Nucleosynthesis: an overview

M. Arnould, N. Prantzos

NUCLEOSYNTHESIS: AN OVERVIEW

M. Arnould[1] and N. Prantzos[2]
[1] Institut d'Astronomie et d'Astrophysique, CP 165,
Université Libre de Bruxelles, Belgium
[2] Institut d'Astrophysique de Paris, France

Résumé

A toutes les époques et échelles astrophysiques, les réactions nucléaires ont joué et continuent à jouer un rôle dominant en ce qui concerne aussi bien l'énergétique que la production des nucléides (nucléosynthèse). Après une brève revue de la composition chimique et isotopique observée dans divers objets de l'Univers, et en particulier dans le système solaire, les prédictions de la nucléosynthèse primordiale dans le cadre d'un modèle de Big Bang sont présentées, ainsi que les ingrédients de base nécessaires à la construction de modèles de l'évolution chimique des galaxies. Une attention toute particulière est portée à l'évaluation de la contribution nucléosynthétique stellaire au travers d'une analyse des épisodes importants de combustion nucléaire à l'intérieur des étoiles en explosion ou non et d'une discussion de la nucléosynthèse concomitante. L'accent est mis sur les incertitudes astrophysiques et nucléaires qui empêchent encore d'accéder à une compréhension claire des caractéristiques, et en particulier des compositions, observées pour une grande variété d'objets astrophysiques.

Abstract

At all times and at all astrophysical scales, nuclear reactions have played and continue to play a key role. This concerns the energetics as well as the production of nuclides (nucleosynthesis). After a brief review of the observed composition of various objects in the universe, and especially of the solar system, the predictions of primordial nucleosynthesis in the framework of Big Bang models are presented, and the basic ingredients that are required in order to build up models for the chemical evolution of galaxies are sketched. Special attention is paid to the evaluation of the stellar yields through an overview of the important burning episodes and nucleosynthetic processes that can develop in non-exploding or exploding stars. Emphasis is put on the remaining astrophysical and nuclear physics uncertainties that hamper a clear understanding of the observed characteristics, and especially compositions, of a large variety of astrophysical objects.

1. Introduction

Astrophysics, the union of astronomy and physics, applies physical laws investigated on earth to the vast and diverse laboratory of space. As such, it is essentially an interdisciplinary field. In particular, cosmology, every branch of astronomy, astronautics, elementary particle, nuclear, atomic and molecular physics, geo- and cosmochemistry have to bring their share to the common adventure.

These lectures deal with the very special interplay between nuclear physics and astrophysics. This interplay comes about namely because nuclear reactions play a pivotal role in the powering of many astrophysical objects, as well as in the production of the nuclides observed in various locations in the Universe.

The hypothesis that the energy production in the Sun and other stars results from thermonuclear reactions has likely been formulated for the first time by Russell (1919), shortly followed by Perrin (1920) (e.g. Schatzman and Praderie 1990). A myriad of further works have substantiated those early ideas beyond doubt. In addition, nuclear reactions are also able to transform nuclear species into others. They thus constitute the key building blocks of the nucleosynthesis models. These models aim at interpreting the present composition of the universe and of its various constituting objects, as well as the variations with time of that composition. As an important subset of that very ambitious program, the solar system composition has been at the center of an intense activity.

Some nucleosynthesis models proposed during the period 1947-1950 assumed that the nuclides were built in a primordial state of the universe [see e.g. Alpher and Herman (1953) for a review]. In spite of some attractive features, those models failed to explain the mounting evidence that all stars do no exhibit the same surface composition. They were also unable to explain the presence of the unstable element technetium discovered by Merrill (1952) at the surface of certain stars.

The problems encountered by those models of primordial nucleosynthesis put to the forefront the idea already expressed earlier by Hoyle (1946) that stars are likely to be major nucleosynthesis agents. That stellar nucleosynthesis model, substantiated by the seminal works of Burbidge et al. (1957) and Cameron (1957), is now widely recognized as being able to explain the origin of the vast majority, if not all, of the naturally occurring nuclides with mass numbers $A \geq 12$ (e.g. Trimble 1975, Arnould 1980, 1986a, Woosley 1986, for reviews). The situation regarding the light nuclides (D, ^{3}He, ^{4}He, ^{6}Li, ^{7}Li, ^{9}Be, ^{10}B and ^{11}B) is different and less clear-cut in certain cases (see Sect. 4). In addition, the problem of the origin of H is outside the realm of the nucleosynthesis models. It is instead a question which is addressed by astrophysicists and particle physicists building up "baryosynthesis" models (e.g. Fritzsch 1986).

2. Composition of the Universe : some basic facts, and a general theoretical framework

The observational basis for the elaboration of nucleosynthesis scenarios consists of the analysis of the electromagnetic radiation at various wavelengths originating from a large variety of emitting locations in the universe: galaxies (especially our own), interstellar medium, and stars of various

types (especially the Sun). Important data also come from the study of the very minute amount of the matter of the universe accessible to man. That matter is comprised for its very largest part in the solar system.[1] The rest is in the form of galactic cosmic rays.[2]

It is not possible to review here the myriad of information available to-date about the composition of a large variety of objects and locations in the Universe (e.g. Trimble 1975, Arnould 1980, 1986a, for reviews). The present discussion is limited to a very brief overview of the situation.

The first general point which has to be stressed is that the large variety of possible sources of information clearly appears associated with some uniformity of composition, as most strikingly exemplified by the fact that hydrogen and helium are by far more abundant than the heavier species in the whole observable universe. A great diversity of elemental and/or isotopic abundances appear, however, to be superimposed on that uniformity. This is the case not only between various classes of observed objects, but also within one given class. For example, (i) the Earth is far from having a uniform composition, (ii) various types of meteorites exist, exhibiting more or less large elemental composition differences, whereas (iii) the abundances of various nuclides at the surface of the stars may vary with the assumed age, the galactic position and the stellar class. Obviously, such a variety of compositions constitutes a problem when trying to set up a coherent nucleosynthetic model. At the same time, that diversity may provide in some instances an invaluable source of information on the chemical evolution of the stars and galaxies.

Unfortunately, the composition information is still very often incomplete, imprecise, or even contradictory. In fact, the most reliable set of data is no doubt provided by the solar system and the Sun. Despite the diversity mentioned above, and within the remaining uncertainties, qualitative similarities are discovered to exist between the (elemental or isotopic) solar system abundances and those measured in a vast body of astrophysical objects. This is why the solar system abundances are sometimes referred to as *universal abundances*, and are regarded as a "standard" for testing nucleosynthesis models.

2.1. Elemental Composition of the Solar System

A milestone in the development of nucleosynthesis models has been the realization that, in spite of large differences between the elemental compositions of constituent members, it was possible to derive a meaningful set of abundances likely representative of the composition of the material from which the solar system formed some 4.6×10^9 yr ago. Such an elemental abundance distribution is displayed in Fig. 1. It is largely based on abundance analyses in a special class of rare meteorites (CI1 carbonaceous chondrites) considered as the least-altered samples of primitive solar matter presently available (e.g. Anders and Grevesse 1989). Solar information, which now comes in quite good agreement with CI1 data for a large variety of

[1] The main solar system sources of information are the meteorites, planets (especially the Earth), the Moon and solar energetic particles. In a not too remote future, matter from comets will probably be brought back to the Earth by space missions. A larger sample of planetary material will also be made available.

[2] The galactic cosmic rays are made of accelerated material from our Galaxy. However, the most energetic cosmic rays might come from extragalactic sources.

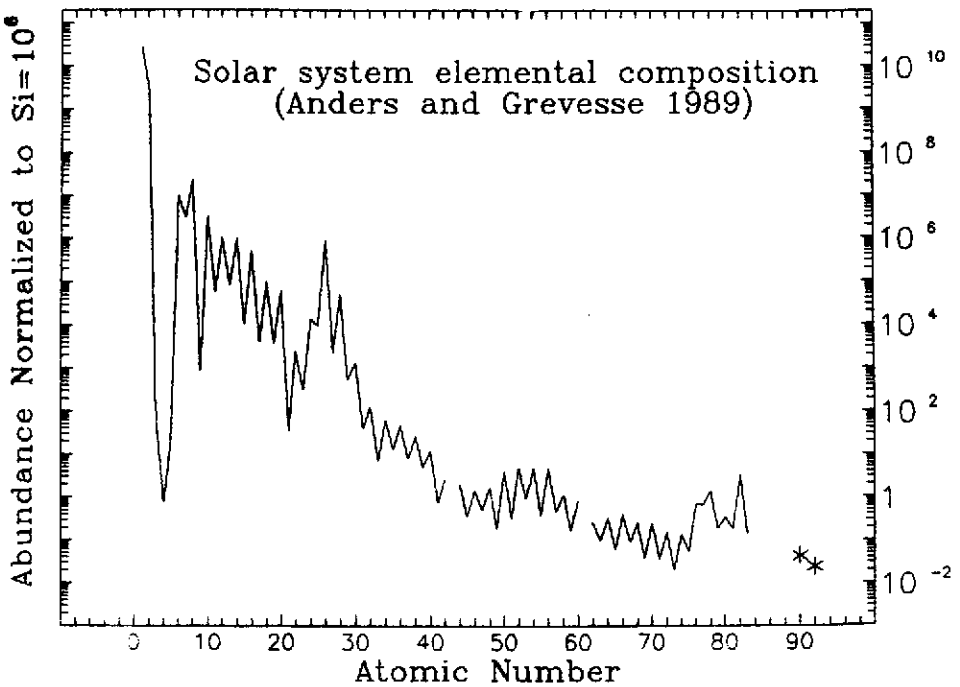

Fig.1. **Bulk solar system elemental composition (data from Anders and Grevesse 1989).**

elements (Anders and Grevesse 1989), has to be used for the volatile elements H, He, C, N, O and Ne, whereas interpolations guided by theoretical considerations are still required in some cases (Ar, Kr, Xe, Hg).

Starting from the composition displayed in Fig. 1, it is possible to account for the differences between the elemental compositions of the various solar system constituents in terms of a large variety of secondary physico-chemical and geological processes.

2.2. Isotopic Composition of the Solar System

If the secondary processes mentioned above have been of primary importance for the differentiation between the elemental abundances of various solar system objects, it seems that they have played only a minor role as far as the isotopic composition is concerned, except in some specific cases. This fact manifests itself through the extremely high homogeneity of the bulk isotopic composition of most elements within the solar system.

In such conditions, terrestrial materials have been classically adopted as the primary standard for the isotopic composition characteristic of the primitive solar nebula. However, the choice of the most representative isotopic composition of H and the noble gases raises certain specific problems.

2.3. Bulk Solar System Composition and Universal Abundances

The solar system composition (SC) derived from Fig. 1 and from the isotopic abundances discussed in Sect. 2.2 is displayed in Fig. 2. As already noticed previously, that SC is sometimes viewed as representative of universal abundances.

Without going into details, some characteristics of the SC are worth noticing :

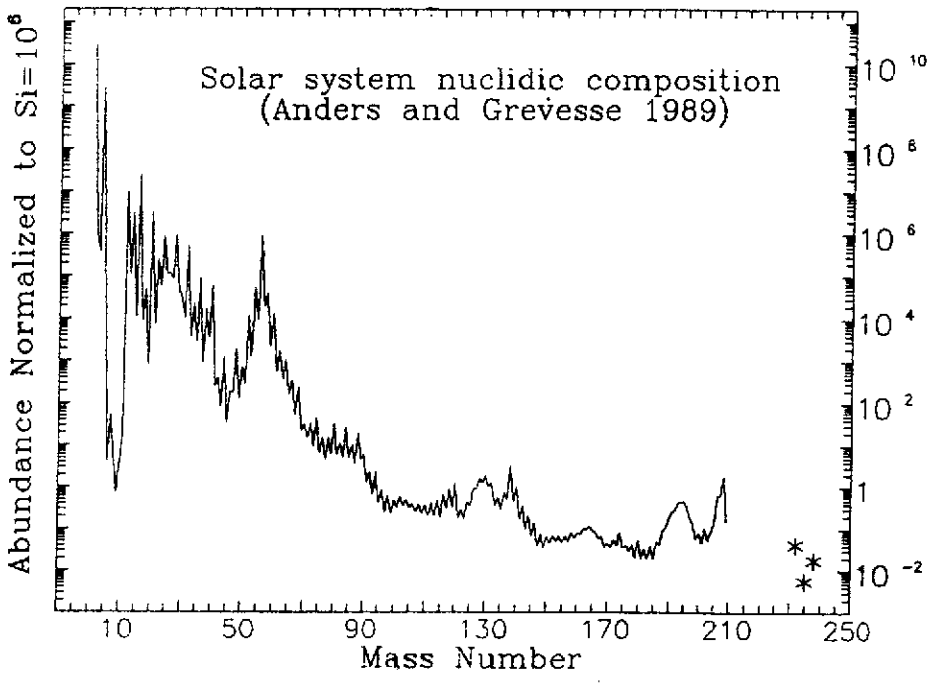

Fig.2. Bulk solar system nuclidic composition (data from Anders and Grevesse 1989).

1) by far, H and He are the most abundant species;
2) Li, Be, and B are extremely underabundant with respect to the neighboring light nuclei;
3) some abundance peaks are superimposed on a curve which is decreasing with increasing mass number A. Apart from the most important one centered around ^{56}Fe ("iron peak"), peaks are found at $A = 4n$ nuclei ($A \leq 56$). In addition, a broad peak is observed in the $A \approx 80 - 90$ region, whereas double peaks show up at $A = 130 - 138$ and $195 - 208$.

For practical purposes, and especially for establishing a useful connection between observations and nucleosynthesis models, it is of interest to split the $A \geq 70$ SC curve into three distributions providing separately the abundances of the stable nuclei located at the bottom of the valley of nuclear stability, in the neutron deficient, and in the neutron-rich regions. Such a splitting of the abundance curve can be made clearer by considering a portion of the nuclidic chart (Fig. 3). For even values of the mass number A, more than one stable isobar may exist. The stable (even Z) neutron-rich isobar, if any, is classically referred to as a r-nucleus. In Fig. 3, ^{142}Ce, ^{148}Nd, ^{150}Nd, or ^{154}Sm belong to such a class. All the long-lived actinides are also classified as r-nuclei. The stable (even Z) isobar located at the bottom of the valley of stability is referred to as a s-nucleus. In Fig. 3, ^{142}Nd, ^{148}Sm or ^{150}Sm belong to this category. Finally, the stable (even Z) isobar located in the neutron-deficient region, like ^{144}Sm in Fig. 3, is called a p-nucleus. The two very long-lived odd-odd nuclei ^{138}La and ^{180}Ta are also classified as p-nuclei. The remaining odd-A nuclei are referred to as sr-nuclei. Such a classification and terminology is intimately related to the current views on the origin of the heavy elements, the s-, r-, and p-nuclei being ascribed to the so-called s-, r-, and p-processes (Sect. 8).

The abundances of the s-, r- and p-nuclei resulting from the splitting of the SC distribution are displayed in Fig. 4. It is especially worth noticing that the double peak structures mentioned

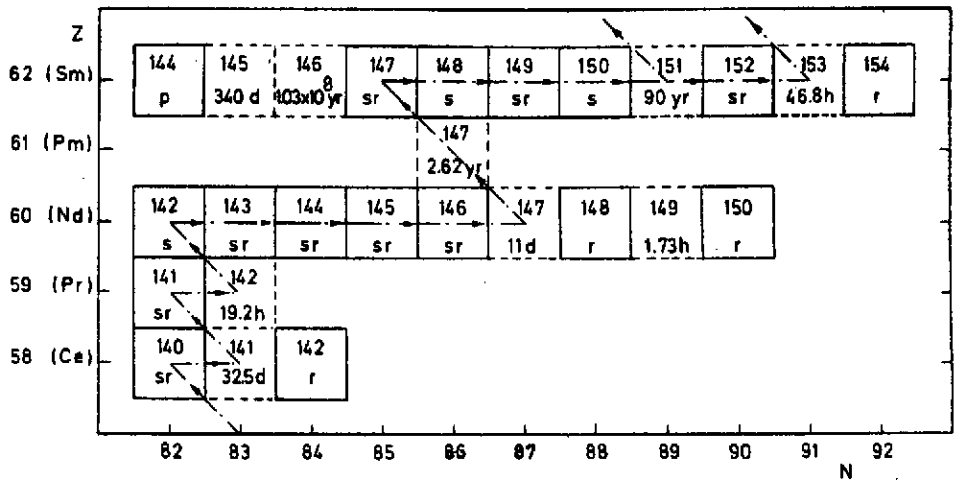

Fig.3. A portion of the nuclidic chart. The stable nuclei are represented by black squares, and their s-, r-, p-, or sr-character is indicated. The $\beta-$unstable nuclides are shown with dashed squares, and their $\beta-$decay half-lives are given. The dash-dotted line represents a typical chain of transformations involved in the process responsible for the synthesis of the s-nuclei (Sect. 8).

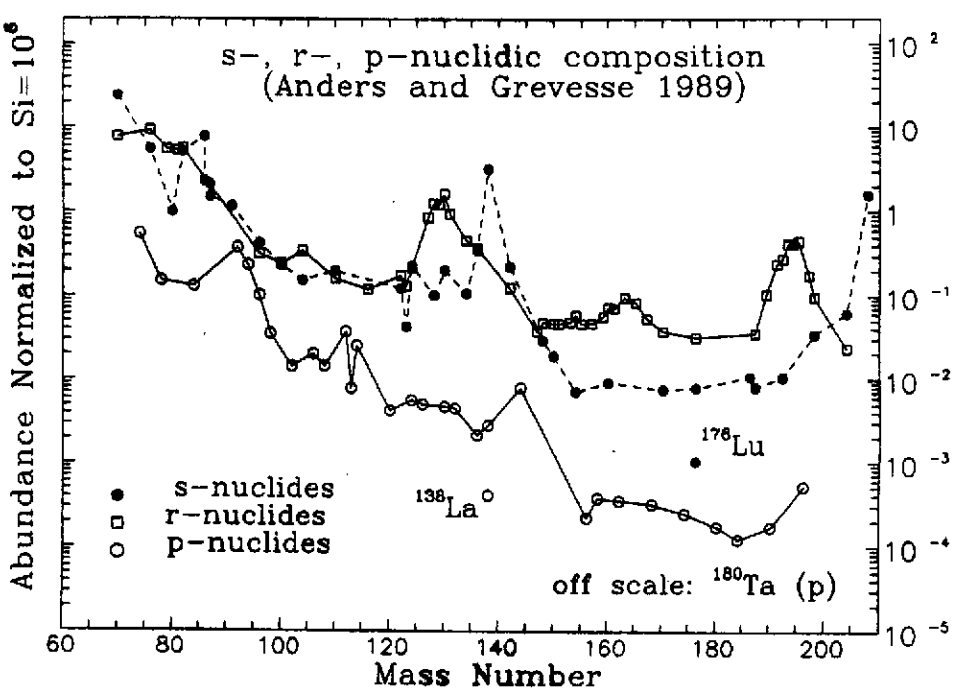

Fig.4. The solar system abundances of the s-, r-, and p-nuclei resulting from the splitting of the SC displayed in Fig. 2, and the classification schematized in Fig. 3. The nuclei which have a mixed sr-character are not shown.

previously are now resolved into a s-component ($A = 138$ and 208) and a r-component ($A = 130$ and 195). In addition, the p-nuclei appear to be $100 - 1000$ times less abundant than the corresponding more neutron-rich isobars, while their distribution roughly parallels the s-nuclei abundance curve (note, however, the very low abundance of the two odd-odd p-nuclei ^{138}La and ^{180}Ta). The abundances of the sr-nuclei are also separated into a s- and an r-component, such

a splitting involving, however, some uncertainty (Käppeler et al. 1989). In Fig. 4, only pure s- or r-nuclides are shown, or s- (r-) nuclides for which the estimated r- (s-) contribution does not exceed 10%.

2.4. Isotopic Anomalies in the Solar System

It has been realized recently (essentially after 1973) that a minor fraction of the solar system material might have an isotopic composition different from the bulk one (Sect. 2.3), after due correction for the operation of the known mechanisms of isotopic fractionation.

Even if only a very minute amount ($\leq 10^{-4} M_{\odot}$, where $M_{\odot}$ represents the mass of the Sun) of the solar system material appears to be concerned, it is generally believed today that such a discovery might necessitate very profound changes in the classical ideas regarding the history and physical state of the very early solar nebula. In particular, evidence is now accumulating concerning the existence of isotopic heterogeneities in the solar nebula just before the start of condensation of solids (in complete contradiction with the "canonical" models of the solar nebula).

It has been speculated that such an "anomalous" material might originate from nearby or remote stars, particularly exploding ones (novae, supernovae). It is well beyond the scope of the present review to provide a detailed discussion of such anomalies, and we simply refer to extensive reviews and discussions of these problems (e.g. Wasserburg 1985, Anders 1987, Arnould 1987). Let us just emphasize that several anomalies due to the in-situ decay of radionuclides have been observed. This is a strong indication for the presence of species with half-lives $t_{1/2} \geq 10^5$ yr in the early solar system. The possible presence of such short-lived (in astronomical standards!) nuclei in some meteoritic material may have far-reaching consequences for the modeling of the early solar system.

2.5. Understanding the Composition of the Universe and the Solar System: the Modern Alchemy

Much theoretical work has attempted to answer the question of the very origin of the abundances observed in various places and objects in the universe. A key guideline in the development of those nucleosynthesis models has been the early realization that the SC displayed in Fig. 2 demonstrates quite convincingly that a correlation exists between abundances and nuclear properties. In particular, a nuclide is more abundant than its neighbors if it is nuclearly more stable. Thus, Fig. 2 clearly exhibits the imprint of some nuclear "alchemy" the details of which have to be unraveled.

Nucleosynthesis models call for two broad classes of nuclear reactions: thermonuclear processes and non-thermal (loosely referred to as "spallation") nuclear transmutations. The former ones can take place at a "primordial" or cosmological level (Big Bang), as well as inside stars during the galactic era. It has been speculated that they could also develop in putative pregalactic very massive or "supermassive objects" that might have formed after the Big Bang. On the other hand, spallation reactions might occur in the interstellar medium (through interactions with galactic cosmic rays), and at the surface or surroundings of stars (through interactions with stellar energetic particles). Some models also call for the operation of spallation reactions at a cosmological or pregalactic level. It is currently thought that primordial nucleosynthesis is

responsible for the production of the "lightest" nuclides H, D, ^{3}He, ^{4}He, and (part of) ^{7}Li (see Sect. 4), while spallation reactions formed ^{6}Li, (most of) ^{7}Li, Be and B. All the other nuclides, from ^{12}C to U, are thought to originate in stars, either during their non-explosive evolutionary phases ("quiescent nucleosynthesis"), or in stellar explosions ("explosive nucleosynthesis").

As said previously, the solar system is the object of the universe which provides the most complete set of high quality abundance data, and has been at the center of an intense activity in the field of nucleosynthesis. It is widely accepted today that the bulk solar system material is made of the ashes of many nucleosynthetic events that could mix in the interstellar medium (or at least in that portion of it to be incorporated in the Solar System) before isolation of the protosolar nebula from the general galactic material. The remaining reservoir(s) contain(s) the minute amount of isotopically anomalous solar system material. They might originate from a very limited number of astrophysical events (perhaps even a single one), in dramatic contrast with the bulk material reservoir. The chemical peculiarities observed at the surface of certain stars have also to be interpreted in terms of in situ nuclear reactions, the products of which can find their way to the stellar surfaces. [3]

A necessary (but not sufficient!) condition for building up reliable models for stellar surface abundances, for the SC and for the meteoritic anomalies is to have as a good knowledge as possible of the rate of the nuclear reactions that can be responsible for abundance changes in the astrophysical locations of relevance. Section 3 is devoted to a brief discussion of thermonuclear reactions of astrophysical interest.

3. Thermonuclear Reactions in Astrophysics: Some Generalities

3.1. Charged Particle Reactions

Thermonuclear reactions between charged particles which are of interest in stellar evolution and in nucleosynthesis are essentially proton and α-particle captures by targets with mass number $A \lesssim 60 - 70$. In certain cases, inverse (γ, p) or (γ, α) photodisintegrations may also play an important role, even on nuclei much heavier than those of the iron group. This is especially the case in the p-process of nucleosynthesis (Sect. 8). Furthermore, the fusion of some light heavy ions, like $^{12}\mathrm{C} + ^{12}\mathrm{C}$, $^{12}\mathrm{C} + ^{16}\mathrm{O}$, $^{16}\mathrm{O} + ^{16}\mathrm{O}$, is also very important in astrophysics.

Much work has been devoted to the study of nuclear reactions with charged particles in astrophysical plasmas. For details, the reader is especially referred to Filippone (1986), Thielemann et al. (1986a), Rolfs et al. (1987), Rolfs and Rodney (1988), and references therein, as well as to the lectures by Descouvemont and by Thibaud at this School. Here, we limit ourselves to some brief comments. As discussed in more detail in the next sections, astrophysical thermonuclear reactions take place typically at temperatures in the $10^6 \lesssim T \lesssim 10^{10}$ K range. In such conditions, it can be shown on grounds of semi-quantitative considerations that the corresponding reaction energies of astrophysical interest vary roughly between some keV and 10 MeV (c.m.), the lowest energies relating more particularly to the lowest-Z species, as well as to

[3] However, some abundance patterns observed at the surface of certain stars or in the interstellar medium are now known not to be due to nuclear reactions, but instead to chemical phenomena, diffusion, or gravitational settling.

non-explosive stellar evolutionary phases, which are characterized by lower temperatures than the corresponding explosive burnings. In any case, those energies of astrophysical interest are generally much lower than the Coulomb barrier energy. As a consequence, the corresponding cross sections are extremely small (very often below the nanobarn), and are thus very difficult to measure, or even impossible to reach with present-day techniques. In such conditions, a widely adopted procedure is to use a model in order to extrapolate the cross sections measured at higher (and lowest possible) energies. Theoretical uncertainties therefore combine with purely experimental ones.

In many other instances, the situation is still much less favorable, no experimental data being available, at least below the Coulomb barrier. That problem is especially acute in nucleosynthesis models, which require the knowledge of a very large body of nuclear data. In addition, unstable targets, as well as targets in excited states, have sometimes to be considered, especially in the field of explosive nucleosynthesis. In such conditions, the cross sections to be used have to rely entirely on theoretical estimates based in particular on more or less well founded systematics, especially for intermediate and heavy nuclei. Needless to say that reaction rates evaluated in such a way are especially uncertain. Last but not least, one must realize that the rates for thermonuclear reactions taking place in a stellar plasma may have to be corrected for various effects. In particular, the role of the electron screening of the nuclear charges has to be considered with great care, and is very difficult to evaluate reliably in certain regimes (e.g. Thielemann and Truran 1986, and references therein).

Let us also note that, under certain stellar circumstances, the nuclei can become bound in a crystalline lattice. Nuclear reactions can take place in such conditions, referred to as the pycnonuclear regime, as a result of the quantum zero point energy which allows for the tunnelling of a nucleus from its lattice point to that of another nucleus. Pycnonuclear reaction rates are still very uncertain (e.g. Salpeter and Van Horn 1969, Dufour and Dietrich 1990). This has important consequences namely on the modeling of the late evolution of white dwarf stars (Hernanz et al. 1988).

3.2. Neutron Reactions

Neutron captures are considered to be important for the synthesis of certain rare $A \lesssim 70$ species, as well as for the production of the stable $A \gtrsim 70$ s-, sr- and r-nuclei (Sect. 8). Furthermore, (γ, n) photodisintegrations can be important for the synthesis of the r-, sr- and p-nuclei (Sect. 8), while neutron-induced fission might play a role in the production of the actinide r-nuclei.

Relevant energies for neutron captures in astrophysical sites range roughly between 10 and 500 keV. A review of experimental data concerning neutron capture reactions at energies of astrophysical interest may be found in Bao and Käppeler (1987) and Käppeler et al. (1989). In many cases, and especially in the study of the r-process, where a very large number of unstable targets have to be dealt with, experimental data are badly lacking. Considerations about theoretical predictions for neutron capture rates may be found in Thielemann et al. (1986a).

3.3. Beta Decays

Weak interactions are important in a host of stellar evolution and nucleosynthesis models. In

astrophysical sites, β-decay rates may be substantially different from their laboratory values, terrestrially stable nuclei even becoming unstable in certain situations. Such differences may be due namely to (i) the possible decay from thermally populated parent excited states, (ii) the partial or total ionization of atoms, (iii) the capture of free electrons, positrons, and even neutrinos. Furthermore, β-decay rates for nuclei far from the line of nuclear stability are required in many nucleosynthesis models (p- or r-process; see Sect. 8). Many of those questions have already been investigated by several authors (e.g. Takahashi and Yokoi 1987; Bender et al. 1988; Möller and Randrup 1989, and references therein).

On the other hand, β-delayed (single or multiple) neutron emission, as well as β-delayed fission may play some role at the termination of the r-process (e.g. Thielemann et al. 1983; Hoff 1986), and thus in the evaluation of the production ratio of the actinide r-nuclei (Sect. 8). In addition to the uncertainties associated with the β-transitions themselves, the evaluation of the delayed particle emission or fission rates are of course affected by still further poorly predictable quantities characterizing the radiation, neutron or fission channels.

Finally, it has to be emphasized that weak interaction neutral currents have various important implications in astrophysics (e.g. Freedman 1977).

3.4. Alpha Decays and Spontaneous Fission

Spontaneous fission may play some role at the termination of the r-process, and provide a "last touch" to the predicted final yields of the r-nuclei. In the canonical r-process model (Sect. 8), this mechanism is, however, of secondary importance compared to neutron-induced fission. As already emphasized previously, fission barriers, half-lives and yields of interest for the r-process are still very poorly predictable.

On the other hand, α-decays are expected to shape the redistribution of $A \geq 210$ material r-processed into the Bi, Pb, U and Th regions. The evaluation of this effect can be performed on grounds of experimentally known α-decay rates. Alpha-decays of nuclei far from the line of stability might also play a role in some nucleosynthesis models. The prediction of those decay probabilities has not yet reached the desirable level of reliability.

3.5. Nuclear Reaction Networks

Energy generation or nucleosynthesis predictions are derived from the solution of a "nuclear reaction network" defined as a set of nuclear species coupled by a set of nuclear reactions and decays. Mathematically, such a solution is particularly simple in special conditions, such as the quasi-equilibrium Si burning, and, especially, the nuclear statistical equilibrium (NSE; Sect. 6). In other conditions, a set of coupled first order non linear differential equations of the form

$$\frac{dY_m}{dt} = -\lambda_m Y_m + \sum_{k \neq m} \lambda_k^{(m)} Y_k - \sum_k Y_m Y_k [mk] + \sum_{\substack{k \neq m \\ l \geq k}} Y_k Y_l [kl]^{(m)} + \cdots \qquad (3.1)$$

has to be solved. In Eq. (3.1), Y_m is the abundance of nuclei m, related to the number of nuclei m per unit volume by $N_m = \rho Y_m N_A$, ρ being the mass density and N_A the Avogadro number. The other symbols in Eq. (3.1) are as follows: (1) $\lambda_k^{(m)}$ is the rate of photodisintegration or of β-decay of nucleus k leading to the formation of nucleus m ($k \neq i$); λ_m is obtained by summing

over all the possible photodisintegrations or β-decays of nucleus m; (2) $[kl]^{(m)}$ is related to the rate $r_{kl}^{(m)}$ of the reaction between nuclei k and l, leading to the formation of nuclei m, by $[kl]^{(m)} = \rho N_A r_{kl}^{(m)}$. It has to be noted that elastic scattering is of no interest in the problem at hand. This is also true for inelastic scattering, except possibly in certain special situations involving isomeric states; $[kl]^{(m)}$ is obtained by summing over all the possible exit channels in the $k + l$ reaction. Equation (3.1) must also include terms corresponding to reactions involving more than two particles in the entrance channel. For the sake of conciseness, such terms have not been written down explicitly. It is important to note that the coefficients in Eq. (3.1) are in general very sensitive functions of temperature and density, which in turn can vary extremely rapidly with time in explosive situations (e.g. Arnould 1980, Woosley 1986).

For obvious practical purposes, limitations are imposed on the size of the reaction networks. An "educated guess" of the best suited network for a given purpose requires some a priori knowledge of the range of physical conditions one might have to deal with. This particularly concerns temperatures, densities and initial compositions. One further needs to know which nuclear reactions and β-decays may have a chance to be important in these estimated conditions.

4. Primordial Nucleosynthesis: a Probe of Cosmology and Particle Physics

The standard hot Big Bang model provides a very successful and economical description of the evolution of the (observable) Universe, from temperatures as high as $T \sim 10^{12}$ K ($t \sim 10^{-4}$ s after the "bang") until the present epoch ($T \sim$3 K, $t \sim (10 - 20) \times 10^9$ yr). The observational evidence testifying for the validity of the model is threefold:

- The *universal expansion*, discovered by Hubble in 1929: all galaxies, except those of the Local Group, are receding from us (and from each other) with velocities v proportional to their distances r following $v = H\, r$. The *Hubble parameter H(t)* measures the rate of universal expansion. Its current value is $H_0 \sim$ 50-100 km/s/Mpc (1 Mpc = 3.26 10^6 light years), and its inverse $t_H \sim H_0^{-1} \sim$ 10-20 10^9 yr (*Hubble time*) is a measure of the age of the Universe.

- The *cosmic* (microwave) *background radiation* (CBR in the following), discovered by Penzias and Wilson in 1965: its spectrum fits with astonishing precision a blackbody of temperature $T_0 = 2.735 \pm 0.006$ K (COBE 1990, Fig. 5), and its angular uniformity ($\Delta T/T < 10^{-4}$) combined with its presumed homogeneity (Cosmological Principle) strongly argue for a hot and homogeneous early Universe, where matter and radiation were in equilibrium. The "last scattering surface", i.e. the epoch when matter and radiation "decoupled", is situated at a temperature $T \sim$3000 K, corresponding to an age of a few 10^5 years after the "bang".

- The *cosmic abundances* of D, ^{3}He, ^{4}He, ^{7}Li: these light nuclides are predicted to be synthesized in the hot early Universe, at temperatures $T \sim 10^9 - 10^8$ K ($t \sim 10^2 - 10^3$ s). The successful comparison of their predicted abundances with inferred determinations of their primordial ones is a real triumph of the standard model. At the same time, it is by far the most stringent test we have of it, constraining severely its parameters. Notice that the epoch of Big Bang nucleosynthesis (BBN), being the earliest period in the life of the Universe from which we have "relics" from a well understood process (i.e. the abundances of the light nuclides),

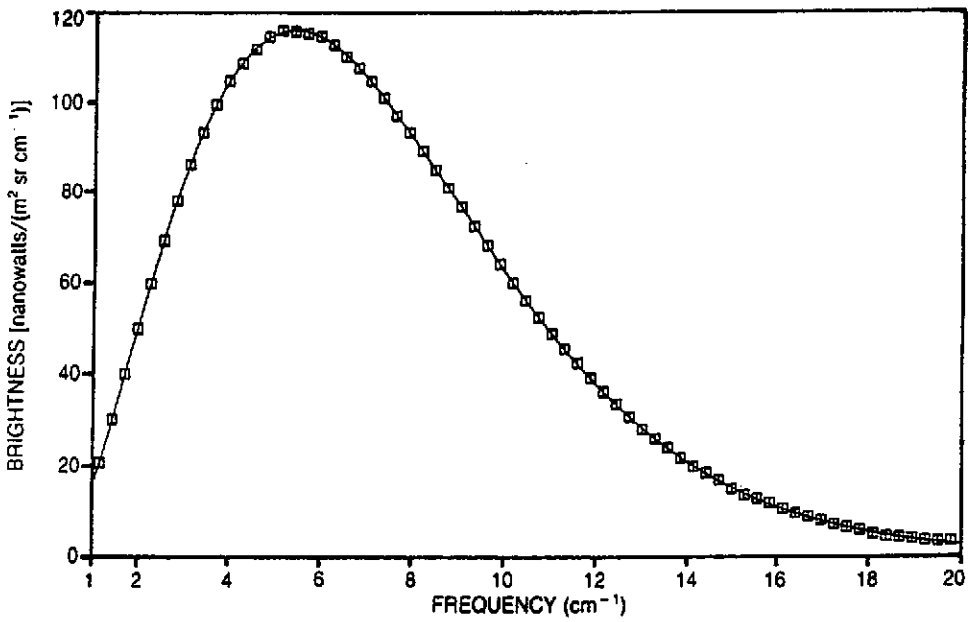

Fig.5. Cosmic microwave backround spectrum, measured by the Far Infrared Absolute Spectrometer aboard the Cosmic Background Explorer (COBE) launched in November 1989. The fit to a Planck blackbody curve yields a temperature $T = 2.735 \pm 0.006$ K. At the level of 1% of peak brightness, these new observations show no deviation from a perfect blackbody spectrum.

is a gateway to the Very Early Universe, where particle energies were much higher than those accessible to present-day accelerators. The importance of a continuous scrutiny of the BBN predictions is thus manifest.

4.1. Thermodynamics of the Early Universe

The two fundamental assumptions underlying BBN are that: 1) General Relativity offers a valid description of gravity, and 2) the Universe once was hotter than $\sim 10^{11}$ K, so that statistical equilibrium was established between all of its components (e.g. Weinberg 1972, Kolb and Turner 1990). The basic cosmological equation, describing the expansion of the Universe under the gravitational attraction of its material content, is ***Friedmann's equation***, which reads (assuming that the cosmological constant is zero)

$$(\frac{\dot{R}}{R})^2 - \frac{8\pi}{3} G\rho = \frac{k}{R^2} \tag{4.1}$$

where ρ is the average density, k a constant related to space-time curvature, and $R(t)$ a dimensionless *scale factor* (distances in the expanding Universe increase following $r = Rr_0$, where r_0 is a distance at some reference epoch) the time derivative of which is $\dot{R}(t)$. [4] Eq. (4.1) can be cast in the form

$$\frac{k}{H^2 R^2} = \frac{\rho}{3H^2/8\pi G} = \frac{\rho}{\rho_c} - 1 = \Omega - 1 \tag{4.2}$$

[4] Although (4.1) is a general relativistic equation, it can also be obtained in the framework of Newtonian mechanics by requiring energy conservation for a test particle on a sphere of radius R and mass $M = 4\pi/3\rho R^3$, expanding adiabatically with velocity $v = \dot{R}$, i.e. $E = v^2/2 - GM/R = const.$. The difference with general relativity is in the interpretation of ρ (matter density in classical mechanics, matter + energy density in relativity) and k (a simple constant in classical mechanics).

where $H = \dot{R}/R$. This expression defines the *critical density* $\rho_c = 3H^2/8\pi G$, and the *density parameter* $\Omega = \rho/\rho_c$. For k = (1, 0, -1), $\Omega(>,=,<)1$, and $\rho(>,=,<)\rho_c$, corresponding to a closed, flat, or open Universe respectively.

The present average *density of matter* in the Universe is poorly known. If only luminous matter is considered (i.e. stars in galaxies, made essentially of *baryons*), then $\rho_{B,0} \sim 2 \times 10^{-31}$ gcm^{-3} (corresponding number density: $n_{B,0} \sim 510^{-7}$ cm^{-3}). However, the rotation curves of galaxies (i.e. the observed "rotational velocity vs. galactocentric distance" relationship) require ~10 times more matter than the luminous one, which could be either in baryonic or non-baryonic form. On the other hand, the *density of radiation*, essentially in CBR photons, is $\rho_{\gamma,0}(\propto T_0^4) \sim 5 \times 10^{-34}$ gcm^{-3} (and the corresponding number density of photons $n_{\gamma,0}(\propto T_0^3) \sim 500$ cm^{-3}), i.e. much less than the material density (*matter dominated* Universe). All these values are considerably smaller than the *current critical density* $\rho_{c,0} = 3H_0^2/8\pi G \sim 10^{-29}$ gcm^{-3}. It thus seems that the Universe is *open*.

The density of the Universe has not always been dominated by matter. Number densities of all species (i.e. n_B, n_γ etc.) are indeed inversely proportional to the expanding volume (i.e. $n \propto R^{-3}$), and the same is true for the corresponding *mass density* $\rho_m \sim \rho_B = n_m m_B \propto R^{-3}$ (m_B being the mass of a baryon). On the other hand, the equivalent energy *density of radiation* $\rho_\gamma = n_\gamma hc/\lambda \propto R^{-4}$ (since the wavelength of a photon $\lambda \propto R^{-1}$, being "stretched" by the universal expansion). This means that sometime in the past (in fact shortly before the matter-radiation decoupling period, at $T \sim$ a few 10^4 K) the Universe has been *radiation dominated*. Notice that the *baryon/photon ratio* $\eta = n_B/n_\gamma \sim 10^{-9}$ remains ~ constant throughout the evolution of the Universe (i.e. from just before the BBN period until now, since the contribution of stellar radiation turns out to be negligible). This makes it a very useful parameter, connecting the early Universe of BBN with the observable one.

The present-day Universe is very close to being flat, and it can be shown that it was even more so in the past. For $k = 0$ and with an appropriate equation of state, the evolution of the thermodynamic variables of the Universe can be deduced from Eq. (4.1) and the assumption of adiabatic expansion [see Eq. (4.7)]. Notice that *time* is not a good variable, since we do not know if we are allowed to extrapolate our physical laws to arbitrarily high temperatures, i.e. back to $t = 0$. *Temperature* is used instead, which fixes the ***number of relativistic degrees of freedom*** of the system

$$g^*(T) = \Sigma g_B (\frac{T_B}{T})^4 + \frac{7}{8} \Sigma g_F (\frac{T_F}{T})^4 \qquad (4.3)$$

where B and F stand for bosons and fermions, respectively (the factor 7/8 being due to fermion statistics), and where the possibility of components with different temperatures (i.e. thermally decoupled from the cosmic plasma) is taken into account. In equilibrium, the *total density*

$$\rho \sim \rho_R \sim 1/2\ g^*(T)\ \rho_\gamma = 1/2\ g^*(T)\ \alpha T^4 \qquad (4.4)$$

(α is the radiation constant) is essentially determined by the number of relativistic species, since the density of non-relativistic species of mass m in equilibrium is severely hindered by the Boltzmann factor [$\rho_m = mn_m \sim m \exp(-mc^2/kT)$]. Through Eq. (4.1), Eq. (4.4) then fixes the ***expansion rate***

$$H = \dot{R}/R \sim (\frac{8\pi}{3} G\rho)^{1/2} \sim 2\ (g^*)^{1/2}\ G^{1/2}\ T^2 \qquad (4.5)$$

which also measures the rate of change of the thermodynamic properties of the system [Notice the important (and counter-intuitive!) result of a faster expansion for a larger density]. On the other hand, the rates of the various reactions (weak, strong, electromagnetic) in the cosmic plasma depend generally on temperature folowing

$$\Gamma \sim n(T)\ \sigma(T)\ v(T) \sim T^{\nu} \tag{4.6}$$

where n is the particle density, σ the reaction cross-section, and v the average particle velocity. Since $n \propto R^{-3} \propto T^3$, $\nu > 3$, so that $\Gamma/H \propto T^{\mu}$ ($\mu > 1$) decreases during the expansion. As long as $\Gamma > H$ (i.e. the reactions are faster than the expansion), equilibrium is maintained, redistributing energy among the various components of the cosmic plasma. In contrast, when $\Gamma < H$ the reactions can no more keep in pace with the expansion and the affected species drop out of equilibrium (*decoupling*).

At temperatures greater than the rest mass of some particle S ($kT > m_S c^2$), pair creation by the background radiation maintains particle densities $n_S = n_{\overline{S}} \sim n_\gamma$. When temperature drops below that threshold ($kT < m_S c^2$), particle-antiparticle annihilation is not balanced anymore by pair creation and, in principle, $n_S = n_{\overline{S}} < 10^{-17} n_\gamma$. However, no antimatter has been found in the observable Universe ($n_B >> n_{\overline{B}}$ for baryons), except in cosmic rays, where it comes as a secondary product of high energy interactions. Moreover, $(n_B - n_{\overline{B}})/n_\gamma = \eta \sim 10^{-9} >> 10^{-17}$, as we saw before. This observed *excess of matter over antimatter* is unexplained in standard Big Bang models, where it is assumed as initial condition. It finds an explanation in the framework of Grand Unified Theories (GUT's), where it is produced (*baryogenesis*) during GUT symmetry breaking, at temperatures $T \sim 10^{27}$ K (e.g. Kolb and Turner 1989).

4.2. Primordial Nucleosynthesis: Results and Uncertainties

For our purpose, we start the description of the primordial Universe at temperatures $T \sim 10^{12}$ K (~100 MeV), with a mixture of one non-relativistic baryon (p and n) for every $\sim 10^9$ relativistic species ($\gamma, e^-, e^+, \nu, \overline{\nu}$), all of them in statistical equilibrium. Since the leptonic degrees of freedom dominate the total mass-energy density, we are in the *Leptonic Era*. The assumption of adiabatic expansion ($dE + pdV = 0$) gives

$$\frac{d}{dt}(\rho R^3) + p d(R^3) = 0 \tag{4.7}$$

which, combined to Eqs. (4.1) and (4.4) and the equation of state for radiation (i.e. $p = 1/3\rho$), leads to a useful formula for the time dependence of temperature during the whole radiation dominated epoch:

$$T\ (\mathrm{K}) \sim 1.2\ 10^{10}\ (g^*)^{-1/4}\ t(\mathrm{s})^{-1/2} \tag{4.8}$$

It follows that $T \sim 10^{12}$ K at $t \sim 10^{-4}$ s. This timescale is larger than the characteristic timescales of the various interactions (weak, strong or electromagnetic) at that temperature, so that the assumption of statistical equilibrium (starting hypothesis for the standard BBN scenario) is fully justified.

At $t \sim 0.1$ s ($T \sim 3 \times 10^{10}$ K ~4 MeV), neutral current weak interactions (i.e. $e^+ + e^- \rightleftharpoons \nu + \overline{\nu}$) become slower than the expansion ($\Gamma_{WEAK} \propto T^5$, whereas $H \propto T^2$). Neutrinos decouple

then from the thermal plasma and expand adiabatically thereafter with a neutrino temperature $T_\nu \propto R^{-1}$ (this is the "last scattering" epoch for neutrinos; detection of the cosmic neutrino seas would provide a direct "view" of the Universe as it was ~0.1 s after the "bang"). However, charged current weak interactions (i.e. $n + e^+ \rightleftharpoons p + \overline{\nu}$ and $e^- + p \rightleftharpoons n + \nu$), proceeding at a rate $\Gamma \propto \tau_n^{-1}$ ($\tau_n \sim 890$ s being the neutron lifetime) are still sufficiently fast to maintain the neutron/proton ratio at its equilibrium value $n/p \sim \exp(-Q/kT)$, where $Q = (m_n - m_p)c^2 \sim 1.28$ MeV. At those temperatures, $(n/p)_{equilibrium} \sim 1$.

At $t \sim 1$ s ($T \sim 10^{10}$ K ~ 1 MeV), charged current weak interactions become slower than the expansion. The n/p ratio essentially "freezes" at its equilibrium value at that *decoupling temperature* T_*: $(n/p)_* \sim \exp(-Q/kT_*) \sim 0.18$. Neutron decay ($n \rightarrow p + e^- + \overline{\nu}$) still continues to operate, slowly modifying the "freeze-out" ratio: $n/p = (n/p)_* \exp(-t/\tau_n)$.

At $t \sim 10$ s ($T \sim 3 \times 10^9$ K ~ 0.5 MeV), photons are no longer sufficiently energetic to create $e^- - e^+$ pairs, which disappear leaving behind 1 e^- for every $\sim 10^9$ photons, so that charge conservation w.r.t protons is respected. The photon bath is slightly "heated" by the transfer of the annihilation entropy, but not the neutrino seas which are decoupled. From now on, the corresponding temperatures are related by $T_\nu = (4/11)^{1/3} T_\gamma$ (leading to a current neutrino temperature $T_{\nu,0} \sim 2$ K, too low for them to be detected). The disappearence of $e^- - e^+$ pairs marks the end of the Leptonic Era and the beginning of the *Radiation Era*, which will end $\sim 10^5$ yr later.

During all that time, nuclear reactions could not form any composite nuclei because of the "deuterium bottleneck". As a result of its relatively small binding energy ($BE_D \sim 2.2$ MeV), deuterium is photodisintegrated as soon as it is formed by $p + n \rightarrow D$, its abundance being kept to tiny equilibrium amounts $n_D/n_B \sim \eta \exp(-BE_D/kT)$. Even when $kT < BE_D$, the large value of $\eta^{-1} \sim 10^9$ allows for a large photon population in the high energy tail of the Planck spectrum (i.e. $E_\gamma > BE_D$) that is able to keep destroying deuterium efficiently. Since three-particle reactions are quite improbable at those densities ($\rho_B \sim 10$ gcm^{-3}), no heavier nuclei can be formed either. Only when temperature drops down to $\sim 9 \times 10^8$ K (~ 0.1 MeV, at $t_D \sim 200$ s) does the deuterium bottleneck "break", leading to the production of substantial amounts of D. The n/p ratio at that time is $(n/p)_0 \sim (n/p)_* \exp(-t_D/\tau_n) \sim 0.15$, not very different from the "freeze-out" value.

This is the starting point of *primordial nucleosynthesis* (Wagoner et al. 1967, Schramm and Wagoner 1977). Dozens of other reactions become operative, i.e. D+p $\rightleftharpoons$ ^{3}He+γ, D+n $\rightleftharpoons$ ^{3}H+γ etc. (Fig. 6), bringing nuclei in statistical equilibrium. Since ^{4}He is the most tightly bound nucleus in that region, almost all the neutrons present at that time are finaly incorporated into ^{4}He. This allows an easy evaluation of its final mass fraction X_4. Before ^{4}He formation, the (number *and* mass fraction X) abundances of neutrons and protons were related by $(n/p)_0 = (X_n/X_p)_0 \sim 0.15$. As $X_{n,0} + X_{p,0} = 1$, we obtain $X_{p,0} \sim 0.87$ and $X_{n,0} \sim 0.13$. Neutrons combine with an equal amount of protons to form ^{4}He, so that we are left with $X_p = X_{p,0} - X_{n,0} \sim 0.74$ and $X_4 \sim 1 - X_p \sim 0.26$ after Big Bang. In other words, a quarter of the baryonic mass of the Universe is transformed into ^{4}He. The result of this rough calculation compares fairly well with the observed amount of ^{4}He in the Universe ($X_{4,obs} \sim 25\%$), which cannot be accounted for by stellar nucleosynthesis.

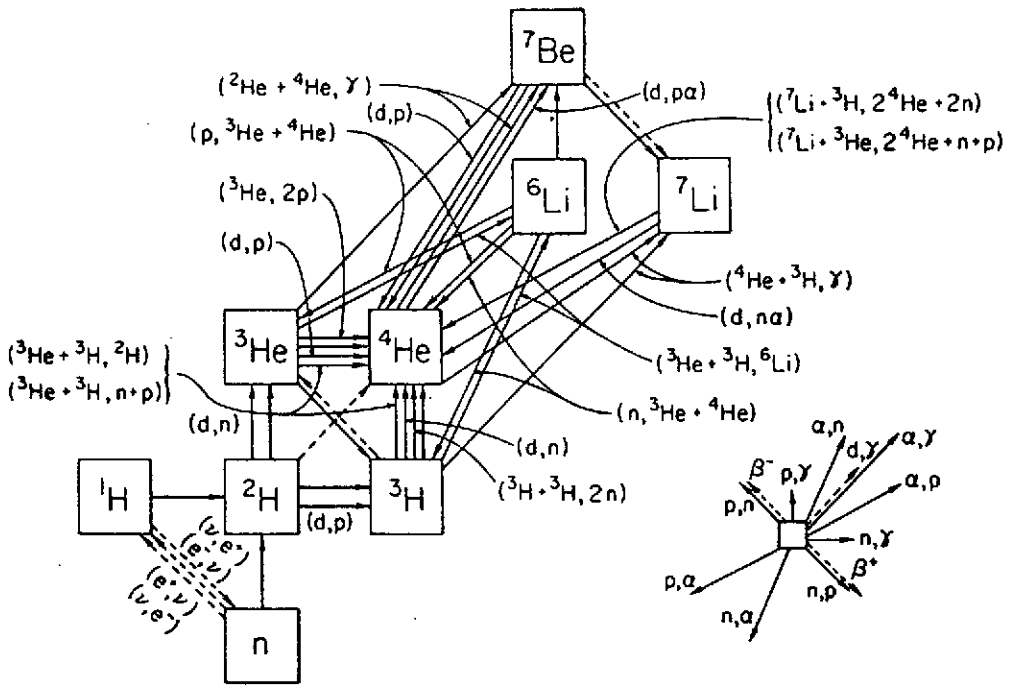

Fig.6. Reaction network with the most important reactions for standard primordial nucleosynthesis models. Unstable nuclei with mass $A = 8$ do not allow to go beyond ^{7}Li in such models.

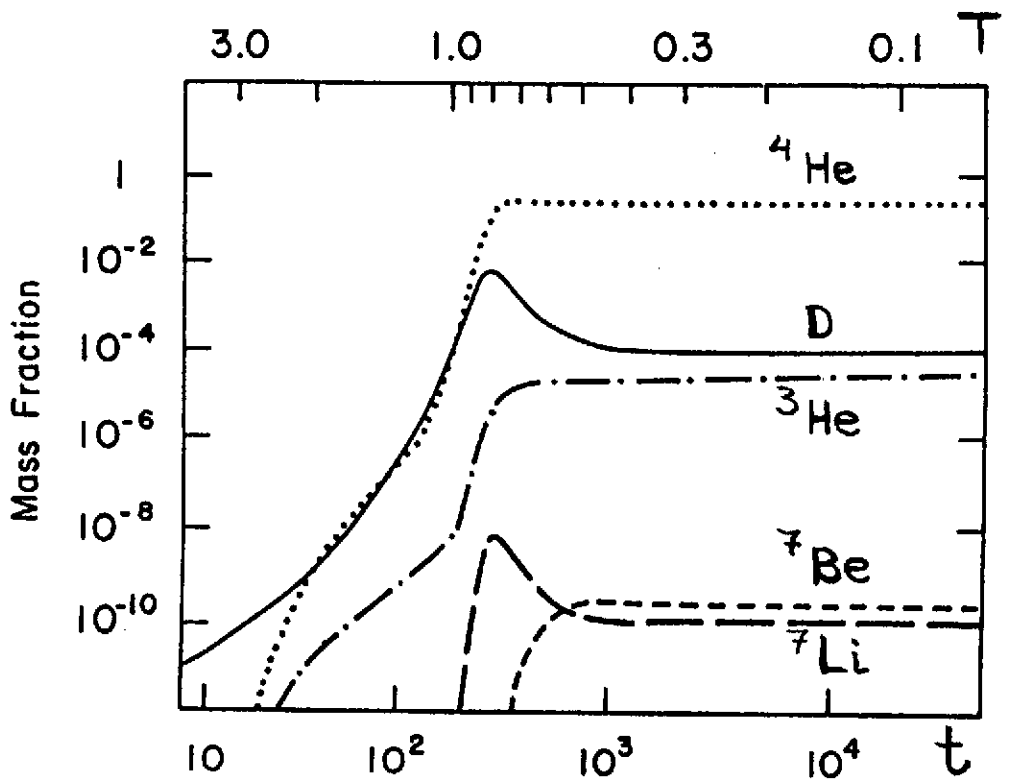

Fig.7. Evolution of the abundances of light nuclides in standard Big Bang nucleosynthesis calculations, as a function of time t (*down*, in s), or temperature T (*up*, in 10^9 K). Nucleosynthesis really starts at $t \sim 200$ s, with the breaking of the "deuterium bottleneck" (see text). ^{7}Be eventually decays to ^{7}Li, with a half-life of ~54 days.

The nuclear flow stops essentially at ^{4}He, because there are no stable nuclei with mass $A = 5$ or $A = 8$. The combination of the most abundant nuclei, protons and ^{4}He, via two-particle reactions always leads to unstable $A = 5$ nuclides. Even if ^{4}He combines with rarer nuclei, like ^{3}H or ^{3}He, $A = 7$ nuclides are produced, which, when hit by (abundant) protons or (rare) neutrons yield mass $A = 8$. [5]. Nucleosynthesis stops when temperature drops to $\sim 310^8$ K ($t \sim 10^3$ s), so that the Coulomb barriers can not be penetrated any more. Eventually, ^{3}H decays to ^{3}He and the $A = 7$ nuclei transform into ^{7}Li, while all the protons remain as hydrogen. Thus, as shown in Fig. 7, BBN transforms the composition of the primordial Universe into (by mass) $\sim 75\%$ H, $\sim 25\%$ ^{4}He, and traces of D($\sim 10^{-4}$), ^{3}He($\sim 10^{-4}$) and ^{7}Li($\sim 10^{-10}$). In such conditions, all the other nuclides are expected to form later in stars.

The BBN yields are essentially determined by the competition between the various reaction rates and the expansion rate. The latter depends on the (unknown) total density ρ, fixed by the number of relativistic degrees of freedom g^*, while the former depends on the (also unknown) densities of the various interacting species (e.g. $\eta = n_B/n_\gamma$ for baryons) and, of course, on the rates of the relevant two-body reactions.

The Big Bang (i.e. primordial) ^{4}He yield (traditionally referred to as Y_p if expressed by mass) depends upon η, N_ν [which parametrizes the number of "light" species (i.e. $mc^2 < 1$ MeV) other than γ, e^-, and e^+], and τ_n (the neutron lifetime, which determines the rates for all the weak processes that interconvert neutrons and protons). It is almost insensitive to the rates of the thermonuclear reactions, since, for $\eta > 3 \times 10^{-11}$, all the available neutrons at "freeze-out" are converted in ^{4}He. In fact, Y_p is a monotonically increasing function of η, N_ν and τ_n. The dependence on η is weak: larger η means that the D bottleneck "breaks" earlier, with more neutrons available (since they had less time to decay after the "freeze-out") to form a larger Y_p. More light species (i.e. larger N_ν) means a faster expansion, since [Eq. (4.4)] $H \sim 2.4 g^{1/2} G^{1/2} T^2$, with $g_{Leptonic\,Era} = g_\gamma + 7/8(g_e + N_\nu g_\nu) = 43/4$ for a mixture of photons with $g_\gamma = 2$ (2 spin states), electron-positron pairs with $g_e = 4$ (2 spin states) and $N_\nu = 3$ neutrino-antineutrino species with $g_\nu = 2$ (*only one helicity state*). In turn, a faster expansion implies an earlier decoupling with a larger abundance of neutrons to form ^{4}He. An increase in τ_n has the same effect, since the slower rate of weak interactions ($\Gamma \propto \tau_n^{-1}$) leads to an earlier "freeze-out" and larger amounts of neutrons available.

As shown in Fig. 8, the primordial yields of D and ^{3}He are particularly sensitive to the density of interacting nuclei during BBN, i.e. to η. Their abundances are found to decrease with increasing η, since higher densities favour their larger destruction into ^{4}He. A larger expansion rate H, on the other hand, leads to a larger yield of D and ^{3}He, since the reactions responsible for their destruction stop earlier in that case.

The situation is somewhat different for ^{7}Li: its primordial abundance as a function of η has

---

[5] A loophole around the $A = 8$ gap can be found if $n/p > 1$ initially, so that excess neutrons exist. In the standard BBN, $n/p < 1$, but in *inhomogeneous* BBN scenarios, one can find regions with $n/p > 1$. Such scenarios, involving coexisting neutron-rich and proton-rich "bubbles" at the epoch of primordial nucleosynthesis, have been proposed recently and raised much excitement. The nucleosynthesis consequences of that non-standard model have been studied in many places (e.g. Malaney and Fowler 1989, Kajino and Boyd 1990, Thielemann and Wiescher 1990)

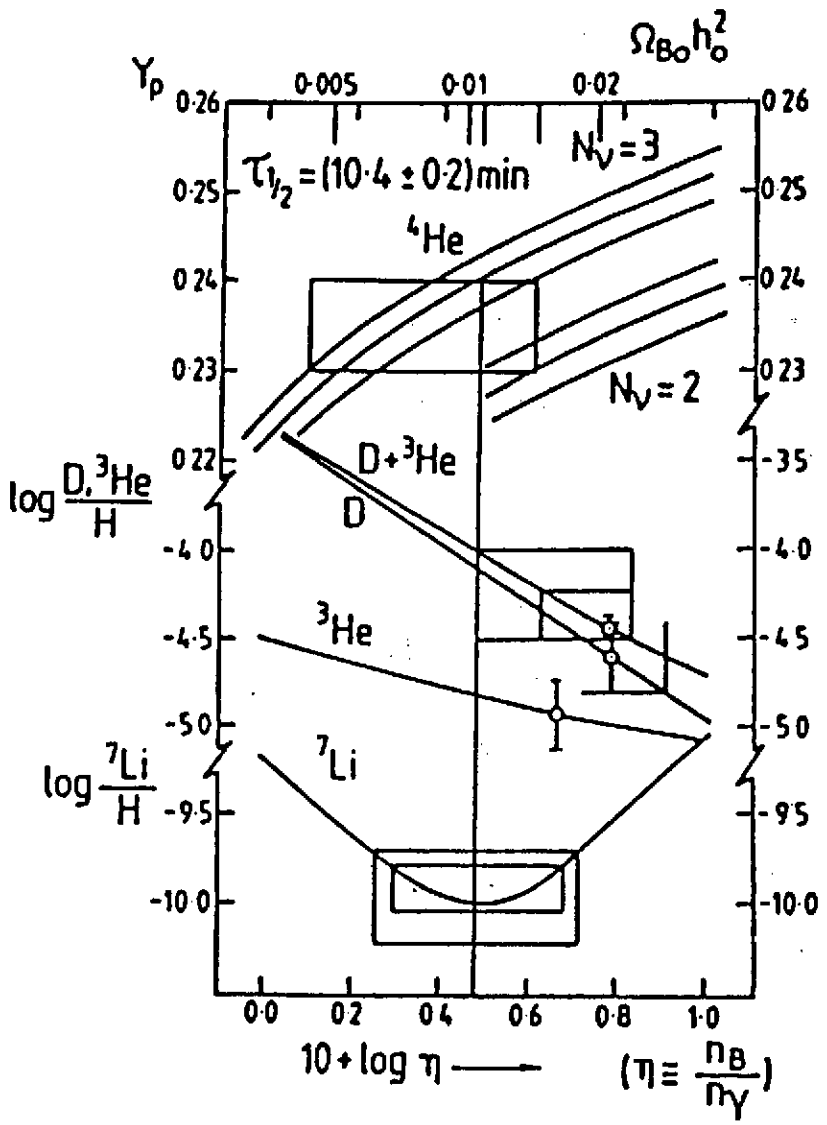

Fig.8. Abundances of light nuclei in standard Big Bang nucleosynthesis calculations, plotted as a function of the baryon/photon ratio η (down), or equivalently, the baryonic density parameter (up) $\Omega_{B,0}h_0^2 = 0.0036(\eta/10^{-10})(T_0/2.73)^3$ (see text). The calculations (Yang et al. 1984) are performed for $N_\nu = 2$ and 3 neutrino species, respectively, and for a neutron half-life of $\tau_{1/2} = 10.4 \pm 0.2$ min (three curves for each N_ν are shown for ^{4}He). Current observationally inferred primordial abundances are indicated by vertical lines for each nuclide, while horizontal lines show the acceptable values for η.

a minimum situated (by accident?) in the range of interest for cosmology, i.e. $10^{-10} < \eta < 10^{-9}$. This is due to its two-fold production mechanism, through $^3\mathrm{He}(\alpha,\gamma)^7\mathrm{Li}$ at low densities (yield decreasing with η), and through $^3\mathrm{H}(\alpha,\gamma)^7\mathrm{Be}$ at high densities (yield of ^{7}Be increasing with η).

The *uncertainties* in BBN yields due to nuclear reaction rates are relatively small. The rates of most of the relevant reactions are known to better than ~10-15%, and the impact on the corresponding yields is less than ~ 2-3 % for D, ^{3}He, ^{4}He. The situation is worse for ^{7}Li: current uncertainties on its production and destruction rates do not allow to evaluate its primordial yield to better than a factor of ~2. Finally, let us mention the increasing precision in the estimate of the neutron lifetime, for which the new (1990) world average is: $\tau_n = 890\pm4$ s ($\tau_{1/2}$=10.3 min).

This current uncertainty has a minor impact (less than 2 percent) on the primordial ^{4}He yield (a thorough analysis of current uncertainties of BBN yields is made by Krauss and Romanelli 1990, and Olive et al. 1990).

4.3. Comparison with Observations: Constraints on Physics and Cosmology

The primordial yields of a recent BBN calculation shown in Fig. 8 as a function of η are compared to abundances inferred from observations (to be analyzed below). An impressive agreement between theory and observation is obtained, covering more than 9 orders of magnitude in abundances for a relatively narrow range in η! This agreement constitutes one of the triumphs of the standard Big Bang model, arguing strongly for its validity, and suggesting that primordial abundances could be used to constrain poorly known cosmological (η, Ω_B) and physical (N_ν) parameters (Yang et al. 1984, Schramm 1990), as well as the models of the chemical evolution of our galaxy (Audouze 1986).

Before, however, turning to the use of BBN as a "probe" of cosmology and particle physics, we should briefly mention some of the difficulties associated to the obsevational determination of primordial abundances (see also Boesgaard and Steigman 1985, and Arnould and Forestini 1989). Indeed, the relationship of the BBN yields (produced $\sim 10^9$ yr before the first stars were formed) to the light element abundances that we observe today [either in the interstellar medium (age $\sim$0), the solar system (age $\sim 4.5 \times 10^9$ yr), or the oldest stars (age$\sim 10^{10}$ yr)], is not a trivial one. Several astrophysical processes may indeed have affected (and they certainly did!) the light element abundances during stellar and galactic evolution.

The abundance of deuterium has been determined in solar system studies (meteorites, solar wind, Jupiter's atmosphere) and by UV absorption studies of the local interstellar medium (ISM). A firm lower limit D/H$>10^{-5}$ has been established for the deuterium/hydrogen ratio (by number). D is a very fragile nucleus, easily destroyed by D(p,γ)^{3}He at temperatures as low as $T \sim 5 \times 10^5$ K, i.e. during stellar formation. Because of that fragility, no astrophysical site seems able to produce substantial D amounts. Its observed abundance is then a firm lower limit to the primordial one: $(\mathrm{D/H})_p > 10^{-5}$, and allows to put a firm upper limit to $\eta < 10^{-9}$. Because of its fragility, D cannot be used to constrain η from below.

The abundance of ^{3}He has been measured in solar system samples (meteorites, solar wind). Since D was burned to ^{3}He during the formation of the Sun, those measurements represent the sum of D+^{3}He: $[(\mathrm{D}+^3\mathrm{He})/\mathrm{H}]_{pre-\odot} \sim 4 \times 10^{-5}$. On the other hand, measurements in galactic HII (ionised hydrogen) regions give $^3\mathrm{He/H} \sim (1-15) \times 10^{-5}$, which means that ^{3}He has been produced during galactic evolution. ^{3}He is indeed synthesized in stars by D(p,γ)^{3}He, but it is also transformed into ^{4}He at temperatures $T > 7 \times 10^6$ K. Its *net yield* is positive for relatively low-mass stars (i.e. $M < 2-5\,M_\odot$), and negative for more massive ones, where it is destroyed by a (difficult to evaluate) factor $f \sim 2-4$ (the upper bound being rather extreme; stars destroying their initial ^{3}He by that large amount would overproduce ^{4}He and metals during galactic evolution). With those arguments, the inequality

$$(\frac{D+{}^3He}{H})_p < (\frac{D}{H})_{pre-\odot} + f(\frac{{}^3He}{H})_{pre-\odot} = f(\frac{D+{}^3He}{H})_{pre-\odot} + (1-f)(\frac{D}{H})_{pre-\odot} \quad (4.9)$$

can be established. Then, the pre-solar abundances of D and D+^{3}He can be used to derive an

upper bound to primordial $[(D+^3He)/H]_p < (8 \text{ to } 13) \times 10^{-5}$ for $f = (2 \text{ to } 4)$, which leads to a lower bound for $\eta > (4 \text{ to } 3) \times 10^{-10}$.

The situation is much more complicated for ^{7}Li which is also very fragile and destroyed at $T \sim 10^6$ K, i.e. in the inner, convective, regions of young stars. The difficulty lies in the fact that it can also be produced to various extents in several astrophysical sites [i.e. spallation reactions in cosmic rays, nova explosions, or red giant stars in the asymptotic giant branch phase]. Young (population I) stars have an abundance of ^{7}Li/H$\sim 10^{-9}$, while old (population II) stars have ^{7}Li/H$\sim 10^{-10}$ (as discovered by Spite and Spite 1982), and it seems natural to admit that the pop II lower abundance is closer to the primordial one. However, ^{7}Li can be easily destroyed at the base of the convective envelope of the lowest mass stars, and this could have been the case for the old and low mass pop II stars, which might then have been born with more ^{7}Li than presently observed at their surfaces. Recent (and intense!) observational and theoretical activity on that topic (e.g. Rebolo et al. 1988, Deliyannis et al. 1990) now favors the former and more natural interpretation, namely that the pop II ^{7}Li/H $\sim (1.4 \pm 0.2) \times 10^{-10}$ abundance is indeed representative of the primordial one. This value is very close to the minimum in the ^{7}Li/H vs. η curve, which allows to put a new, independent, constraint on η from both above and below: $10^{-10} < \eta < 7 \times 10^{-10}$ (taking into account uncertainties on the ^{7}Li production in BBN due to nuclear reaction rates). The combined results for D, ^{3}He and ^{7}Li give then: $4(3) \times 10^{-10} < \eta < 7(10) \times 10^{-10}$ (numbers in parenthesis being more conservative limits), i.e. the baryon to photon ratio is determined to better than 50%!

The current baryonic density parameter: $\Omega_{B,0} = \rho_{B,0}/\rho_{c,0}$ (where $\rho_{c,0} = 3H_0^2/8\pi G$ and $\rho_{B,0} = m_B n_{B,0} = m_B \eta \alpha T_0^3$, since $n_{\gamma,0} = \alpha T_0^3$) is related to the observed quantities $h_0 = H_0/(100 \text{ km/s/Mpc})$ (current expansion rate) and $T_0 \sim 2.73$ K (current CBR temperature) through the baryon/photon ratio η by

$$\Omega_{B,0} = 0.0036\, h_0^{-2}\, (\eta/10^{-10})\, (T_0/2.73)^3 \qquad (4.10)$$

With the current uncertainties on h_0 $(0.5 < h_0 < 1)$ and η $(3 \times 10^{-10} < \eta < 10 \times 10^{-10})$ we obtain $0.01 < \Omega_{B,0} < 0.12$. Thus, primordial nucleosynthesis clearly indicates that *baryons cannot close the Universe* (notice the good agreement between the upper limit on Ω_B obtained from BBN and the one obtained from the rotation curves of galaxies).

Observations of ^{4}He in galactic and extragalactic (metal poor) HII regions are used to determine its primordial abundance. Since ^{4}He is also synthesized in stars by H burning, some of the observed ^{4}He is clearly not primordial. Since stars also produce metals (i.e. nuclides heavier than He nuclei), some correlation should be expected between the abundances (by mass) of He (Y) and metals (Z), i.e. lower Y with lower Z. Such a trend is indeed observed in HII regions between Y and the C, O, or N mass fractions (Fig. 9). Extrapolation to $Z = 0$ then gives the primordial ^{4}He abundance, currently evaluated to lie in the $0.23 < Y_p < 0.24$ range. The Y_p upper limit seems to rule out the possibility of $N_\nu = 4$. The upper limit allowed from BBN is now $N_\nu = 3.4$. This strong cosmological constraint on particle physics (actually, the strongest constraint on N_ν during the 80's) has been recently confirmed by the LEP measurements of the Z^0 width: $N_\nu = 2.96 \pm 0.14$, from the ALEPH, DELPHI, L3 and OPAL collaborations (e.g.

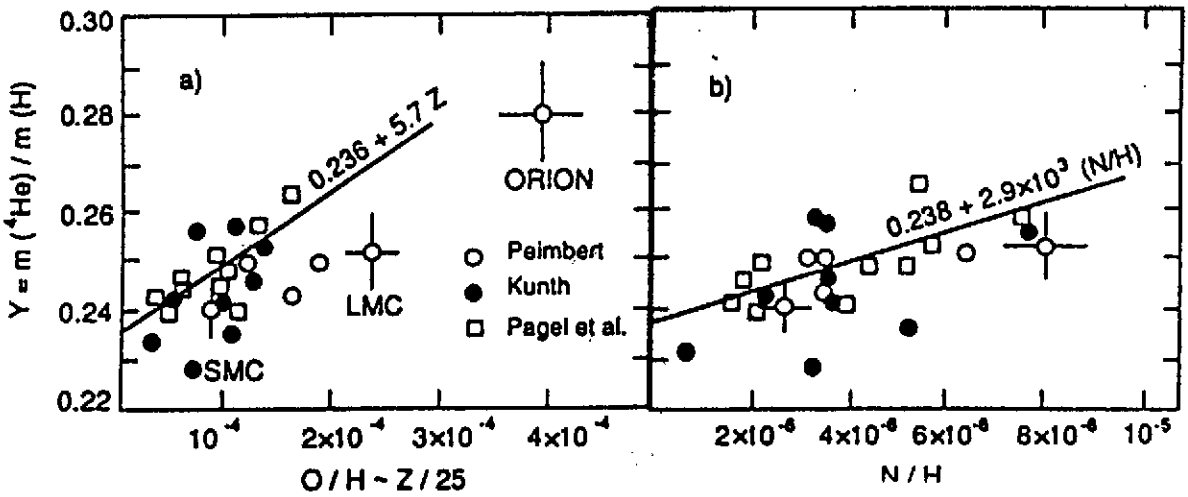

Fig.9. Observations of the ^{4}He abundance in HII regions, as a function of the abundances of O [part a)] and N [part b)]. Extrapolation to zero abundances for O or N allows then to estimate the primordial ^{4}He mass fraction: $0.23 < Y_p < 0.24$.

Schramm 1990). [6]

Finally, notice that if it turns out that $Y_p < 0.225$ or $^7\mathrm{Li/H} < 10^{-10}$, the standard BBN model with $N_\nu = 3$ will be in serious difficulty. In that sense, standard BBN is a falsifiable theory.

A major event following the Big Bang is the formation of galaxies through mechanisms that are far from being fully understood to-day, and the discussion of which goes beyond the scope of these lectures. In fact, we will limit ourselves to a sketch of the way the composition of galaxies changes with time. This formidable problem, commonly referred to as the chemical evolution of galaxies, has indeed to be tackled by nuclear astrophysics.

5. Principles of Stellar Nucleosynthesis and Galactic Chemical Evolution

The way a galaxy evolves chemically is represented in a very sketchy manner in Fig. 10. Let us consider the interstellar medium (ISM) (made of gas and dust) just after galaxy formation. Its composition is assumed to be essentially the one emerging from the Big Bang, the standard model of which just predicts the presence of significant amounts of H, D, ^{3}He, ^{4}He and ^{7}Li (Sect. 4). Part of the ISM material is used to make stars which, through a large variety of nuclear reactions, transform the composition of their constituting material during their evolution. At one point or another during that evolution, some material may be returned to the ISM through

[6] Notice, however, that BBN and LEP are sensitive to different things: LEP counts the number of species with $mc^2 < 45$ GeV coupled to Z, while BBN depends on all *relativistic degrees of freedom* during the Lepton Era, some of which (e.g. a very light Higgsino or photino) might not be coupled to the Z. If ν_τ turns out to be heavy it should not be counted in N_ν, and some place would be left for some other light species. The current experimental mass limit $m_{\nu_\tau} < 35$ MeV does not allow to conclude.

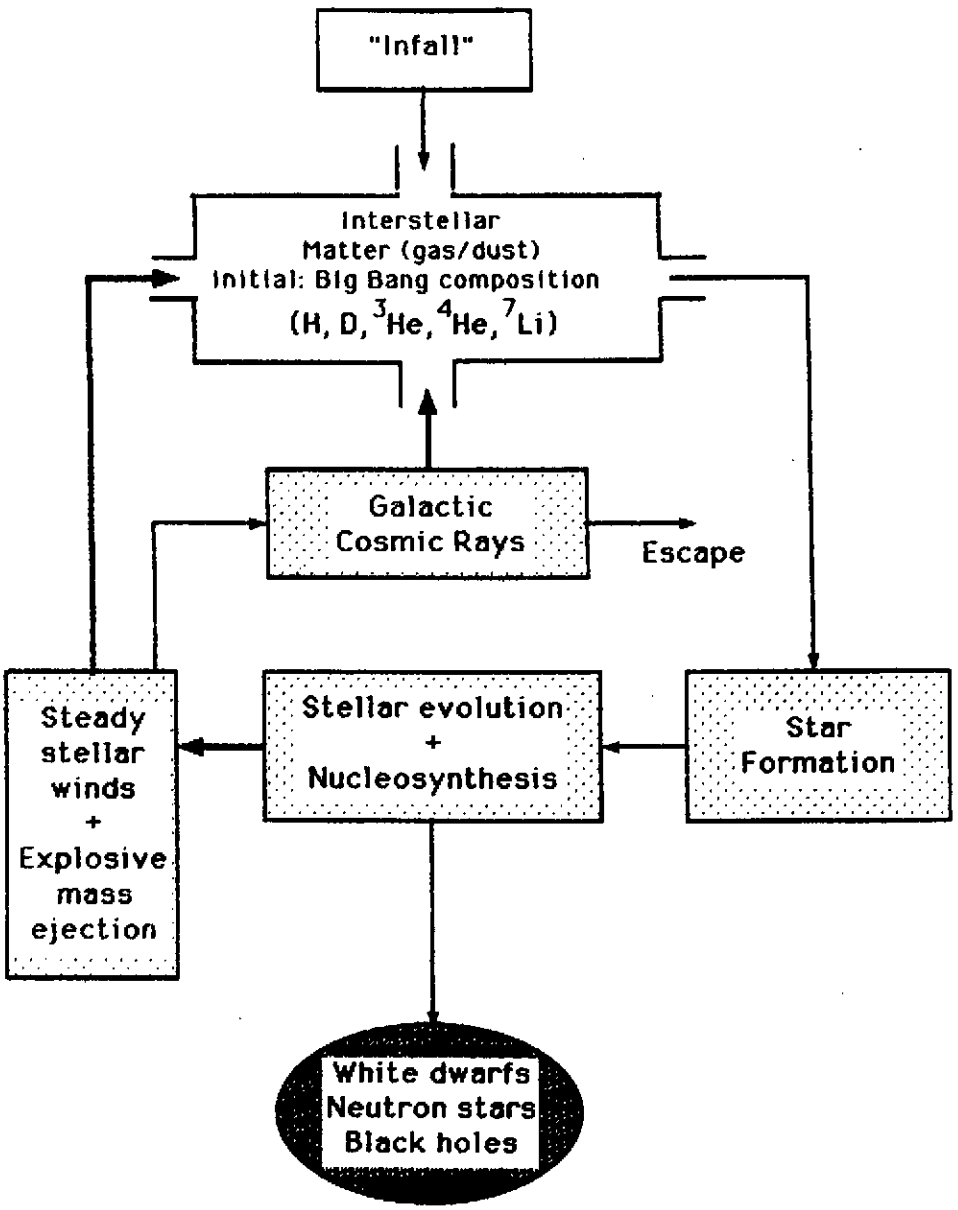

Fig.10. A very schematic picture of the galactic "blender".

various mechanisms (see below). In general, all the stellar material with altered composition is not returned to the ISM. Part is locked up in stellar residues (white dwarfs, neutron stars, or black holes) and normally does not contribute to the subsequent chemical evolution of the galaxies.

Also note that a tiny fraction of the matter ejected by stars can be accelerated to galactic cosmic-ray energies. Those high-energy particles can interact with the ISM material and be responsible through spallation reactions for the ^{6}Li, ^{9}Be, and ^{10}B content of the galaxies, and especially of the disk of our own Galaxy. That mechanism can also produce ^{7}Li and ^{11}B (see e.g. Arnould 1986b, and Arnould and Forestini 1989 for reviews). At least in spiral galaxies like our own, some fraction of the galactic cosmic-ray nuclei might escape the galactic disk. Some part of the supernova ejecta might also be ejected from the disk (this is not sketched in Fig. 10).

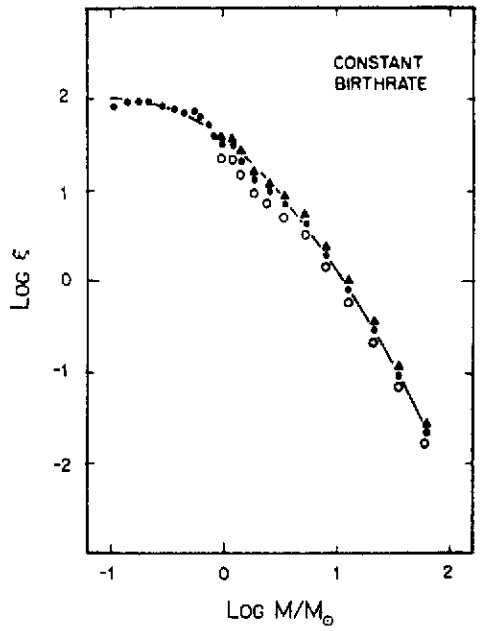

Fig.11. An Initial Mass Function (IMF) relevant to the disk of our Galaxy in the solar neighborhood, assuming that the stellar birthrate is constant in time. The IMF ξ is expressed in stars(parsec)$^{-3}$(log $\frac{M}{M_\odot}$)$^{-1}$ (adapted from Miller and Scalo 1979).

In contrast, some material, possibly of Big Bang composition, might infall on the galactic disc from the galactic halo, and "dilute" the material processed by stars.

One basic ingredient of the models for the chemical evolution of the galaxies is the stellar creation function, that is the number of stars born per unit area of the galactic disk (in spiral galaxies) per unit mass range and unit time interval. That question has been discussed at length by e.g. Scalo (1986). As supported to a large extent by phenomenological considerations, and also for obvious reasons of modelling facilities, it is generally assumed that the stellar creation function is separable into a function of time only (the stellar birthrate, which, in the neighborhood of the Sun at least, is found not to vary widely with time), and a function of mass only, referred to as the *Initial Mass Function* (IMF). An IMF constructed in such a way from observational data is represented in Fig. 11. The main result of such a study is that, in the solar neighborhood at least, but also in more general situations, the IMF is more or less steeply decreasing with increasing stellar mass, at least in the $M \gtrsim M_\odot$ range.

Another main ingredient of the galactic chemical evolution problem is the *mass and composition of the matter ejected by a star with a given initial mass.* That quantity is referred to as the stellar *yields.* Its evaluation requires the modelling of the evolution of stars with initial masses in a broad range of values (essentially between $1M_\odot$ and $100M_\odot$), as well as of the concomitant nucleosynthesis. A detailed discussion of that question can be found in the following textbooks or review articles: Cox and Giuli (1968), Sugimoto and Nomoto (1980), Arnould (1980), Clayton (1983), Iben and Renzini (1983), Bowers and Deeming (1984), Chiosi and Maeder (1986), Nomoto and Hashimoto (1988).

In short, and as pictured very schematically in Fig. 12, the evolution of the central regions

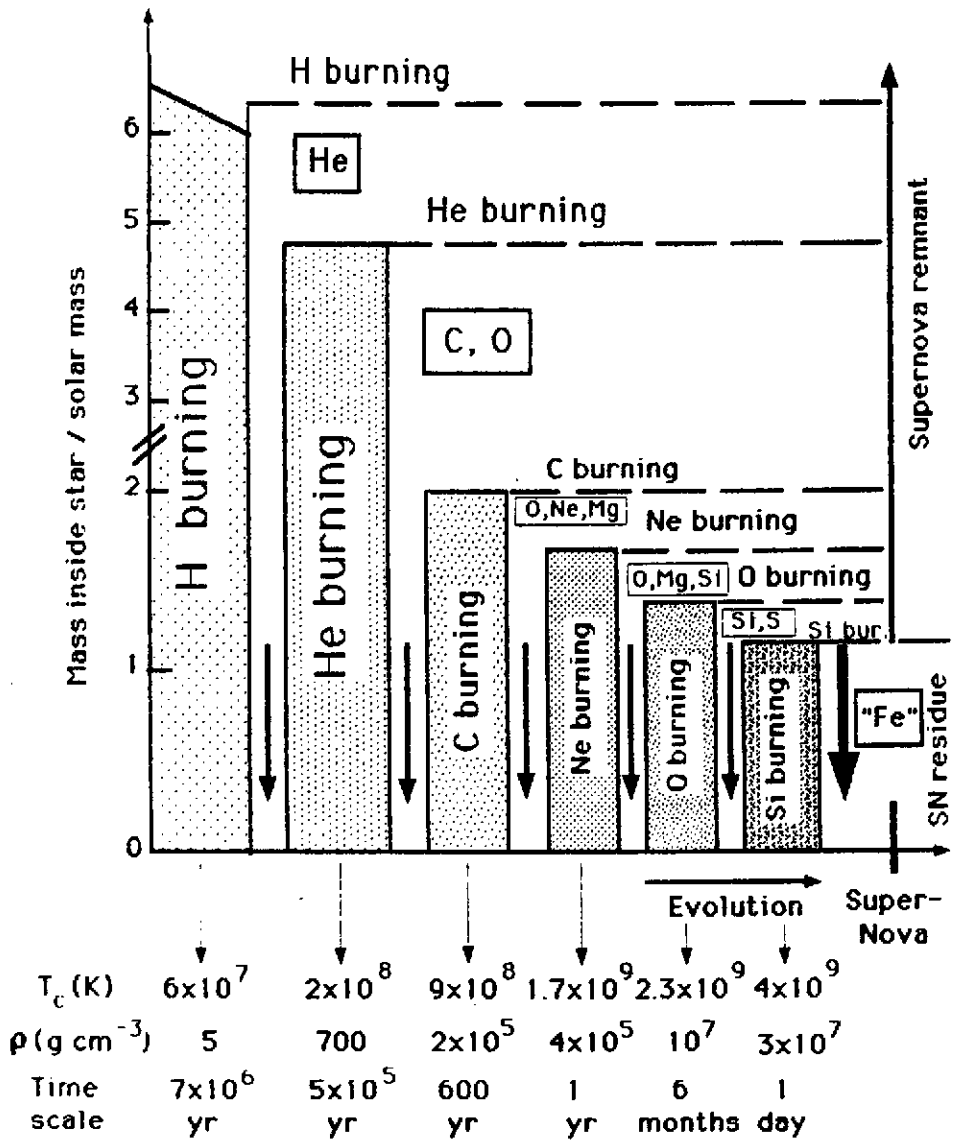

Fig.12. Schematic representation of the evolution of the internal structure of a $M = 25M_\odot$ star. The hatched zones correspond to nuclear burning stages. A given burning phase starts in the central regions, and then migrates into thin peripheral burning shells. In between central nuclear burning phases are episodes of gravitational contraction (downward arrows). The chemical symbols represent the most abundant nuclear species left after a given nuclear burning mode ("Fe" symbolizes the iron peak nuclei, with $50 \lesssim A \lesssim 60$). If the star explodes as a (Type II) supernova, the most central parts may leave a "residue", while the rest of the stellar material is ejected into the ISM, where it is observed as a supernova "remnant".

of a star is made of successive "controlled" thermonuclear burning stages and of phases of gravitational contraction. The latter phases are responsible for a temperature increase, while the former ones produce nuclear energy and lead to composition changes. The sequence of nuclear burning stages is discussed in greater detail in Sect. 6. Let us simply emphasize here that such a sequence develops in time with nuclear fuels of ever increasing charge number Z, and at temperatures increasing from several 10^6 K to about 4×10^9 K. Concomitantly, the duration of the successive nuclear burning phases decreases dramatically. In fact, all those general trends are quite intimately correlated.

Figure 12 also depicts schematically that a nuclear burning phase, once completed in the central regions, migrates into a thin peripheral shell. As a consequence, the deep stellar regions look like an onion with various "skins" of different compositions. In fact all stars do not necessarily experience all the burning phases displayed in Fig. 12: while massive ($M \gtrsim 10 M_{\odot}$) stars go through all these burning episodes, lower mass stars stop their nuclear history after completion of central He burning.

If a star can go through all the burning phases of Fig. 12, it is seen to develop an iron core that is lacking further nuclear fuels. In fact it becomes dynamically unstable and implodes. Through a very complex chain of physical events, that implosion can, in certain cases at least, turn into a catastrophic supernova explosion referred to as a Type II supernova. [7] That explosion is accompanied by the ejection into the ISM of a substantial fraction of the star to form a so-called supernova remnant. In the adopted picture, the whole of the stellar mass is not returned to the ISM. The innermost parts are bound into a so-called residue, which may be a neutron star (observable as a pulsar if it is magnetized and rapidly rotating), or even a black hole. If a general consensus has been reached on the description of massive star explosions sketched above, many very complicated astrophysics and nuclear physics questions still require much work. The interested reader can find details about the physics of Type II supernovae in e.g. Trimble (1982, 1983), Woosley (1986), Woosley and Weaver (1986), or Schaeffer (this volume).

The Type II supernova explosions described above are not the only way for stars to return material to the ISM. In particular, various stars (especially Red Giants, or hot O-type and Wolf-Rayet stars) are observed to suffer steady (non-explosive) stellar winds. Planetary nebula ejections also contribute to the recycling of material into the ISM. The dominant mechanism(s) for the restitution of matter to the ISM is(are) depicted schematically in Fig. 13 as a function of the initial stellar mass. The fraction of this mass that is ejected is also shown.

Nothing has been said up to now on the evolution of stars in binary systems. The effects of a binary companion on the evolution of a star are complicated and far from being fully explored. However, as a substantial fraction (perhaps $\gtrsim 50\%$) of all stars belong to binary systems, such questions are of great importance. In fact, many different types of observed astronomical events are now interpreted in terms of phenomena occurring in binary systems. It is beyond the scope of these lectures to examine such questions in detail (see e.g. Thomas 1977, de Loore 1980, Sugimoto and Nomoto 1980, Nomoto 1986, Woosley 1986, and references therein). Let us just emphasize that one of the most important characteristics of the evolution of binary systems is the existence of episodes during which matter is transferred from one component to the other. Several very interesting phenomena may be connected to such mass exchanges. In particular, various instabilities of nuclear origin may develop in the transferred material at the surface of the accreting component. In addition to such "surface" effects, the very evolution of the two stars is also affected, the bulk stability of one of them being even possibly threatened by the eventual development of various instabilities. As a result, binary systems may return material

[7] Type II supernovae are defined as those showing hydrogen lines in their spectra. It is likely that most, if not all, of the exploding massive stars still have some hydrogen envelope left, and thus exhibit such a feature

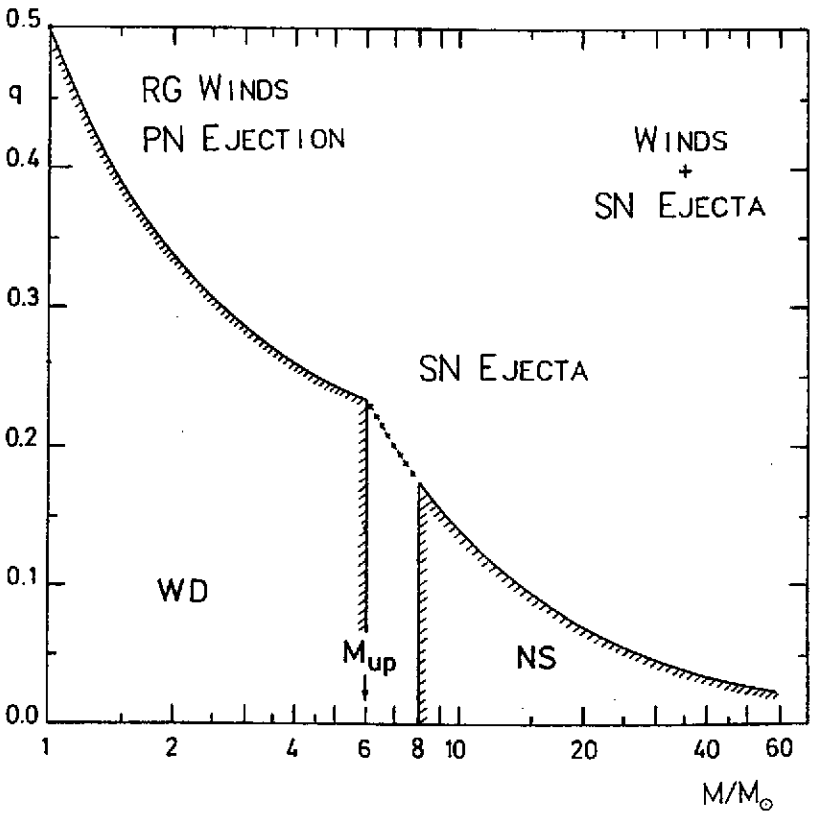

Fig.13. Schematic representation of the fraction q of the initial mass M of a single star that remains bound in a white dwarf (WD) or neutron star (NS) residue at the end of its evolution. The rest of the stellar material is ejected mostly by the indicated mechanisms. Stars with initial masses up to Mup are assumed to end their lives as WD, while those with $M \gtrsim 8M_\odot$ are considered to leave a $1.4M_\odot$ NS. In the remaining $M_{up} \lesssim M \lesssim 8M_\odot$ range, stars might explode without leaving a residue. This overall picture is still affected by various uncertainties.

to the ISM through non-explosive events, or even (Type I) [8] supernova explosions. They thus play a specific and important role in the chemical evolution of galaxies.

In order to model the chemical evolution of galaxies, the precise composition of the material returned from stars to the ISM by the various mechanisms mentioned above remains to be evaluated. This requires a detailed study of the nucleosynthesis accompanying stellar evolution. That question is examined in Sects. 6 and 8.

6. Stellar Nuclear Reactions up to the Fe peak

We very briefly review here some chains of reactions that play an important role in the energy generation or in the nucleosynthesis up to the iron peak nuclides during the non-explosive or explosive phases of stellar evolution. Reactions of importance for the production of heavier nuclides are discussed in Sect. 8.

[8] Type I supernovae are defined as those lacking hydrogen lines in their observed spectra. Various subtypes of this class of objects are known to exist. The explosion of accreting white dwarfs in binary systems is most commonly related to Type Ia supernovae

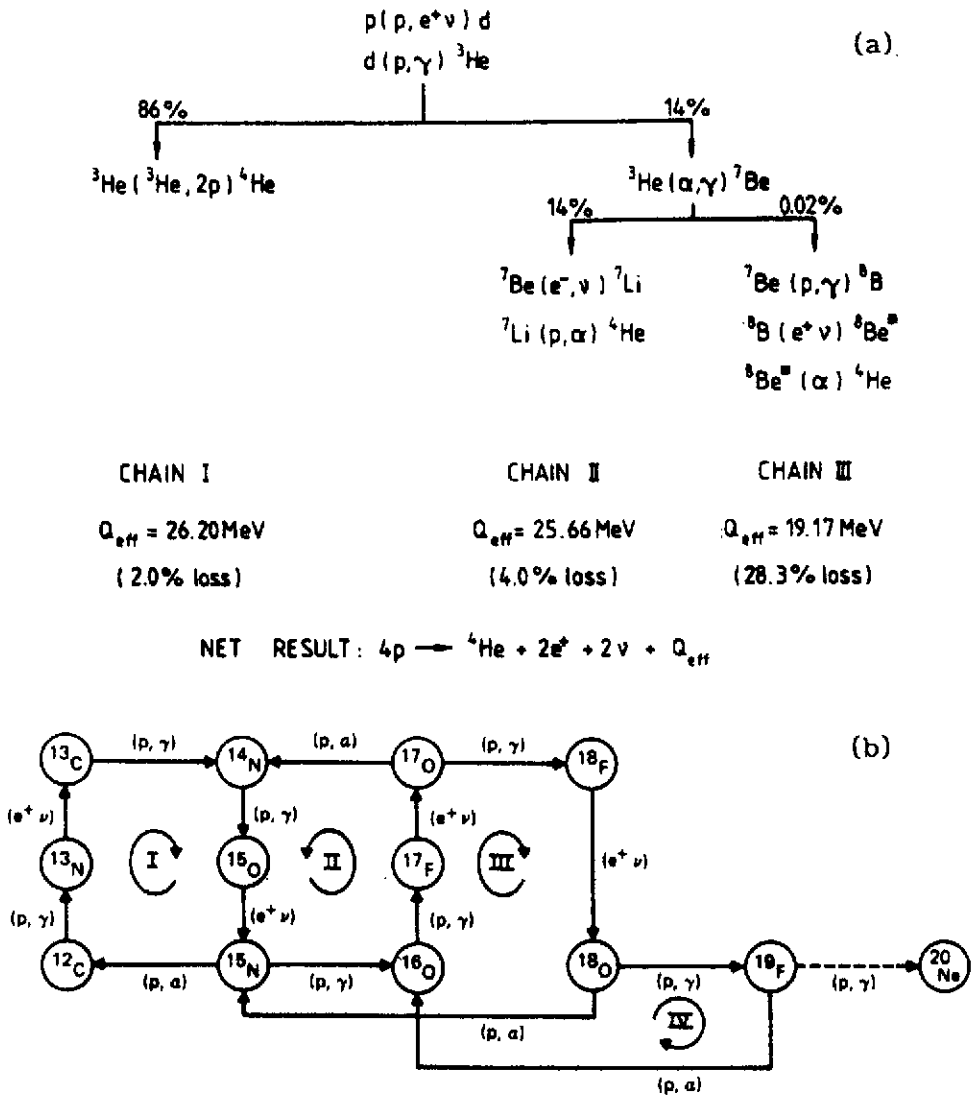

Fig.14. The major non-explosive H-burning modes (from Rolfs and Rodney 1988): (a) reactions of the p-p chains. They develop at $T \gtrsim 10^6$ K, and have the main effect of transforming H into ^{4}He. The Q_{eff} values include the loss of energy by the escaping neutrinos; (b) reactions of the cold CNO cycles. They develop at $T \gtrsim 10^7$ K. Their main role is the transformation of H into ^{4}He, and of most of the initial C, N and O nuclei into ^{14}N.

6.1. The Various H-burning Modes in Non-explosive Situations

In non-explosive stellar environments, H burns essentially through the so-called "cold" p-p chains or CNO cycles, which involve the reactions displayed in Fig. 14. The relative importance of those two modes as far as the energy production is concerned depends upon the stellar mass and the initial composition. Details about this, and other astrophysics or nuclear physics aspects of the cold p-p chain and CNO cycles can be found in many places (e.g. Rolfs and Rodney 1988), and need not be repeated here. Let us simply recall that the rates of several of the reactions involved are still somewhat uncertain, and may affect various predictions [as in the famed solar neutrino problem (e.g. Turck-Chièze et al. 1988; Bahcall and Ulrich 1988, and references therein)]. Independent of those uncertainties, the main nucleosynthetic role of the p-p

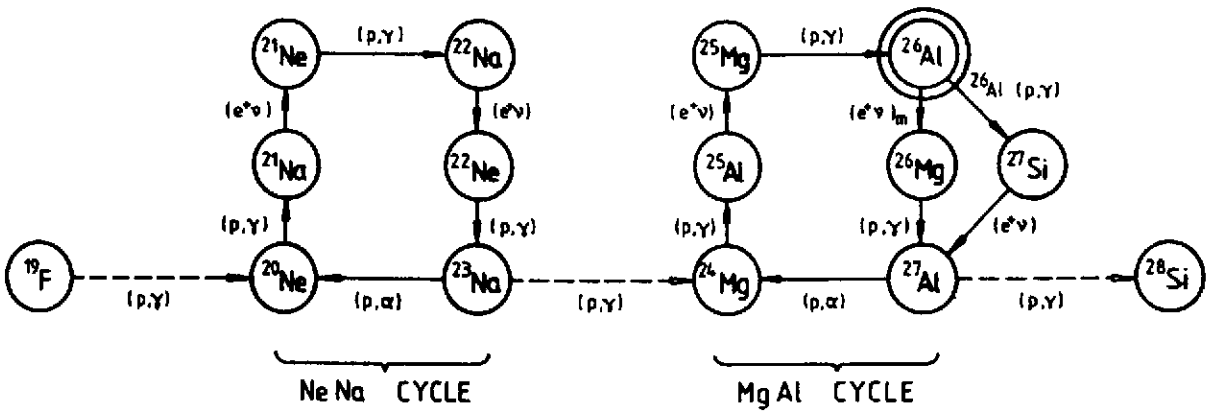

Fig.15. Reactions involved in the cold NeNa and MgAl chains. They develop mainly at $T \gtrsim (2-3) \times 10^7$ K (from Rolfs and Rodney 1988).

and CNO reactions is the transformation of H into ^{4}He. An additional effect of the CNO cycles is the transformation of almost all of the initial C,N,O content of the burning regions into ^{14}N.

Some hydrogen can also be consumed through the cold NeNa and MgAl cycles displayed in Fig. 15. Those burning modes most likely play a minor role in the stellar energy budget. In contrast, they are of importance in the synthesis of Na or Al, as well as of the Ne and Mg isotopes, especially in massive stars (e.g. Prantzos et al. 1986, Rolfs and Rodney 1988). Most importantly, the MgAl chain might also synthesize ^{26}Al, which is a very interesting radionuclide, as briefly mentioned in Sect. 6.2.2.

Many nuclear physics uncertainties still affect the nucleosynthesis predictions relating to the NeNa and MgAl chains, as reviewed in e.g. Arnould (1985), or Rolfs et al. (1987) [see also Iliadis et al. (1989) for recent experimental data concerning some reactions of the MgAl chain, and some of their nucleosynthetic consequences].

6.2. Explosive Hydrogen Burning

Hydrogen burning can also take place explosively in a variety of sites related in particular to the accretion of H-rich material on compact objects (white dwarfs, or even neutron stars), or in dynamically unstable supermassive ($M \gtrsim 10^4 M_\odot$) stars, the very existence of which is still speculative (for reviews of explosive H-burning sites, see e.g. Arnould 1980, Wallace and Woosley 1981, Woosley 1986).

As already emphasized previously, a given nuclear fuel burns explosively at temperatures that are typically higher than those characterizing the non-explosive combustion. As a result of those higher temperatures, charged particle, and especially proton captures on unstable nuclei can compete more and more successfully with their decay. This situation results from the high temperature sensitivity of the charged particle reactions, while the relevant (β^+)-decays are essentially temperature independent. The "hot" p-p, CNO or NeNa-MgAl chains, as well as the so-called rp- or αp-processes then replace the cold modes, the switching temperatures depending of course on the rates of proton and α-captures by key unstable nuclei. The precise characterization of the H-burning modes thus requires a reliable knowledge of these rates. We briefly identify and discuss below some of the important reactions involved in the hot H-burning

Region	Chain/Process	Reaction Sequence
A	*pp*-III	$^7Be(p, \gamma)^8B(\beta^+\nu)^8Be(\alpha)^4He$
	pp-IV	$^7Be(p, \gamma)^8B(p, \gamma)^9C(\beta^+\nu)^9B(p)^8Be(\alpha)^4He$
B	*pp*-II	$^7Be(e^-, \nu)^7Li(p, \alpha)^4He$
C	*pp*-V	$^7Be(\alpha, \gamma)^{11}C(\beta^+\nu)^{11}B(p, 2\alpha)^4He$
D	rap-I	$^7Be(p, \gamma)^8B(p, \gamma)^9C(\alpha, p)^{12}N(p, \gamma)^{13}O(\beta^+\nu)^{13}N(p, \gamma)^{14}O$
	rap-II	$^7Be(\alpha, \gamma)^{11}C(p, \gamma)^{12}N(p, \gamma)^{13}O(\beta^+\nu)^{13}N(p, \gamma)^{14}O$
	rap-III	$^7Be(\alpha, \gamma)^{11}C(p, \gamma)^{12}N(\beta^+\nu)^{12}C(p, \gamma)^{13}N(p, \gamma)^{14}O$
E	rap-IV	$^7Be(\alpha, \gamma)^{11}C(\alpha, p)^{14}N(p, \gamma)^{15}O$
F	rp	$^{14}O(\alpha, p)^{17}F(p, \gamma)^{18}Ne(\beta^+\nu)^{18}F(p, \alpha)^{15}O$
		$^{15}O(\alpha, \gamma)^{19}Ne(p, \gamma)^{20}Na$

Fig.16. Reactions of the hot pp-chain that are dominant in the regions of the $T - \rho$ plane delineated in Fig. 17 (from Wiescher et al. 1989).

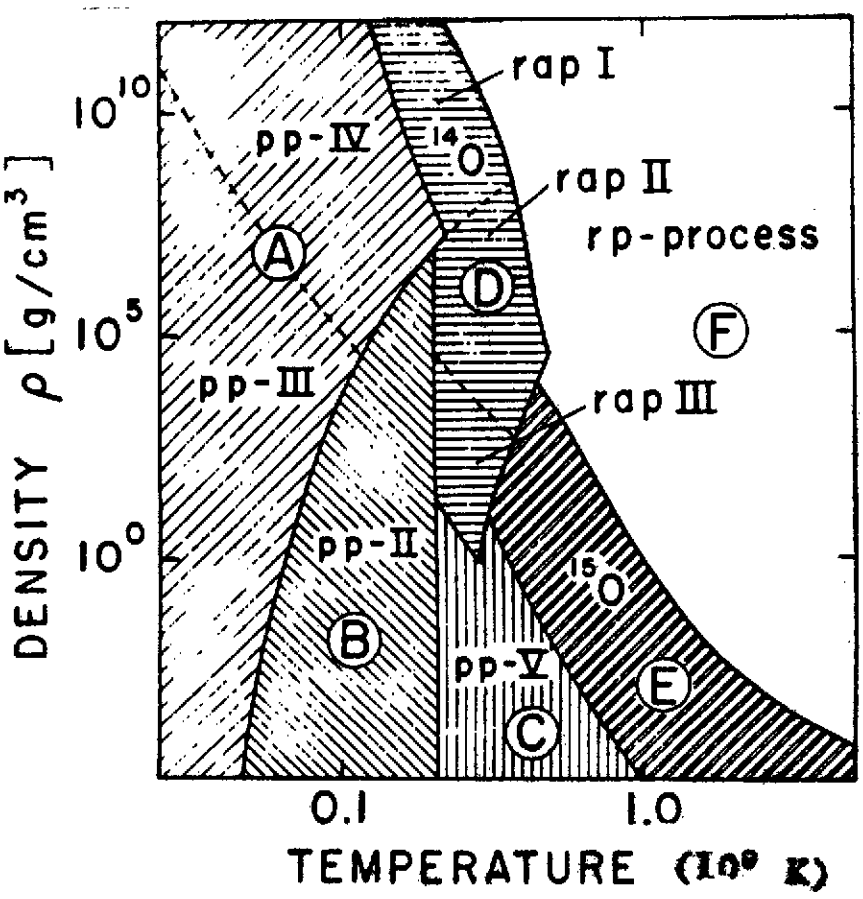

Fig.17. Temperature and density conditions at which the different hot pp-chains of Fig. 16 are expected to operate (see Wiescher et al. 1989 for the criteria used in this delineation).

modes.

6.2.1. The hot p-p mode. As discussed by Arnould and Nørgaard (1975) and, more recently, by Wiescher et al. (1989), the classical p-p chains can switch to the hot p-p mode when $^{8}B(p,\gamma)$ or $^{8}B(\gamma,p)$ become more rapid than the ^{8}B β-decay. The transformation into the hot p-p chain can also occur when $^{7}Be(\alpha,\gamma)^{11}C$ becomes more rapid than the ^{7}Be proton capture, thus bypassing the formation of ^{8}B. In fact, a variety of hot p-p reaction chains have been identified (Fig. 16). Their development and relative importance depend on the precise temperature and density conditions, as illustrated in Fig. 17.

One or another of the hot p-p chains of reactions could develop in (the still putative) "pre-galactic" stars supposed to be made just of the ashes of the Big Bang nucleosynthesis (e.g. Wiescher et al. 1989). The last decade has seen an increased interest for the modelling of these objects, their existence, evolution and fate being indeed very important in a variety of interesting astrophysical questions. A satisfactory answer to these problems requires in particular a reliable evaluation of the nuclear energy production in these stars, and more specifically the determination of the relative contribution of the hot p-p chains and of the classical 3α He-burning reactions (Sect. 6.3) to the production of ^{12}C.

Some hot p-p reaction patterns could also develop in classical nova explosions resulting from the accretion of material on a white dwarf star. These reactions could possibly allow certain novae to produce substantial amounts of ^{7}Li and ^{11}B (Arnould and Nørgaard 1975).

Reliable conclusions concerning the possible development of one or another of the hot p-p chains of reactions, as well as precise evaluations of the yields of the hot p-p chains in realistic astrophysical situations are hampered by the large uncertainties still affecting many of the potentially important reactions displayed in Fig. 16, and in particular those on unstable nuclei, such as $^{7}Be(p,\gamma)^{8}B$, $^{8}B(p,\gamma)^{9}C$, $^{11}C(p,\gamma)^{12}N$, $^{12}N(p,\gamma)^{13}O$, $^{13}N(p,\gamma)^{14}O$, $^{7}Be(\alpha,\gamma)^{11}C$, or $^{9}C(\alpha,p)^{12}N$. The re-evaluations based on nuclear structure data or on microscopic models proposed recently for the rates of some of these reactions (e.g. Buchmann et al. 1988; Wiescher et al. 1989; Descouvemont 1989a) differ sometimes widely from one another. On the other hand, direct measurements have already been conducted for $^{7}Be(p,\gamma)^{8}B$, and are hoped to be performed for $^{13}N(p,\gamma)^{14}O$ in a near future (see Sect. 6.2.2). Further laboratory work, and especially direct determinations using radioactive ion beam facilities, would obviously be most welcome.

6.2.2. The hot CNO and NeNa-MgAl chains. As discussed in many places (e.g. Audouze et al. 1973; Arnould and Beelen 1974; Wallace and Woosley 1981; Rolfs and Rodney 1988), a major change in the cold CNO cycle occurs when $^{13}N(p,\gamma)^{14}O$ becomes more rapid than the ^{13}N β-decay. In such a case, a hot CNO cycle (Fig. 18) is initiated. Figure 19 provides the switching conditions from the cold to the hot mode, their precise values depending of course upon the still uncertain ^{13}N proton capture rate. Up to now, this rate has been derived from indirect experiments (Wang et al. 1988; Aguer et al. 1989; Fernandez et al. 1989) and from various theoretical estimates (e.g. Descouvemont and Baye 1989). A direct $^{13}N(p,\gamma)^{14}O$ measurement is called for, and, as already said before, is hoped to be obtained in a near future through the development of a radioactive beam facility at Louvain-la-Neuve (Delbar et al. 1988; Darquennes

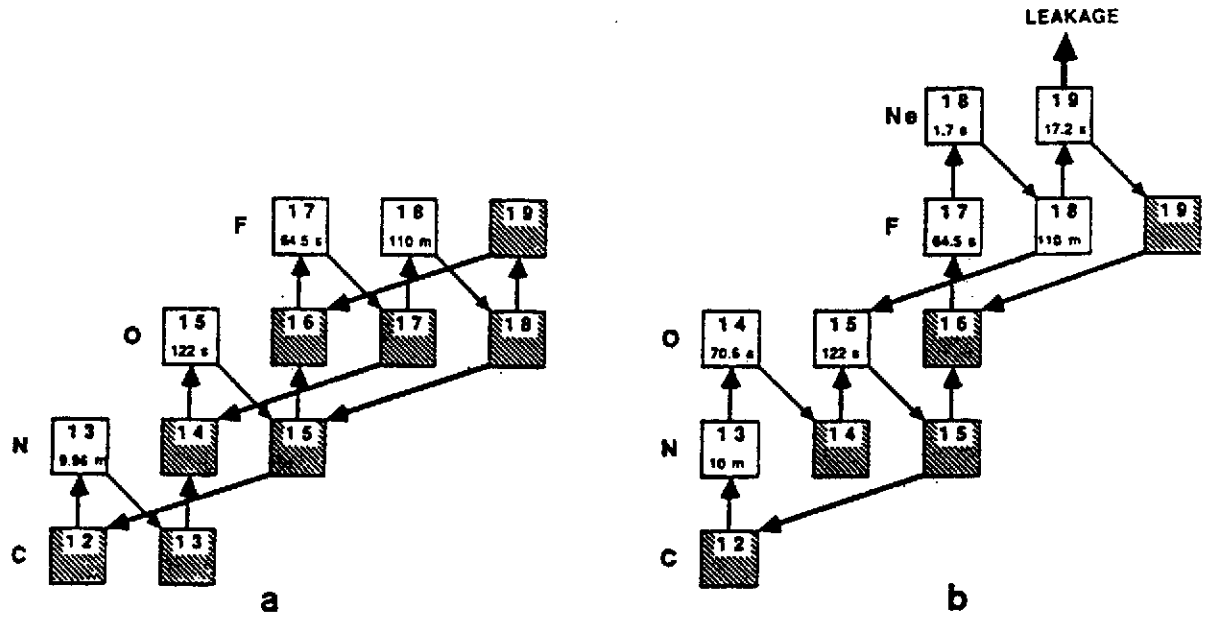

Fig.18. Comparison between the important reactions of (a) the cold CNO cycle [see also Fig. 14(b)], and (b) of the hot CNO chains (from Rolfs et al. 1989).

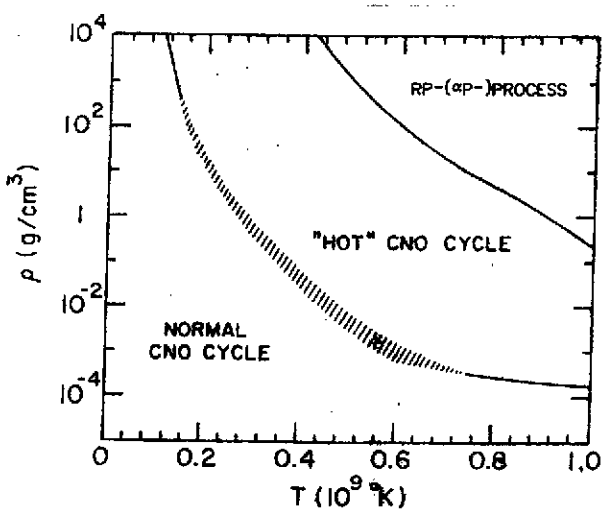

Fig.19. Temperature - density conditions delineating the operation of the cold CNO cycles, the hot CNO chains, and the rp- (or $\alpha p-$) process. The boundary between the cold and hot CNO modes is constructed from the equality between the proton capture rates on ^{13}N or ^{14}N (whichever is smaller) and the sum of the ^{14}O and ^{15}O $\beta-$decay rates, the cross- hatched zone representing the effect of uncertainties in the ^{13}N(p,γ) rate (from Fernandez et al. 1989). The switching from the hot CNO chain to the rp- (or $\alpha p-$) process occurs when ^{15}O(α,γ) or ^{14}O(α,p) becomes faster than the $\beta-$decay of ^{15}O or ^{14}O, respectively, whichever occurs first (from Wiescher et al. 1987).

et al. 1990).

Other proton captures on unstable species are involved in the hot CNO cycle: ^{17}F(p,γ)^{18}Ne (Wiescher et al. 1988), ^{18}F(p,γ)^{19}Ne, ^{18}F(p,α)^{15}O (Wiescher and Kettner 1982), or ^{19}Ne(p,γ)

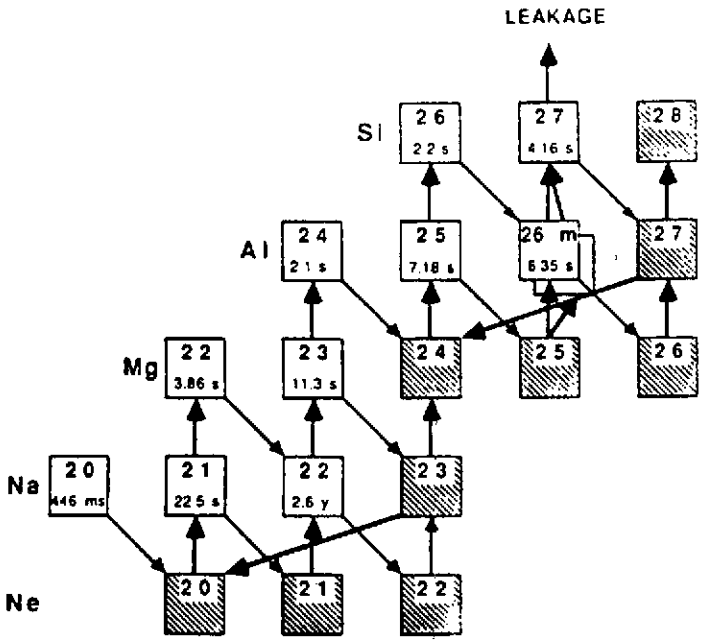

Fig.20. Important reactions of the hot NeNa and MgAl chains (from Rolfs et al. 1989).

^{20}Na [e.g. Kubono et al. (1989), and references therein]. The latter transformation can be responsible for a leakage out of the CNO region to higher masses (see below). The rates of all these reactions are still uncertain.

The cold NeNa and MgAl chains of reactions (Fig. 15) could switch into the hot burning modes in temperature conditions that appear to be quite similar to the operating conditions for the hot CNO chain [e.g. Audouze et al. 1973; Arnould and Beelen 1974; Arnould et al. 1980; Wallace and Woosley 1981; Wiescher et al. 1986). As seen in Fig. 20, it involves many important proton captures on unstable nuclei, like ^{20}Na(p,γ)^{21}Mg, ^{21}Na(p,γ)^{22}Mg, ^{22}Na(p,γ)^{23}Mg, ^{22}Mg(p,γ)^{23}Al, ^{23}Mg(p,γ)^{24}Al, ^{25}Al(p,γ)^{26}Si, ^{26}Al^{g}(p,γ)^{27}Si, ^{26}Al^{m}(p,γ)^{27}Si (where the superscripts g and m refer to the ^{26}Al ground and isomeric states), or ^{27}Si(p,γ)^{28}P, which may be responsible for a leakage out of the Ne to Al mass region. Apart from the proton captures on ^{22}Na (Seuthe et al. 1990) and on ^{26}Al^{g} (Iliadis et al. 1989), the rates of these reactions have never been measured directly, and are evaluated from available spectroscopic information on individual level properties (Wiescher et al. 1986; Wiescher and Langanke 1986; Wiescher et al. 1988a; Kubono et al. 1989). Consequently, they still have to be considered as quite uncertain.

The hot CNO (and hot NeNa-MgAl) mode transforms into the so-called rp- or αp-processes when ^{15}O(α,γ)^{19}Ne or ^{14}O(α,p)^{17}F become more rapid than the corresponding β-decays (e.g. Wallace and Woosley 1981; Woosley 1986). The astrophysical conditions leading to such a switching are illustrated in Fig. 19, the displayed delineation depending of course upon the still quite uncertain α-capture rates on ^{14}O and ^{15}O (Wiescher et al. 1987).

It is expected that the nuclear flow associated with the rp-process can go all the way from the C-N-O region up to, or even slightly beyond, the iron peak through a chain of (p,γ), (γ,p), and (β^{+})-decays (Fig. 21). The leakage out of the C-N-O and the Ne-Na-Mg-Al regions is due in particular to ^{19}Ne(p,γ)^{20}Na and ^{27}Si(p,γ)^{28}P, respectively. With increasing temperatures,

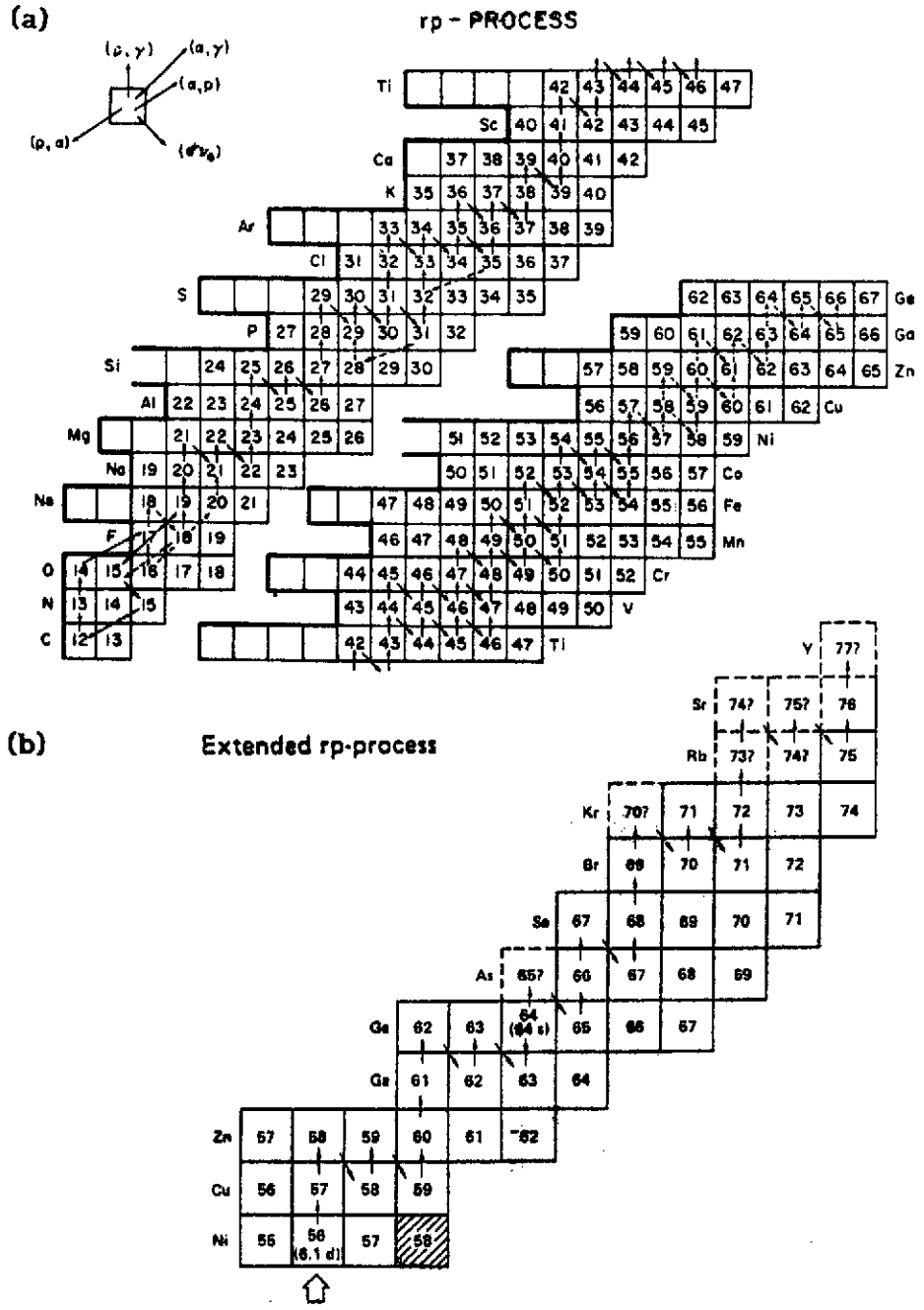

Fig.21. Important reactions of the rp-process: (a) between C and Ge, and (b) above the iron peak nuclei (adapted from Wallace and Woosley 1981, 1984).

(α, p) reactions start playing a more and more important role (e.g. Wallace and Woosley 1981; Wiescher et al. 1987). As seen in Fig. 22, these reactions modify the rp-process path. The rate at which the material can flow from the C-N-O region to heavier species is also affected, as the (α, p) reactions can bypass some relatively slow β-decays. The corresponding reaction pattern has been called the αp-process. In such a case, $^{18}\mathrm{Ne}(\alpha, \mathrm{p})^{21}\mathrm{Na}$ can become the dominant leakage out of the C-N-O region.

The rp- and αp-processes involve a host of reactions on unstable deficient nuclei. Some of these reactions on $A \lesssim 30$ species have already been mentioned above. In the higher mass range,

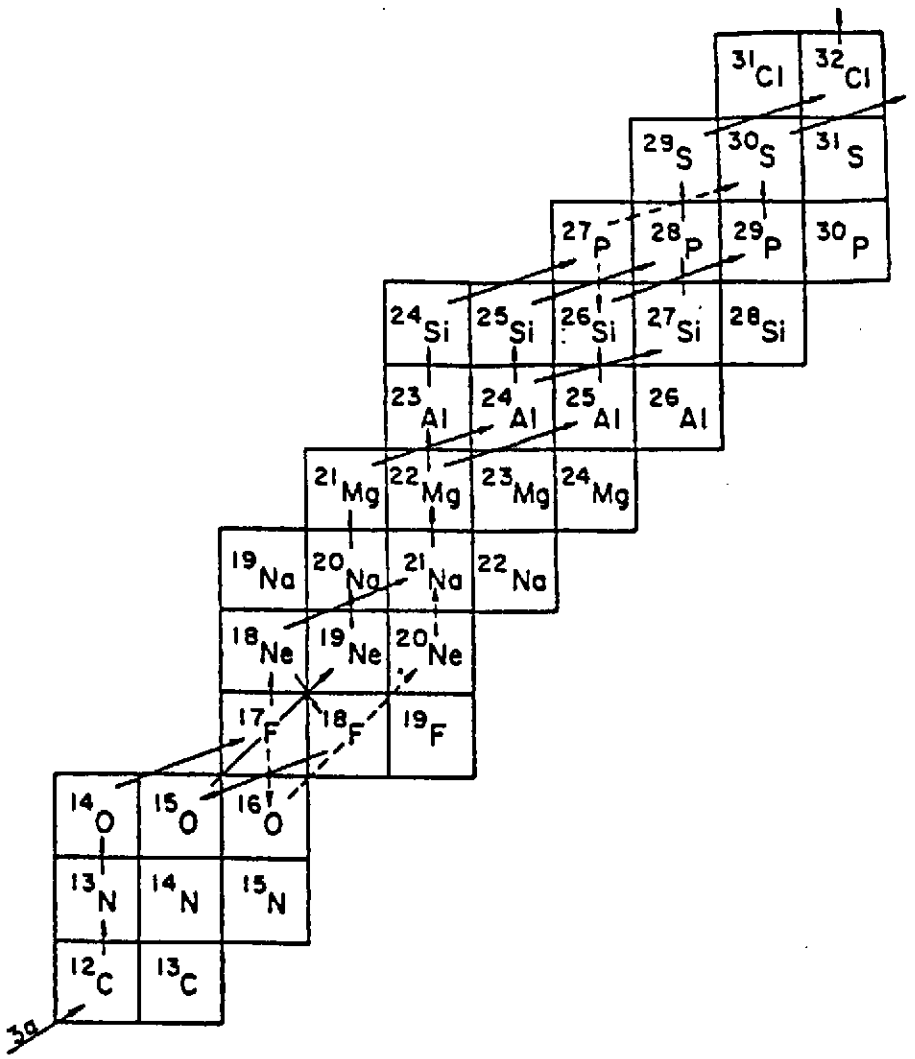

Fig.22. Some important reactions of the αp–process (adapted from Wallace and Woosley 1981).

a limited number of estimates based on individual level properties have been performed (van Wormer et al. 1989; Wiescher and Görres 1989). However, most evaluations rely commonly on a statistical (Hauser-Feshbach) model (e.g. Thielemann et al. 1986a). This procedure appears to be adequate in many cases, particularly in view of relatively high nuclear level densities. In such conditions, the build up of reliable systematics for the key quantities involved in such an approach (such as level density parameters, etc.) would be highly valuable.

Typical astrophysical situations have been identified in which the hot CNO or NeNa-MgAl chains could develop (for a review, see e.g. Woosley 1986). In particular, novae or (still putative) exploding supermassive stars could be such sites. The rp- or αp-process could take place in certain Type I supernovae, or in certain X-ray bursters resulting from the accretion of matter on a neutron star. The modelling of these various objects suffers not only from astrophysical uncertainties, but also from uncertainties related to the poor knowledge of several key reactions involved in the hot H-burning modes of interest. The latter problems have important bearings on the evaluation of the nuclear energy budget, and also of certain nucleosynthetic yields. In the latter respect, and for the sake of illustration, let us emphasize that

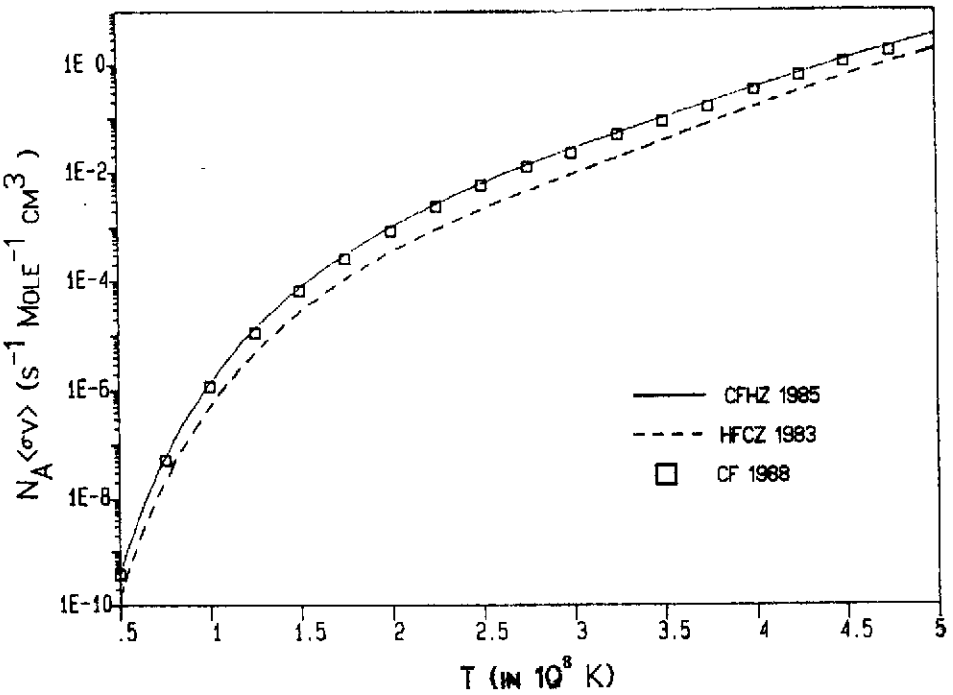

Fig.23. Rates of $^{13}N(p,\gamma)^{14}O$ versus T, as provided by the following compilations: Harris et al. (1983) (HFCZ 1983), Caughlan et al. (1985) (CFHZ 1985), and Caughlan and Fowler (1988) (CF 1988). The true uncertainties on the rate may be larger than the displayed differences.

(i) One of the keys to the hot CNO cycle is $^{13}N(p,\gamma)^{14}O$, the rate of which is still quite uncertain, as discussed above. Figure 23 compares the rates proposed in three recent compilations. It has to be emphasized that the displayed differences between those rates might turn out to be smaller than the true remaining uncertainties. The rate differences exhibited in Fig. 23 translate into uncertainties in the typical temperatures at which the cold CNO cycles switch into the hot CNO cycle, as illustrated partly in Fig. 19. More spectacularly, the uncertainties in the $^{13}N(p,\gamma)^{14}O$ rate are also responsible for poorly reliable predictions of the $^{13}C/^{12}C$ ratio, as displayed in Fig. 24. This is quite unfortunate in view of the now accumulating astrophysical data concerning that abundance ratio in sites where the hot CNO chain is expected to operate, and especially in novae. Other astrophysical situations than the hot CNO cycle have also been identified in which $^{13}N(p,\gamma)^{14}O$ may play an important role (e.g. Jorissen and Arnould 1986, 1989).

(ii) the hot NeNa and the cold or hot MgAl chains could be significant producers of ^{22}Na and ^{26}Al, respectively. These two nuclides are important for γ-ray line astronomy and for cosmochemistry (e.g. Arnould 1985, 1987; Clayton and Leising 1987; Prantzos 1987). More specifically, ^{22}Na is thought to be the progenitor of an extraordinary meteoritic Ne component made virtually of pure ^{22}Ne, and referred to as Ne-E. On the other hand, ^{26}Al has raised much interest following the discovery that it has decayed in situ in various meteoritic inclusions, leading to the observation of a ^{26}Mg excess. The interest for ^{22}Na and ^{26}Al is amplified further by the fact that their β-decays are accompanied with the emission of characteristic γ-ray lines (at 1274 and 1809 keV for ^{22}Na and ^{26}Al, respectively). The ^{26}Al

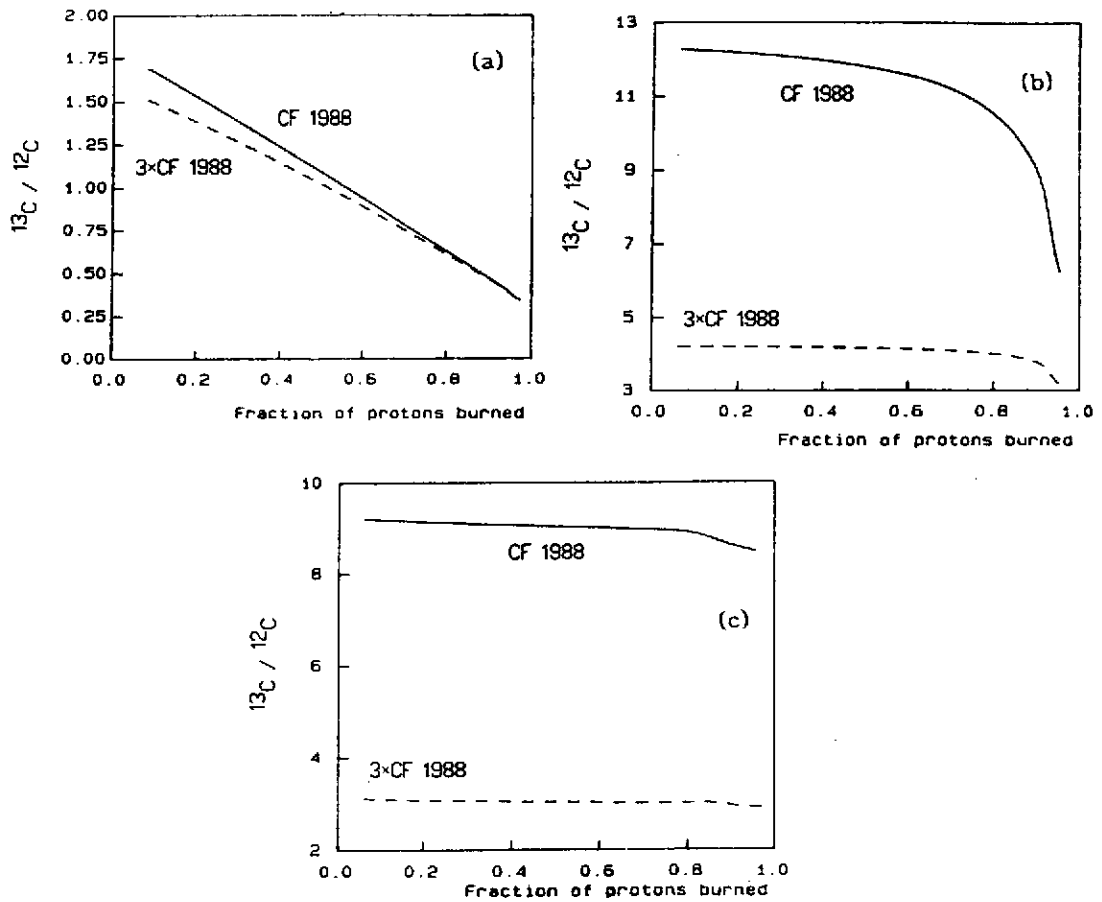

Fig.24. Values of the abundance ratio $^{13}C/^{12}C$ (after complete decay of ^{13}N) resulting from the burning of H in three CNO burning conditions: (a) $T = 8 \times 10^7$ K, (b) $T = 1.4 \times 10^8$ K, and (c) $T = 2 \times 10^8$ K, the density being equal to $10^3 gcm^{-3}$ in all cases. From Fig. 19, cases (b) and (c) are seen to correspond to the hot mode of CNO burning. The computations are performed with the CF 1988 rate for $^{18}N(p,\gamma)^{14}O$ (see Fig. 23), and with a rate which is artificially increased by a factor of 3.

γ-ray line has indeed been observed in the interstellar medium (Mahoney et al. 1984; von Ballmoos et al. 1987), while just an upper limit has been put up to now on the amount of interstellar ^{22}Na (Leising et al. 1988).

The conclusions one can derive about the ability of the hot NeNa and of the cold or hot MgAl chains to account for the meteoritic and γ-ray observations are sensitive to the details of the astrophysical modelling of the appropriate sites (e.g. Arnould 1987), but also to the still uncertain rates of several key reactions on unstable nuclei (e.g. Arnould 1985). Further experimental effort would certainly be of great help in this respect, as are the recent data about the stellar rates of $^{22}Na(p,\gamma)^{23}Mg$ (Seuthe et al. 1990) and $^{26}Al^g(p,\gamma)^{27}Si$ (Iliadis et al. 1989).

6.3. Helium Burning

Non-explosive He burning takes place in stellar layers with temperatures in excess of $\approx 10^8$ K. The calculation of many stellar models (e.g. Iben 1974; Iben and Renzini 1983; Arnett and Thielemann 1985; Chiosi and Maeder 1986; Prantzos et al. 1986; Nomoto and Hashimoto 1988)

Energy generation:

$^4\mathrm{He}(2\alpha,\gamma)^{12}\mathrm{C}(\alpha,\gamma)^{16}\mathrm{O}(\alpha,\gamma)^{20}\mathrm{Ne}$

Neutron source:

$$^{14}\mathrm{N}(\alpha,\gamma)^{18}\mathrm{F}(\beta^+)^{18}\mathrm{O}(\alpha,\gamma)^{22}\mathrm{Ne}\begin{matrix}(\alpha,\gamma)^{26}\mathrm{Mg}\\(\alpha,n)^{25}\mathrm{Mg}\end{matrix}$$

High-temperature burning with effective $^{22}\mathrm{Ne}(\alpha,n)^{25}\mathrm{Mg}$:

$^{22}\mathrm{Ne}(n,\gamma)^{23}\mathrm{Ne}(\beta^-)^{23}\mathrm{Na}(n,\gamma)^{24}\mathrm{Na}(\beta^-)^{24}\mathrm{Mg}$

$^{20}\mathrm{Ne}(n,\gamma)^{21}\mathrm{Ne}(\alpha,n)^{24}\mathrm{Mg}$

$^{24}\mathrm{Mg}(n,\gamma)^{25}\mathrm{Mg}(n,\gamma)^{26}\mathrm{Mg}(n,\gamma)^{27}\mathrm{Mg}(\beta^-)^{27}\mathrm{Al}$

$^{27}\mathrm{Al}(n,\gamma)^{28}\mathrm{Al}(\beta^-)^{28}\mathrm{Si}(n,\gamma)^{29}\mathrm{Si}$ + further *s*-processing

Fig.25. Important reactions in non-explosive He burning (from Arnett and Thielemann 1985). They develop essentially at $T \gtrsim 10^8$ K. The reactions listed under the heading "high-temperature burning" even require $T \gtrsim 3 \times 10^8$ K. The main ashes of He burning are ^{12}C and ^{16}O in proportions depending upon the stellar mass and $^{12}\mathrm{C}(\alpha,\gamma)^{16}\mathrm{O}$ rate. Neutrons can also be liberated, and lead to some s-processing (Sect. 8.1).

clearly show that it represents a major nuclear burning phase in the evolution of a star as far as energy production and nucleosynthesis are concerned.

The main reactions involved in such a burning are indicated in Fig. 25. Of very special interest is the $^{12}\mathrm{C}(\alpha,\gamma)^{16}\mathrm{O}$ reaction, which fixes the $^{12}\mathrm{C}/^{16}\mathrm{O}$ ratio at the end of He burning, as well as the whole subsequent stellar evolution and nucleosynthesis. No wonder then that the evaluation of the rate of that key reaction has been the subject of an unprecedented experimental as well as theoretical effort by nuclear physicists. In spite of that, some uncertainty still subsists (for details, see e.g. Barnes 1986; Descouvemont and Baye 1987; Rolfs and Rodney 1988; Filippone et al. 1989).

Of great importance also during He burning is the neutron production, essentially through $^{22}\mathrm{Ne}(\alpha,\mathrm{n})^{25}\mathrm{Mg}$. This can induce a s-process, as discussed in Sect. 8. In certain special situations, $^{13}\mathrm{C}(\alpha,\mathrm{n})^{16}\mathrm{O}$ could also produce a substantial amount of neutrons during He burning (e.g. Jorissen and Arnould 1986, 1989).

Helium burning can also take place explosively in a variety of sites, and namely in those associated with various explosions of the supernova type, as well as possibly at the surface of certain white dwarfs or neutron stars (e.g. Woosley 1986). The explosive processing of He could also lead to some neutron liberation, and consequently to the development of a "mini" r-process (Sect. 8).

Basic:

$^{12}C\left(^{12}C,\begin{matrix}\alpha\\ p\end{matrix}\right)\begin{matrix}^{20}Ne\\ ^{23}Na\end{matrix}$

$^{23}Na(p,\alpha)^{20}Ne$ $^{23}Na(p,\gamma)^{24}Mg$

Down to 10^{-2} of above:

$^{20}Ne(\alpha,\gamma)^{24}Mg$ $^{23}Na(\alpha,p)^{26}Mg(p,\gamma)^{27}Al$

$^{20}Ne(n,\gamma)^{21}Ne(p,\gamma)^{22}Na(\beta^+)^{22}Ne(\alpha,n)^{25}Mg(n,\gamma)^{26}Mg$

$^{21}Ne(\alpha,n)^{24}Mg$ $^{22}Ne(p,\gamma)^{23}Na$

$^{25}Mg(p,\gamma)^{26}Al(\beta^+)^{26}Mg$

Low-temperature, high-density:

$^{12}C(p,\gamma)^{13}N(\beta^+)^{13}C(\alpha,n)^{16}O(\alpha,\gamma)^{20}Ne$

$^{24}Mg(p,\gamma)^{25}Al(\beta^+)^{25}Mg$

$^{21}Ne(n,\gamma)^{22}Ne(n,\gamma)^{23}Ne(\beta^-)^{23}Na(n,\gamma)^{24}Na(\beta^+)^{24}Mg$ + *s*-processing

Fig.26. Important reactions in non-explosive C burning (from Arnett and Thielemann 1985). They develop mainly at $T \gtrsim 6 \times 10^8$ K. The main ashes of that burning are $20 \lesssim A \lesssim 27$ nuclides. Neutrons can also be liberated, and lead to some s-processing (see Sect. 8.1).

6.4. Carbon Burning

Non-explosive C burning in stars can develop at temperatures that are typically in excess of $\approx 6 \times 10^8$ K. Its importance as far as energy production and nucleosynthesis are concerned depends dramatically upon the ^{12}C amount left at the end of He burning, which is in turn directly related to the $^{12}C(\alpha,\gamma)^{16}O$ rate (Sect. 6.3).

The important reactions involved in C burning are given in Fig. 26. That burning stage raises the very interesting question of the fusion of light heavy ions below the Coulomb barrier, and in particular of the origin of the very pronounced structures observed in the $^{12}C + ^{12}C$ fusion cross section in that energy range. Much experimental and theoretical nuclear physics work has been devoted to that question, as summarized in e.g. Rolfs and Rodney (1988) (see also Descouvemont 1989). C burning mainly produces isotopes of Ne and Mg, as well as Al. Figure 26 also indicates that neutrons can be produced during non explosive C burning. The capture of those neutrons could lead to a limited s-process (Sect. 8).

Carbon burning could also take place explosively in a variety of sites and regimes. It appears that ^{46}Ca (which is a rare isotope in the solar system) and, to a lesser extent, ^{36}S are by far the most overabundant species emerging from that type of burning.

6.5. Neon Burning

That nuclear phase develops at temperatures in excess of 10^9 K, and starts with the photo-disintegration of ^{20}Ne produced by C burning, as it appears in Fig. 27, which summarizes the

Basic reactions:

$^{20}Ne(\gamma,\alpha)^{16}O$ $^{20}Ne(\alpha,\gamma)^{24}Mg(\alpha,\gamma)^{28}Si$

Flows $> 10^{-2}$ *times the above:*

$^{23}Na(p,\alpha)^{20}Ne$ $^{23}Na(\alpha,p)^{26}Mg(\alpha,n)^{29}Si$
$^{20}Ne(n,\gamma)^{21}Ne(\alpha,n)^{24}Mg(n,\gamma)^{25}Mg(\alpha,n)^{28}Si$
$^{28}Si(n,\gamma)^{29}Si(n,\gamma)^{30}Si$
$^{24}Mg(\alpha,p)^{27}Al(\alpha,p)^{30}Si$
$^{26}Mg(p,\gamma)^{27}Al(n,\gamma)^{28}Al(\beta^-)^{28}Si$

At low temperature and high density
(^{22}*Ne left from prior n-rich C burning):*

$^{22}Ne(\alpha,n)^{25}Mg(n,\gamma)^{26}Mg(n,\gamma)^{27}Mg(\beta^-)^{27}Al$

Fig.27. Important reactions in non-explosive Ne burning. They develop essentially at $T \gtrsim 10^9$ K (from Thielemann and Arnett 1985).

important reactions during that nuclear stage. Apart from ^{16}O, the dominantly produced species are the isotopes of Mg and Si, as well as Al and P. Some neutrons can also be produced, leading to a limited s-processing.

Explosive Ne burning can develop in supernova situations, at peak temperatures of $\sim 2\times10^9$ K. It has also been proposed that some synthesis of the p-nuclei could take place in non-explosive or explosive Ne burning (Sect. 8).

6.6. Oxygen Burning

Non-explosive oxygen burning is a major nuclear burning phase during the evolution of a star, especially of a massive one, where $^{12}C(\alpha,\gamma)^{16}O$ is able to transform a substantial amount of ^{12}C into ^{16}O at the He burning stage.

Important reactions during that phase are indicated in Fig. 28. It is especially interesting to notice that continuum electron captures start to play an important role, which will become more and more important during the further evolution.

Explosive O burning may develop in supernova situations, at peak temperatures $\sim 3\times10^9$ K. A large number of species from Si to Fe are produced in substantial quantities. In addition, non-explosive as well as explosive oxygen burning conditions are thought to be the most appropriate for the production of a majority of the p-nuclei (sect. 8).

6.7. Silicon Burning

Non-explosive as well as explosive Si burning exhibits a very complex pattern of nuclear reactions

Basic reactions:

$$^{16}\mathrm{O}\begin{cases}(^{16}\mathrm{O},p)^{31}\mathrm{P}\\(^{16}\mathrm{O},\alpha)^{28}\mathrm{Si}\\(^{16}\mathrm{O},n)^{31}\mathrm{S}(\beta^+)^{31}\mathrm{P}\end{cases}$$

$$^{31}\mathrm{P}(p,\alpha)^{28}\mathrm{Si}(\alpha,\gamma)^{32}\mathrm{S}$$

$$^{28}\mathrm{Si}(\gamma,\alpha)^{24}\mathrm{Mg}(\alpha,p)^{27}\mathrm{Al}(\alpha,p)^{30}\mathrm{Si}$$

$$^{32}\mathrm{S}(n,\gamma)^{33}\mathrm{S}(n,\alpha)^{30}\mathrm{Si}(\alpha,\gamma)^{34}\mathrm{S}$$

$$^{28}\mathrm{Si}(n,\gamma)^{29}\mathrm{Si}\begin{cases}(\alpha,n)^{32}\mathrm{S}(\alpha,p)^{35}\mathrm{Cl}\\(p,\gamma)^{30}\mathrm{P}(\beta^+)^{30}\mathrm{Si}\end{cases}$$

Electron captures:

$$^{33}\mathrm{S}(e^-,\nu)^{33}\mathrm{P}(p,n)^{33}\mathrm{S}$$

$$^{35}\mathrm{Cl}(e^-,\nu)^{35}\mathrm{S}(p,n)^{35}\mathrm{Cl}$$

Massive stars ($M_\alpha = 16\ M_\odot$)*:*

$$^{32}\mathrm{S}(\alpha,\gamma)^{36}\mathrm{Ar}\begin{cases}(\alpha,p)^{39}\mathrm{K}\\(n,\gamma)^{37}\mathrm{Ar}(\beta^+)^{37}\mathrm{Cl}\end{cases}$$

$$^{35}\mathrm{Cl}\begin{cases}(\gamma,p)^{34}\mathrm{S}(\alpha,\gamma)^{38}\mathrm{Ar}\\(e^-,\nu)^{35}\mathrm{S}(\gamma,p)^{34}\mathrm{S}\end{cases}\quad\begin{cases}(p,\gamma)^{39}\mathrm{K}(p,\gamma)^{40}\mathrm{Ca}\\(\alpha,\gamma)^{42}\mathrm{Ca}\begin{matrix}(\alpha,\gamma)^{46}\mathrm{Ti}\\(\alpha,p)^{45}\mathrm{Sc}(p,\gamma)^{46}\mathrm{Ti}\end{matrix}\end{cases}$$

Lower mass stars ($M_\alpha = 4\ M_\odot$)*:*

$$^{31}\mathrm{P}(e^-,\nu)^{31}\mathrm{S}\qquad ^{31}\mathrm{P}(n,\gamma)^{32}\mathrm{P}$$

$$^{32}\mathrm{S}(e^-,\nu)^{32}\mathrm{P}(p,n)^{32}\mathrm{S}$$

$$^{33}\mathrm{P}(p,\alpha)^{30}\mathrm{Si}$$

Fig.28. Important reactions in non-explosive O burning. They develop essentially at $T \gtrsim 2 \times 10^9$ K. The main ashes of O burning are $28 \lesssim A \lesssim 46$ nuclides. "Massive stars" stands here for $M \gtrsim 20 - 25 M_\odot$ stars (from Thielemann and Arnett 1985).

(e.g. Rolfs and Rodney 1988). In short, Si burning, or more exactly "melting", is characterized by a downward flow from Si to C, which can be represented by

$$\gamma + {}^{28}\mathrm{Si} \rightleftharpoons {}^{27}\mathrm{Al} + p$$
$$\gamma + {}^{24}\mathrm{Mg} \rightleftharpoons {}^{23}\mathrm{Na} + p$$

$$\gamma + {}^{28}\mathrm{Si} \rightleftharpoons {}^{24}\mathrm{Mg} + \alpha$$
$$\gamma + {}^{24}\mathrm{Mg} \rightleftharpoons {}^{20}\mathrm{Ne} + \alpha$$
$$\gamma + {}^{20}\mathrm{Ne} \rightleftharpoons {}^{16}\mathrm{O} + \alpha$$
$$\gamma + {}^{16}\mathrm{O} \rightleftharpoons {}^{12}\mathrm{C} + \alpha\,.$$

The arrows pointing to the left indicate that the photodisintegrations are counterbalanced to some extent by the reverse reactions. In addition, and thanks to the nucleons and α-particles freed by the downward flow, an upward flow from ^{28}Si also builds up. It can be represented by

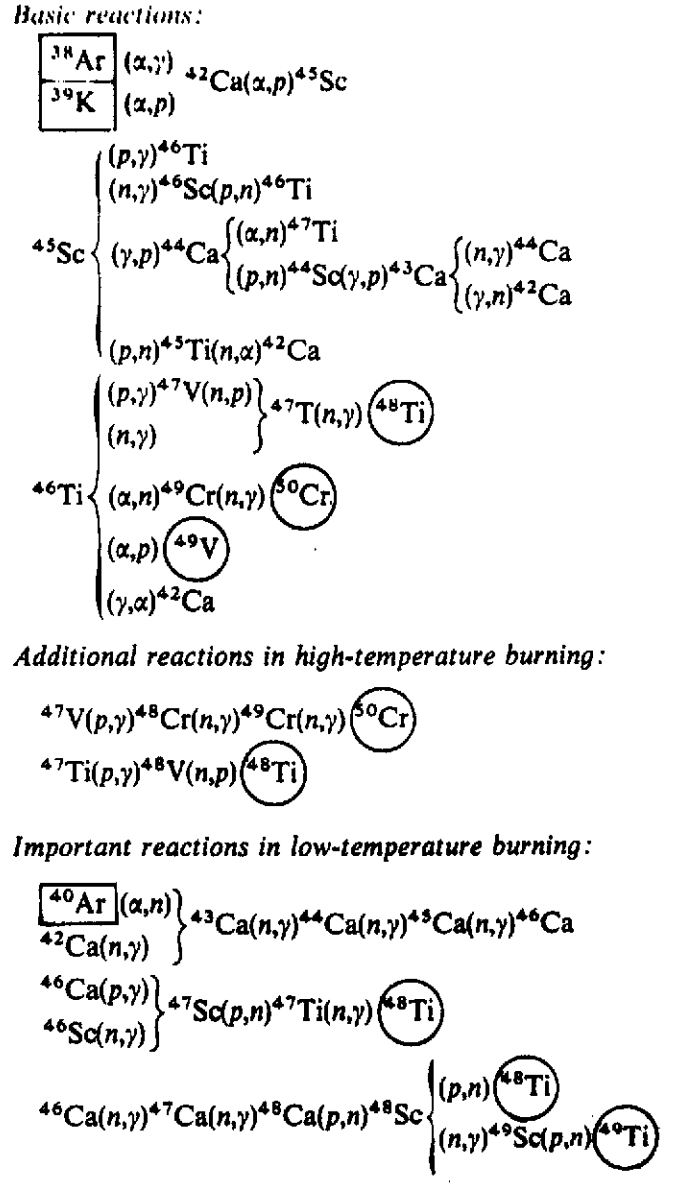

Fig. 29. Important reaction links between the two QSE groups in Si burning. Such a reaction pattern develops essentially at $T \gtrsim 4 \times 10^9$ K (from Thielemann and Arnett 1985).

$^{28}\mathrm{Si} + \alpha \rightleftharpoons {}^{32}\mathrm{S} + \gamma$; $\quad {}^{32}\mathrm{S} + \alpha \rightleftharpoons {}^{36}\mathrm{Ar} + \gamma$; $\quad \ldots$ iron group nuclei.

Considering those two flows originating from ^{28}Si, Si burning may be represented symbolically by

$$2(^{28}\mathrm{Si}) \longrightarrow {}^{28}\mathrm{Si} + 7\alpha \longrightarrow {}^{56}\mathrm{Ni}$$

or

$$2(^{28}\mathrm{Si}) \longrightarrow {}^{28}\mathrm{Si} + 6\alpha + 2n + 2p \longrightarrow {}^{54}\mathrm{Fe} + 2p\,,$$

depending upon the temperatures and densities at which Si burning takes place.

With increasing Si melting, and as a result of the release through photodisintegrations of nucleons and α-particles, followed by their rapid captures at the high temperatures ($T \gtrsim 4 \times 10^9$ K) characterizing that burning stage, groups of nuclei form which are connected by rapid and numerous reactions, and separated by bottlenecks due to slower reactions. For a large enough fraction of burned Si, two such groups of nuclei emerge, comprising $28 \leq A \leq 45$ and $45 \leq A \leq 56$ nuclei, separated by a bottleneck at $A \approx 45$ (e.g. Woosley et al. 1973, Arnould 1980).

In fact, a partial nuclear statistical equilibrium is reached in each of those groups, which are therefore referred to as quasi-statistical equilibrium (QSE) groups. In each QSE group, all the nuclei have the same temporal abundance variations, which can be evaluated from mere statistical mechanics equations just involving temperature, nuclear binding energies, and partition functions. Of course, the abundances in one group relative to the other, as well as of the nuclei not belonging to any QSE group, have to be evaluated by solving a detailed network of nuclear reactions. The most important reactions of such a network are displayed in Fig. 29.

Close to the end of Si burning (mass fractions $\lesssim 0.005$), the two QSE groups mentioned above merge in their turn. In fact, a full nuclear statistical equilibrium (NSE) (e.g. Rolfs and Rodney 1988) between all the nuclear species of the medium can be reached, resulting in the production of the iron group nuclei. As already mentioned in Sect. 5.2.1, that iron core may be at the origin of the subsequent dynamical instability of the star, and eventually of its explosion as a Type II supernova (see Schaeffer, this volume).

Silicon burning occurs explosively not only in those events, but also in Type I supernovae, leading to the production of large quantities of ^{56}Ni ($\sim$0.7 $M_\odot$ per SNIa), whose radioactivity powers the supernova light curve (this is also true for the late light curve of the supernova SN1987A in the Large Magellanic Cloud; Sec. 7). Notice that, through this mechanism, SNIa are currently thought to be the major producers of ^{56}Fe in the Galaxy.

6.8. Summary

Table 1 provides an overview of the nucleosynthetic processes expected to dominate the synthesis of each of the stable nuclides from ^{12}C to ^{64}Zn. In many cases, more than one process may contribute to the galactic abundances of those nuclides.

More details about the He, C, Ne, O and Si burning modes in schematic or realistic non-exploding and exploding model stars can be found in a large variety of papers and reviews. Among others, let us mention Arnett and Thielemann (1985), Thielemann and Arnett (1985), Nomoto (1986), Woosley (1986), El Eid and Prantzos (1988), Nomoto and Hashimoto (1988), and Thielemann (1989, 1990).

Figures 30 and 31 provide two examples of recently calculated supernova yields. Figure 30 displays the composition of the material (assumed to be fully mixed) ejected by the SN1987A Type II supernova (see Sect. 7). Typically, such explosions are predicted to produce a quite broad range of nuclides in relative proportions that are comparable to the solar values in many instances. The most underproduced species are possibly made in other astrophysical sites (e.g.

TABLE 1

Important Processes In the Synthesis of Various Isotopes[a,b]
(adapted from Woosley 1986)

^{12}C	He	^{32}S	O, EO	^{49}Ti	ESi[c], EHe[c]
^{13}C	H, EH	^{33}S	EO	^{50}Ti	nse
^{14}N	H	^{34}S	O, EO	^{50}V	ENe, nse
^{15}N	EH[c]	^{36}S	EC, Ne, ENe	^{51}V	ESi[c]
^{16}O	He	^{35}Cl	EO, EHe, ENe	^{50}Cr	EO, ESi
^{17}O	EH, H	^{37}Cl	EO, C, He	^{52}Cr	ESi[c]
^{18}O	H, EH, He	^{36}Ar	EO, ESi	^{53}Cr	ESi[c]
^{19}F	He, EHe[d]	^{38}Ar	O, EO	^{54}Cr	nse
^{20}Ne	C	^{40}Ar	?, Ne, C	^{55}Mn	ESi[c], nse[c]
^{21}Ne	C, ENe	^{39}K	EO, EHe	^{54}Fe	ESi, EO
^{22}Ne	He	^{40}K	He, EHe, Ne, ENe	^{56}Fe	ESi[c], nse[c]
^{22}Na	EH, ENe	^{41}K	EO[c]	^{57}Fe	nse[c], ESi[c], nse[c]
^{23}Na	C, Ne, ENe	^{40}Ca	EO, ESi	^{58}Fe	He, nse, C, ENe
^{24}Mg	Ne, ENe	^{42}Ca	EO, O	^{59}Co	nse[c], C
^{25}Mg	Ne, ENe, C	^{43}Ca	EHe, C	^{58}Ni	nse, ESi
^{26}Mg	Ne, ENe, C	^{44}Ca	EHe	^{60}Ni	nse[c]
^{26}Al	ENe, EH	^{46}Ca	EC, C, Ne, ENe	^{61}Ni	nse[c], ENe, C, EHe[c]
^{27}Al	Ne, ENe	^{48}Ca	nse	^{62}Ni	nse[c], ENe, O
^{28}Si	O, EO	^{45}Sc	EHe, Ne, ENe	^{64}Ni	ENe
^{29}Si	Ne, ENe, EC	^{46}Ti	EO	^{63}Cu	ENe, C
^{30}Si	Ne, ENe, EO	^{47}Ti	EHe[c]	^{65}Cu	ENe
^{31}P	Ne, ENe	^{48}Ti	ESi[c]	^{64}Zn	EHe[c], nse[c]

[a] Most important process first, additional (secondary) contributions follow.

[b] H = Hydrogen burning; EH = explosive Hydrogen burning, novae.
He = hydrostatic Helium burning; EHe = explosive Helium burning (esp. Type I SN).
C = hydrostatic Carbon burning; EC = explosive Carbon burning.
Ne = hydrostatic Neon burning; ENe = explosive Neon burning.
O = hydrostatic Oxygen burning; EO = explosive Oxygen burning.
Si = hydrostatic Silicon burning; ESi = explosive Silicon burning.
nse = nuclear statistical equilibrium (NSE).

[c] Radioactive progenitor.

[d] Only shell He burning possible; combined H-He burning promising (Goriely et al. 1989)

Arnould 1987). Figure 31 displays the yields from a Type Ia supernova. It appears that this explosion ejects predominantly iron-group nuclei.

As said previously, and in order to build up a model for the chemical evolution of the galaxies, the type of information provided by Figs. 30 and 31 has to be complemented by similar data related to the explosion of single stars of other initial masses and compositions, and of star in binary systems, as well as by a detailed information on the composition of the wind of stars that do not become supernovae. Those composition data would then have to be convoluted with the information on the mass returned by each star to the ISM and with the IMF (see Sect. 5).

Only a minute fraction of such an ambitious program has been completed today in a more or less quantitative way, and the most elaborated models still suffer from major astrophysical and nuclear physics uncertainties.

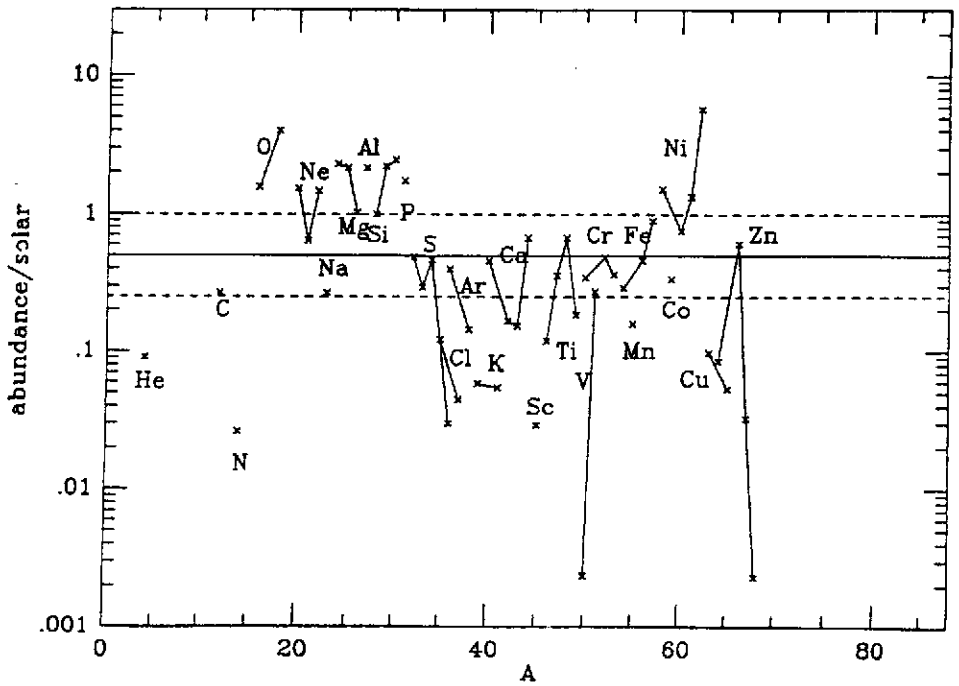

Fig.30. Calculated abundances of the $Z \leq 30$ in the ejecta of the (Type II) supernova SN1987A (see Sect. 7) compared to the bulk SC, and normalized to the solar ^{28}Si abundance (from Thielemann et al. 1989). Different isotopes of the same element are connected by lines.

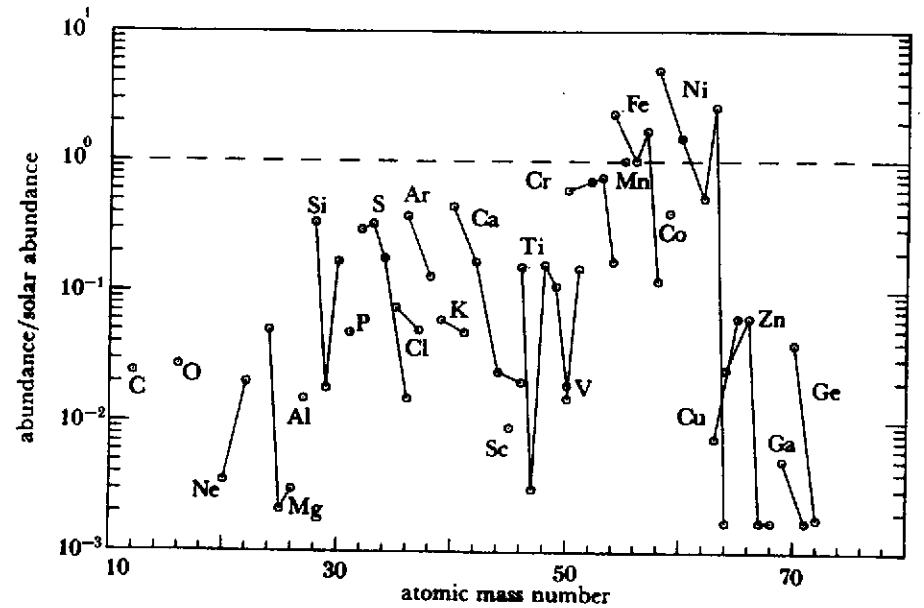

Fig.31. Composition of a Type I supernova ejecta, for elements up to Ge. The yields are normalized to the solar ^{56}Fe abundance (adapted from Thielemann et al. 1986b).

7. The Supernova SN1987A in the Large Magellanic Cloud

The year 1987 will certainly be remembered as an astrophysical milestone due to the appearance

in the Large Magellanic Cloud on Feb. 23 of the first naked-eye observable supernova for the last 386 years. That unique event in modern astronomy, named SN1987A and classified as a Type II supernova in view of the presence of hydrogen lines in its spectrum, is by now one of the most thoroughly studied objects outside the solar system. Many reviews have already been devoted to that supernova (e.g. Arnett et al. 1989; Hillebrandt and Höflich 1989, and references therein), and we limit ourselves here to some brief comments.

The progenitor of SN1987A has been identified as the blue supergiant Sk $-$ 69°202. This came as a surprise, because previously observed light curves of bright Type II supernovae were interpreted in terms of red supergiant explosions. The specific reasons why Sk $-$ 69°202 was blue at the time of its explosion are still being debated, but extensive pre-supernova mass loss and low metallicity (i.e. total abundance of all nuclei heavier than He), or a combination of these two factors, have been offered as the most likely explanations.

From the many studies conducted up to now on SN1987A, it is suggested that Sk $-$ 69°202 was a $20M_{\odot}$ star with a $6M_{\odot}$ helium core and a $10M_{\odot}$ envelope, a few solar masses having been lost prior to the explosion. Even if the details of the Type II supernova explosion mechanism remain elusive (see Sect. 5, and Schaeffer, this volume), it is considered that this phenomenon results from a shock wave generated inside the Fe core, and propagating through the onion-skin structure of the massive pre-supernova star. Several observations of SN1987A are indeed consistent with such a general picture.

One of these observations is the first detection of a burst of neutrinos prior to the optical signal. On the other hand, various observed features of SN1987A provide strong evidence for explosive nucleosynthesis. In particular, its light curve shows, since the end of the first month, an exponential decline which is considered as the clear signature of a powering by the decay of the ^{56}Co expected to be produced in the deep shock-heated Si burning layers. In fact, the light curve observations demand the synthesis of $0.07 \pm 0.01 M_{\odot}$ of ^{56}Ni (transforming afterwards into ^{56}Fe). The produced ^{56}Co has also been identified directly from γ-ray line observations. The detection of X-rays is also in nice support of the production of radionuclides in the supernova explosion, even if radioactivity is certainly not the only source capable of producing the observed SN1987A X-ray emission.

Calculations of the nucleosynthetic yields from SN1987A have been performed on grounds of specific pre-supernova and explosion models. One set of results obtained by Thielemann et al. (1989) is presented in Fig. 30. In this particular case, it is found that only the innermost $2M_{\odot}$ experience a strong explosive processing, while the rest of the material keeps its pre-supernova composition. It has to be emphasized that the predictions of Fig. 30 are constrained by the amount of ^{56}Ni derived from observation. As ^{56}Ni is synthesized in the deepest supernova layers, this translates into a fine tuning of the mass of the ejected material, or, in other words, of the mass of the supernova residue, which is likely to be a neutron star (there is a claim of a pulsar observation in SN1987A; this, however, remains to be confirmed). In fact, the precise value of the ejected mass remains a free parameter in all existing models, as self-consistent calculations predicting a successful explosion with the correct supernova energy are still badly lacking. Only such calculations would predict the amount of ejected material from "first principles". Other uncertainties in the nucleosynthetic production relate to many difficulties in the pre-supernova

modelling and in uncertain rates of various nuclear reactions [in this respect, $^{12}C(\alpha,\gamma)^{16}O$ is of prime importance].

The nucleosynthesis calculations also predict the production of other radioactivities than ^{56}Ni, and in particular of ^{57}Co and ^{44}Ti, which could also power portions of the light curve. On the other hand, other abundance observations than those related to ^{56}Ni can constrain the nucleosynthesis models. However, it has to be stressed that a direct comparison between the calculated and observed abundances suffer from many complications. The observation in SN1987A of elements heavier than iron and the corresponding nucleosynthesis predictions are discussed in Sect. 8.

Obviously, SN1987A has helped improving our understanding of Type II supernovae and of their nucleosynthesis. It has also raised many questions that will certainly keep observers and theoreticians busy for quite a while!

8. Synthesis of the Nuclides Heavier than Iron

The nuclear reactions expected to be of importance in the synthesis of the s-, r- and p-nuclei (Sect. 2.3) have already been listed in Sect. 6. Here, we examine their role in somewhat greater detail, and we attempt to identify the stellar sites where the s-, r- and p-processes develop.

8.1. The s-process

As already stated in Sect. 2.3, the s-process is meant to account for the s-nuclei observed in the solar system (Fig. 4), as well as at the surface of a large variety of stars. Details about the nuclear physics and astrophysics aspects of that process can be found in e.g. Bao and Käppeler (1987), Käppeler et al. (1989), or Prantzos (1989a). Let us just recall here some of its basic features.

The s-process results from the production of neutrons, and from their captures by preexisting ("seed") nuclei (most importantly iron, assumed to be produced in previous stellar generations) on time scales long compared with most β-decay lifetimes. This relative slowness of the neutron captures is at the origin of the identification of that process as the s- (for slow) process. In such conditions, a neutron capture path develops along which a β-unstable nucleus, once produced, has in general time to decay before capturing a neutron. For some nuclides, however, neutron captures can compete with β-decays. This leads to local "branches" along the main path. A typical s-process path with several branches is illustrated in Figs. 3 and 32. They clearly show that the s-process always flows very close to the bottom of the valley of nuclear stability, and "hits" on its way s- or sr- nuclei, while the r- and p-nuclei stay out of its reach. Typical s-process flow paths are obtained for neutron densities n_n in the approximate $10^7 \leq n_n \leq 10^9$ range.

One of the key questions raised by the s-process of course relates to the possibility of producing such neutron concentrations. It now appears that $^{13}C(\alpha,n)^{16}O$ and $^{22}Ne(\alpha,n)^{25}Mg$ are likely to be the most important neutron producing reactions in stars. As already made plausible in Sect. 6, one or another of those reactions could operate during He or C burning (Figs. 25, 26). Additional reactions, like $^{21}Ne(\alpha,n)^{24}Mg$, $^{25,26}Mg(\alpha,n)^{28,29}Si$, or $^{16}O(^{16}O,n)^{31}Si$ could also play some role in certain Ne- or O-burning conditions (Figs. 27, 28).

The precise characterization of the astrophysical sites where the various neutron producing

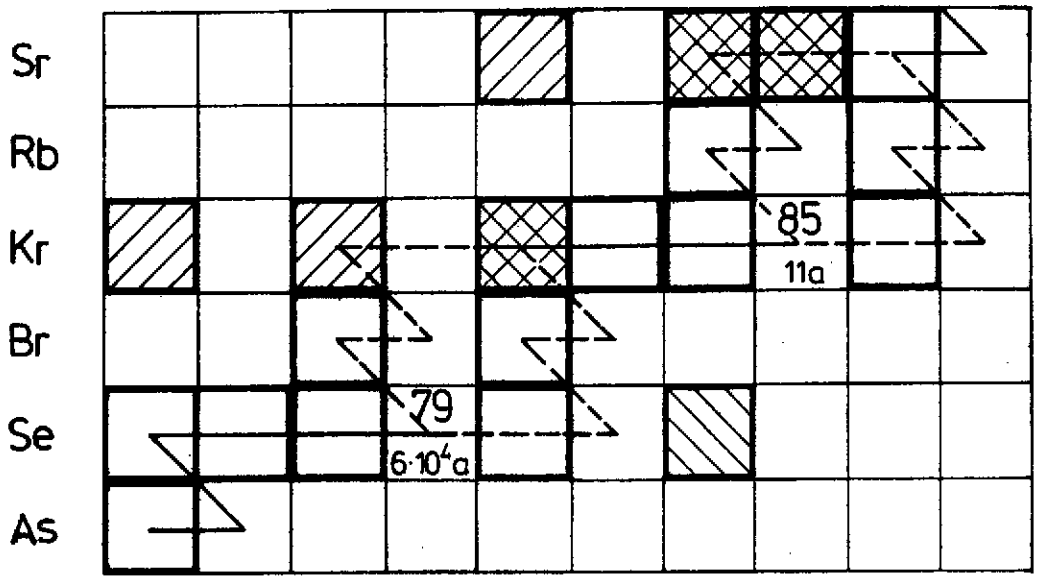

Fig.32. Section of the chart of the nuclides showing a typical s-process path (zigzag line) with two branches at ^{79}Se and ^{85}Kr. Heavy lined squares are stable nuclei. The s-, r- and p-nuclides are represented by XXX , \\\ and /// dashes, respectively (from Schatz 1986).

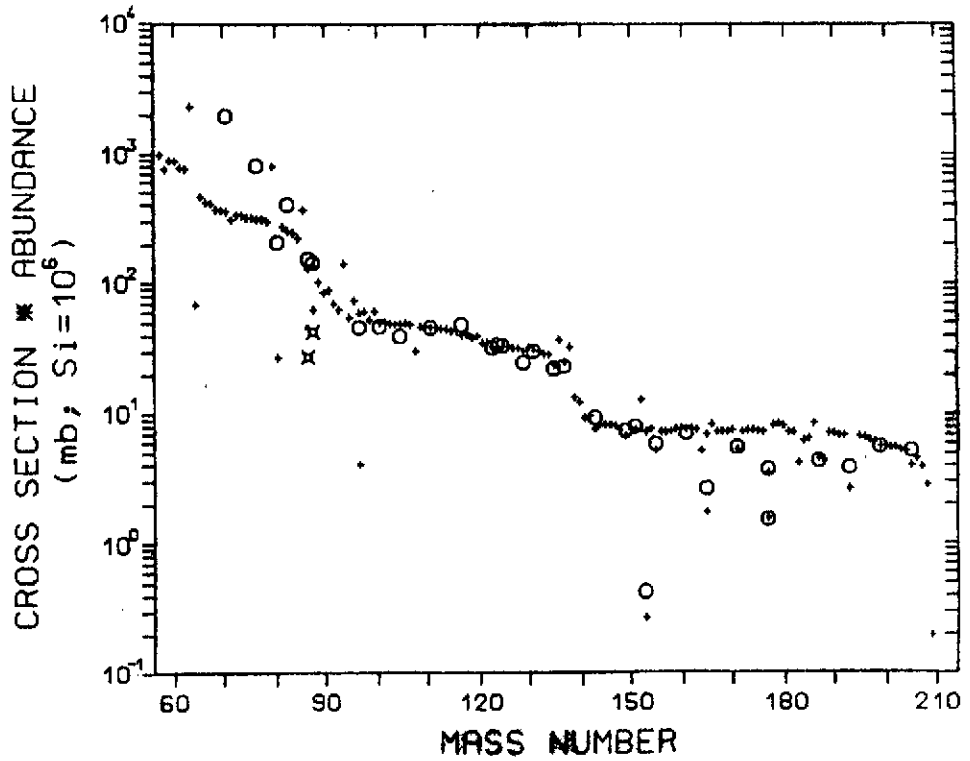

Fig.33. **Values** of σN (product of the 30 keV Maxwellian-averaged radiative neutron capture cross sections by the s-process abundances, normalized to Si = 10^6) resulting from s-process nucleosynthesis in He-rich zones of low mass stars. Open circles represent the values of σN for the solar system s-only isotopes (from Käppeler et al. 1989a). In models of this sort, the $A \lesssim 90$ nuclides are underproduced (with respect to solar).

reactions can operate is the other key aspect of the s-process modelling. Various such sites have already been studied in more or less great detail, namely (i) central He burning in massive ($M \gtrsim 10 M_{\odot}$) stars (e.g. Prantzos et al. 1987, 1988, 1990; Langer et al. 1989), (ii) central C burning in massive stars (Arcoragi et al. 1990), or (iii) shell He burning in highly evolved (asymptotic giant branch) low and intermediate mass ($M \lesssim 10 M_{\odot}$) stars (e.g. Howard et al. 1986; Malaney and Boothroyd 1987; Hollowell and Iben 1989; Jorissen and Arnould 1986, 1989; Käppeler et al. 1989a).

An example of s-process yields obtained in a low-metallicity and low-mass asymptotic giant branch star is presented in Fig. 33 (Käppeler et al. 1989a). In this case, the assumed neutron source is $^{13}C(\alpha,n)^{16}O$. Some agreement appears to be reached between the calculated abundances and those observed in the solar system, at least for mass numbers $A \gtrsim 90$. In fact, Fig. 33 presents the best fit derived by Käppeler et al. (1989a). It is obtained for a metallicity that is $\approx 1/3 - 1/4$ of the solar one.

It has to be emphasized that the astrophysical models underlying those calculations are still quite uncertain (e.g. Arnould 1990, Sackmann and Boothroyd 1990), while many intricacies and uncertainties exist in the involved nuclear physics (Jorissen and Arnould 1986, 1989, Arnould 1990). On the other hand, it remains to be seen if the relative agreement displayed in Fig. 33 is not skrewed up by a contribution from stars with other masses and metallicities to the galactic material making up the solar system (Arnould 1990).

On top of all that, it clearly appears from Fig. 33 that the asymptotic giant branch scenario is enable to account for the solar system content of the $A \lesssim 90$ nuclides. Various calculations (e.g. Prantzos et al. 1987, 1988, 1990; Langer et al. 1989) suggest that the s-process developing during core helium burning in massive ($M \gtrsim 10 M_{\odot}$) stars could produce those nuclides. Figures 34 and 35 present some results obtained in such a framework. Figure 34 exhibits the strong enhancement derived for the $A \lesssim 100$ species, while Fig. 35 shows that indeed such a model can be an important contributor to the $A \lesssim 90$ solar system s-nuclides.

It has been quite traditional to fit the solar system s-nuclei abundance curve by means of parametrized models calling for a specific combination of temperatures ($kT \approx 30$ keV), densities, and superposition of neutron exposures. Figure 36 shows such a fit for the $A \gtrsim 90$ range, a similar model being used in the lower mass range (e.g. Käppeler et al. 1989). Even if realistic astrophysical scenarios providing the conditions required for achieving such a nice fit remain to be found, this parametric approach has the virtue of enabling a separation between the s- and r-nuclidic compositions leading to the curves shown in Fig. 4.

Many interesting data about the s-process are also provided by some chemically peculiar low- or intermediate-mass stars exhibiting s-nuclide enrichments (e.g. the Barium stars). Most of these observations are still difficult to explain in terms of models of the type used to construct Fig. 33 (e.g. Jorissen 1990). The SN1987A supernova (Sect. 7) also brings its share of information about the s-nuclides. It appears in particular that Ba is overabundant in its ejecta by a factor of about 10 compared to solar, with a possible uncertainty of a factor of about 2 (e.g. Hillebrandt and Höflich 1989 for a review). Strontium could also be slightly overabundant. The only detailed s-process calculation performed up to now in order to explain that particular observation (Prantzos et al. 1988) relies on the operation of $^{22}Ne(\alpha,n)^{25}Mg$ during central

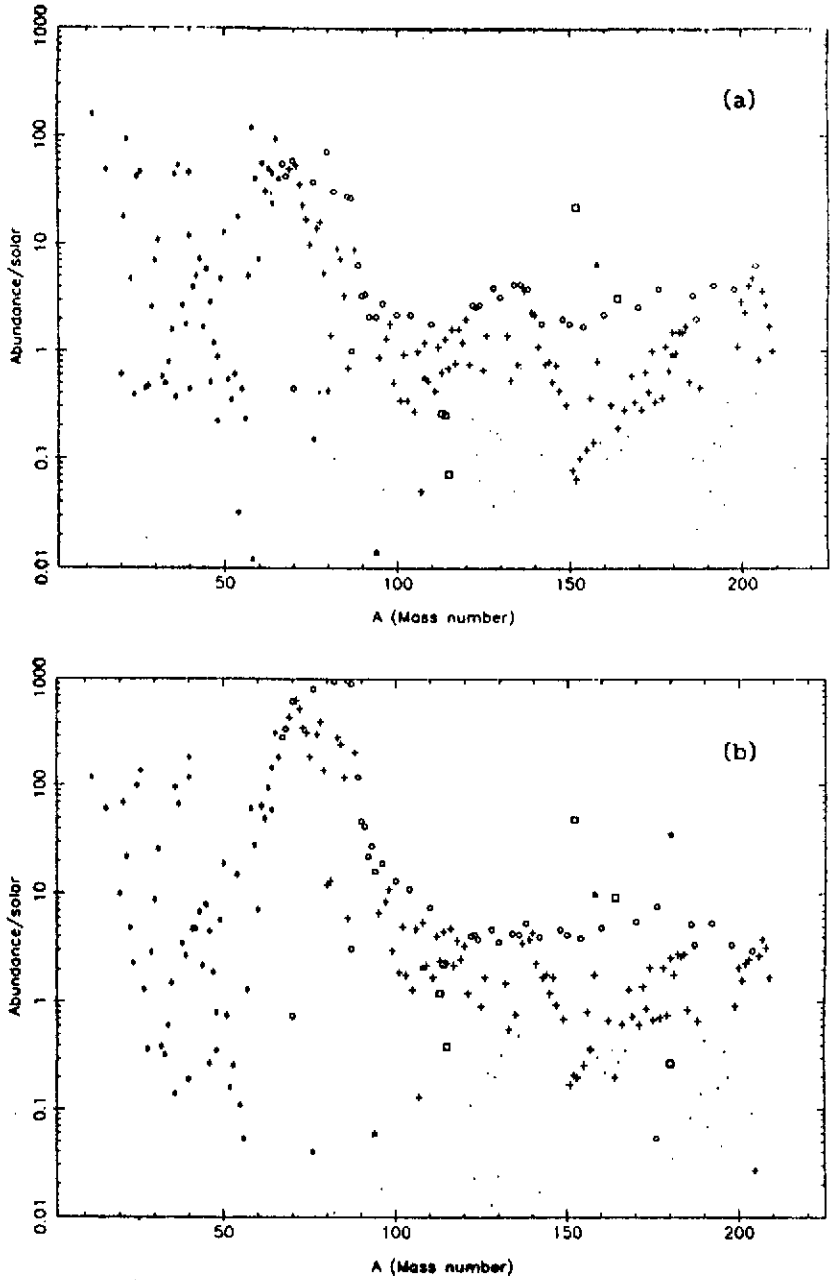

Fig.34. Abundances of s-nuclides at the end of central He burning in the convective core of a star with mass (a) $M \approx 11 - 16 M_{\odot}$, and (b) $M \approx 30 - 45 M_{\odot}$. Note that only nuclides with $A \lesssim 100$ are produced in significant quantities, and that these yields increase with mass M (from Prantzos et al. 1989).

helium burning in a specific model for the SN1987A progenitor. It indeed predicts some Ba overabundance, without, however, being able to account for the largest values compatible with the observations. If these large Ba overabundances are real and not an artifact of the photospheric models, then another neutron capture process had to be at work in the SN1987A progenitor.

In summary, the s-process is certainly the best understood of the mechanisms for the production of the nuclides heavier than iron. In spite of that, it still suffers from various astrophysics and nuclear physics uncertainties. The former ones are especially acute in the scenarios involving

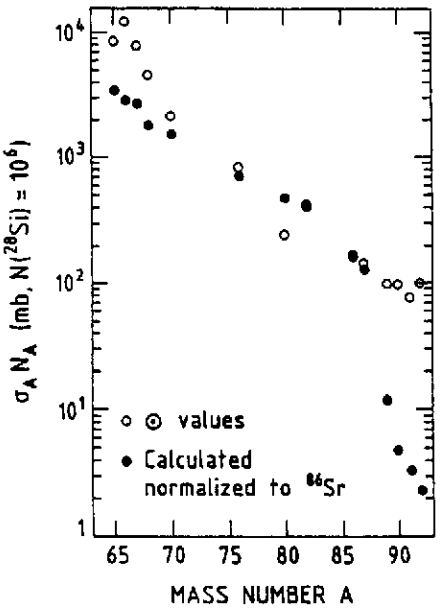

Fig.35. Solar system (circles) and theoretical (dots) σN values (defined in Fig. 33) versus mass number A for the most abundantly produced $65 < A < 90$ nuclides at the end of central He burning in the convective core of massive stars. The theoretical values correspond to the yields from $8 \leq M/M_{\odot} \leq 78$ stars convoluted with an IMF of the type shown in Fig. 11 (from Prantzos et al. 1989).

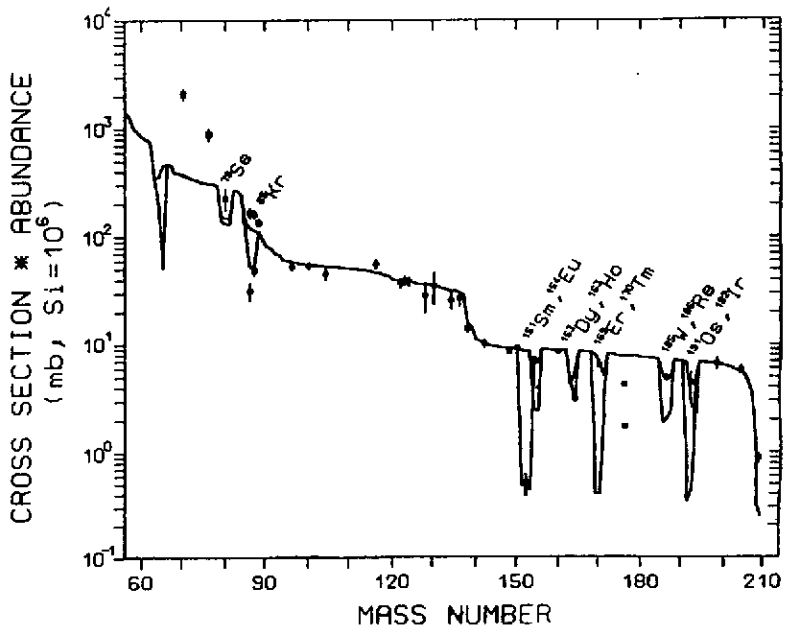

Fig.36. Values of σN (defined in Fig. 33) obtained in the parametrized s-process model for $A \gtrsim 90$ nuclides ("main component") defined by Käppeler et al. (1989) (solid line), compared with the corresponding SC values (black symbols). A different parametrization is needed to account for the σN values of the $A \lesssim 90$ s-nuclei ("weak component"). The effect of branchings along the s-process path is seen to account for the abundances of several relatively rare species (from Käppeler et al. 1989).

the $^{13}C(\alpha,n)^{16}O$, while the rate of this neutron source could be uncertain by a factor of 2-3 at the energies of astrophysical interest (Descouvemont 1987). The rate of $^{22}Ne(\alpha,n)^{25}Mg$ is much more uncertain (Wolke et al. 1989), so that the efficiency of that reaction as a neutron producer cannot be firmly established yet. Other uncertainties concern certain neutron capture rates in typical s-process conditions, or the possibility of thermalization of the ground and isomeric states of some nuclides in such environments. These and other questions of interest for the s-process are discussed at length in e.g. Käppeler et al. (1989).

8.2. The r-process

At the opposite of the s-process, the r- (for rapid) process assumes that neutron captures are more rapid than β-decays, at least in a substantial number of cases, and during a sizable fraction of the duration of the process. In such conditions, a nuclear flow can develop that drives seed nuclei (especially the iron peak) into the very neutron-rich region of the chart of nuclides.

In its simplest form, the r-process model, referred to as the "canonical" model, in fact assumes that temperature, density and neutron concentration remain constant over the whole time scale τ during which the neutron capture process is taking place. In addition, neutron captures are assumed to be always more rapid than β-decays. In such conditions, and as a result of successive neutron captures, the nuclear flow can penetrate deeper and deeper into the neutron-rich regions.

Such a flow encounters nuclei with lower and lower neutron binding energies. As a result, the (n,γ) reactions are slowing down, while the rate of the reverse (γ,n) photodisintegrations is increasing. In such conditions, a $(n,\gamma)-(\gamma,n)$ equilibrium tends to be established for each isotopic chain, in which case the abundances can be quite simply expressed in terms of temperature, n_n, and neutron separation energies S_n.

Once such an isotopic equilibrium is established, (β^-)-decays can eventually take place, leading to a new element for which an isotopic equilibrium is already, or can be, obtained. Such a flow of material to higher and higher Z values takes a special character in the vicinity of neutron shell closures. Due to the especially low S_n values just past a magic number, the flow of material to more neutron-rich species is strongly hindered, so that (β^-)-decays drive the material closer and closer to the valley of nuclear stability, following a path with increasing Z at practically constant N. As a result, the β-decays slow down, as well as the nuclear flow, so that some material accumulates at neutron closed shells. However, the capture chain is merely slowed down, and not stopped: the S_n values at the accumulation point are again high enough for favoring (n,γ) reactions with respect to (γ,n) photodisintegrations. In such conditions, the flow of material towards more neutron-rich species and higher Z values resumes until a new neutron magic number, and thus a new accumulation point, is reached, and then overtaken. The nuclear flow towards increasing Z values is generally believed to be stopped by neutron-induced fissions, which lead to a cycling back of a portion of the material to lower Z values.

After the time interval τ, the canonical r-process model assumes that all nuclear reactions are suddenly frozen. At such a stage, (β^-)-cascades, as well as α-decays (in the $A \geq 210$ region), spontaneous or β-delayed fissions, and single or multiple β-delayed neutron emissions drive the matter towards β-stable nuclei. In particular, the material accumulated at the neutron shell

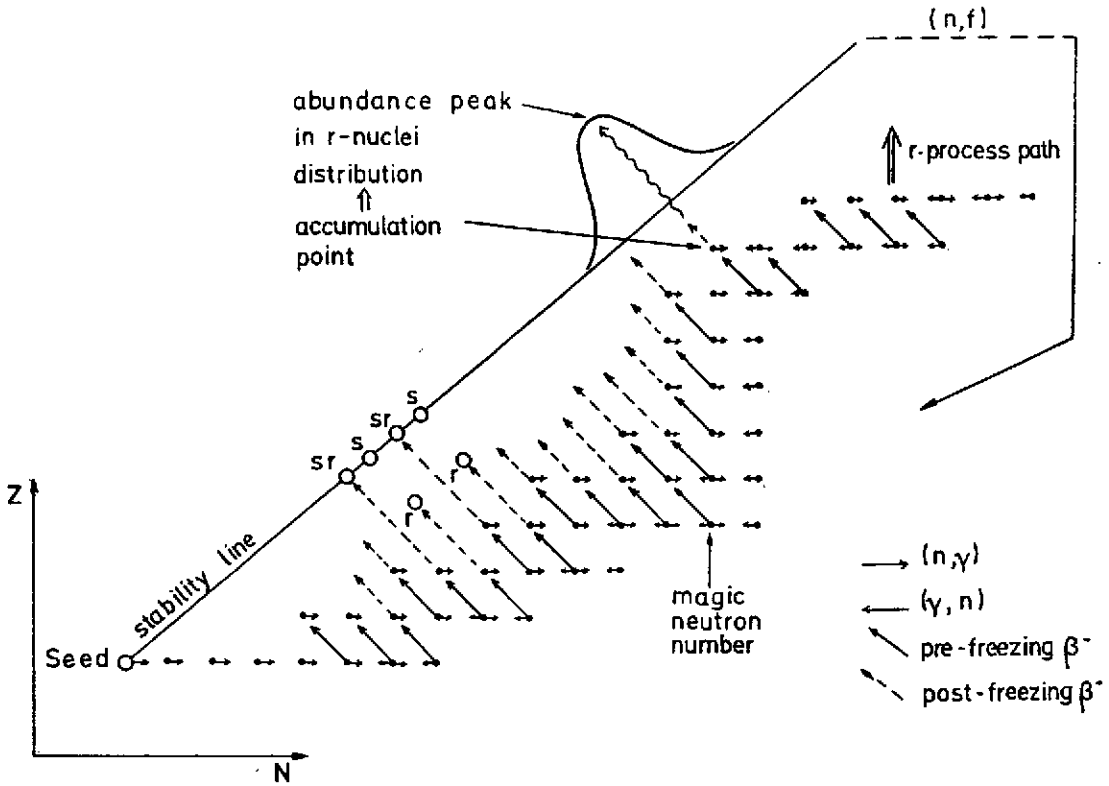

Fig.37. Schematic illustration of the various nuclear transformations involved in the r-process. Various pre- and post-freezing processes are indicated. Other post-freezing mechanisms may operate, like spontaneous or $\beta-$delayed fissions, and $\alpha-$decays (in the $A \geq 210$ range). The origin of the peaks in the solar system r-nuclei abundance curve (Fig.4) is also sketched.

closures during the neutron processing is held responsible for the observed peaks in the r-nuclei abundance distribution (Fig. 4). A typical r-process nuclear flow during the pre- and post-freezing regimes is schematized in Fig. 37. For more details, the reader is referred to e.g. Mathews and Ward (1985).

The canonical r-process described above is internally consistent only for certain ranges of values of the temperature, neutron concentration and time scale τ. Constraints of this nature have been studied in detail, and their violation may in particular invalidate the basic $(n,\gamma) - (\gamma,n)$ equilibrium assumption. This can namely result from a too low neutron concentration, which allows a competition between β-decays and neutron captures. Such a situation could possibly occur for $n_n \lesssim 10^{20}\mathrm{cm}^{-3}$, and is generally referred to as an intermediate or n-process (e.g. Mathews and Ward 1985).

The most detailed n-process models available to date not only drop the assumption of a $(n,\gamma) - (\gamma,n)$ equilibrium, but also consider more realistic astrophysical environments in which temperatures, densities and neutron concentrations do vary in time.

Various locations have in fact been considered as possibly responsible for the very large neutron fluxes that are required for the production of the r-nuclides (e.g. Mathews and Ward 1985; Thielemann 1989, for reviews and references). Originally, the r-process was thought to develop at the base of the material ejected during a Type II supernova explosion, that is just outside the supernova residue (see Fig. 12). An exemple of yields calculated in such a model are

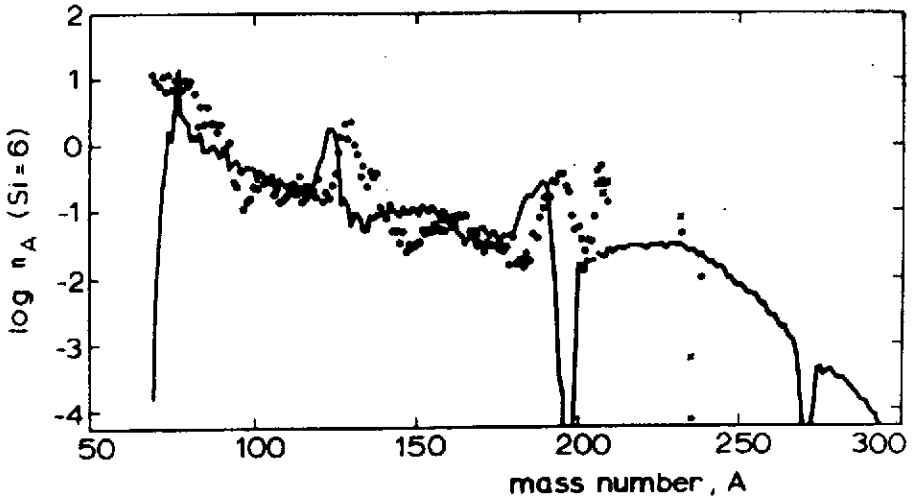

Fig.38. Abundances calculated in a model of the r-process taking place at the mass cut between the supernova residue and remnant material (solid line). They are compared with the observed solar system abundances (from Hillebrandt et al. 1976).

displayed in Fig. 38. None of the predictions of that type is able to reproduce the solar system r-nuclei abundances (Fig. 4) under physically plausible conditions. It has also to be emphasized that all of them suffer from very severe astrophysical uncertainties, related in particular to the description of the layers located at the mass cut between the supernova residue and remnant. On the other hand, the confrontation between calculated and observed abundances of the r-nuclides could provide some information and constraints on the location of that mass cut and on the r-process models. This can be applied in particular to SN 1987A (Sect. 7). In order to satisfy various observational constraints on the composition of this supernova, and in particular on its amount of ejected ^{56}Ni, Thielemann et al. (1989) conclude that no material enriched with r-nuclides can be ejected from the layers just outside the mass cut.

The r-process model presented above has been extended in order to examine the influence of the rotation of the supernova core, which could perhaps cause jet-like ejections of r-nuclides at the poles. However, the precise efficiency of such a mechanism at the galactic level remains to be determined.

In view of the difficulties encountered by the supernova core models, other supernova locations have been suggested, like the exploding He-rich layers of massive stars, in which neutrons can be liberated by ^{22}Ne$(\alpha,\mathrm{n})^{25}$Mg. Figure 39 displays the r-nuclei abundances calculated in such a model. That "He-driven r-process" also suffers from many astrophysical difficulties. In particular, it appears not to be efficient enough to account for the solar system r-nuclei abundances in plausible astrophysical situations. The ^{13}C$(\alpha,\mathrm{n})^{16}$O neutron source has also been suggested, and abundances predicted in such a modified He-driven r-process are presented in Fig. 40. It has to be emphasized that not only the required level of efficiency, but even the very existence of ^{13}C$(\alpha,\mathrm{n})^{16}$O in the considered conditions have not been substantiated by existing stellar models.

Deeper C-rich zones of a massive star processed explosively at the supernova stage have also been considered as a possible site for the r-process. The neutrons may be produced by

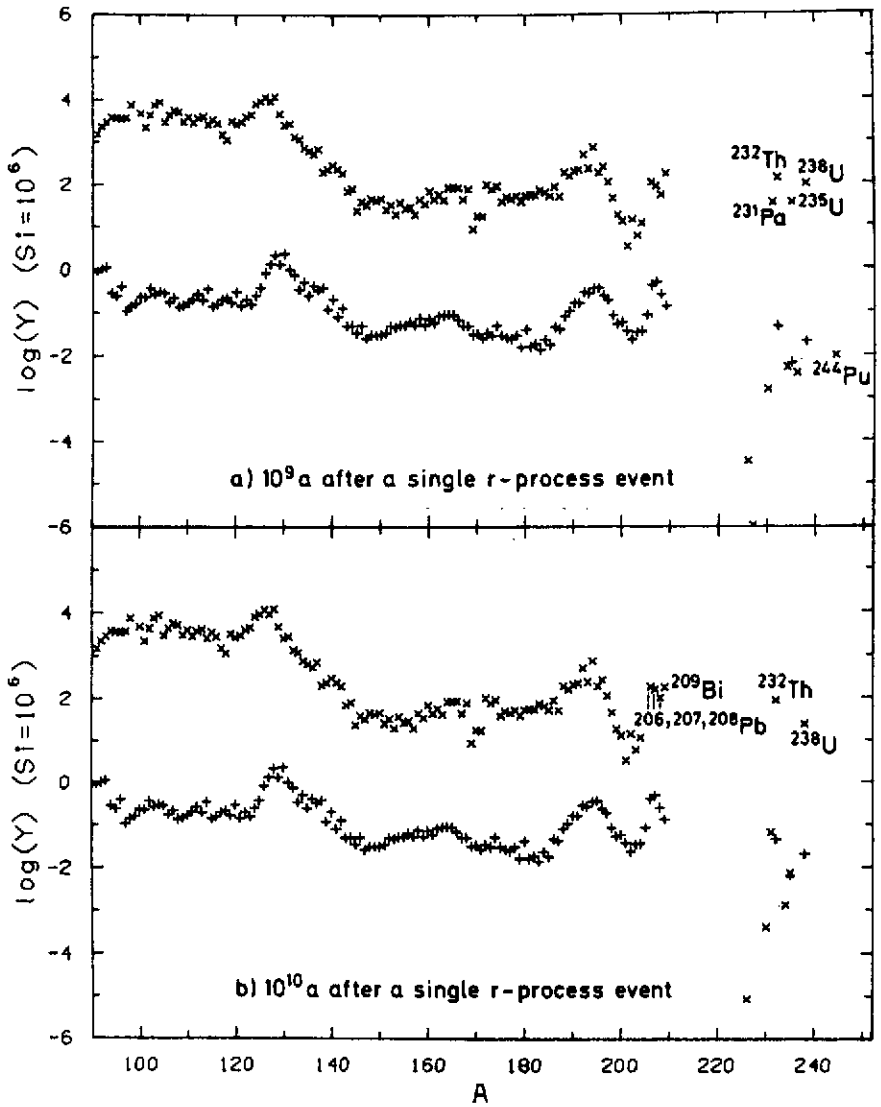

Fig.39. Predicted r-nuclei abundances (x), 10^9 or 10^{10} yr after the operation of a He-driven r-process in which the neutrons are produced by $^{22}\mathrm{Ne}(\alpha,\mathrm{n})^{25}\mathrm{Mg}$. They are compared with the solar system r-nuclei abundances (+) (from Thielemann et al. 1983).

$^{22}\mathrm{Ne}(\alpha,\mathrm{n})^{25}\mathrm{Mg}$. As in the case of the He-driven r-process, the major problem with this model is the lack of sufficient neutrons to produce the total solar system content of r-nuclei. However, the production of some r-nuclei in the He- or C-driven r-processes cannot be excluded, and might provide an explanation for certain isotopic anomalies in meteorites (Sect. 2.4).

Another suggested site is the He core of low mass ($M \lesssim 2M_\odot$) stars, in which He starts burning more or less violently (He flash). In such a model, it is assumed that protons are convectively mixed into the He core, producing neutrons through $^{12}\mathrm{C}(\mathrm{p},\gamma)^{13}\mathrm{N}(\beta^+)^{13}\mathrm{C}(\alpha,\mathrm{n})^{16}\mathrm{O}$. For adequately selected conditions, the r-nuclei abundances calculated in such a scenario are qualitatively the same as in Fig. 40. On top of the fact that detailed models of the He flash are still largely lacking, it appears unlikely that the bulk solar system r-process nuclei can be accounted for in such a way, basically for the same reasons as in the case of the He- or C-driven

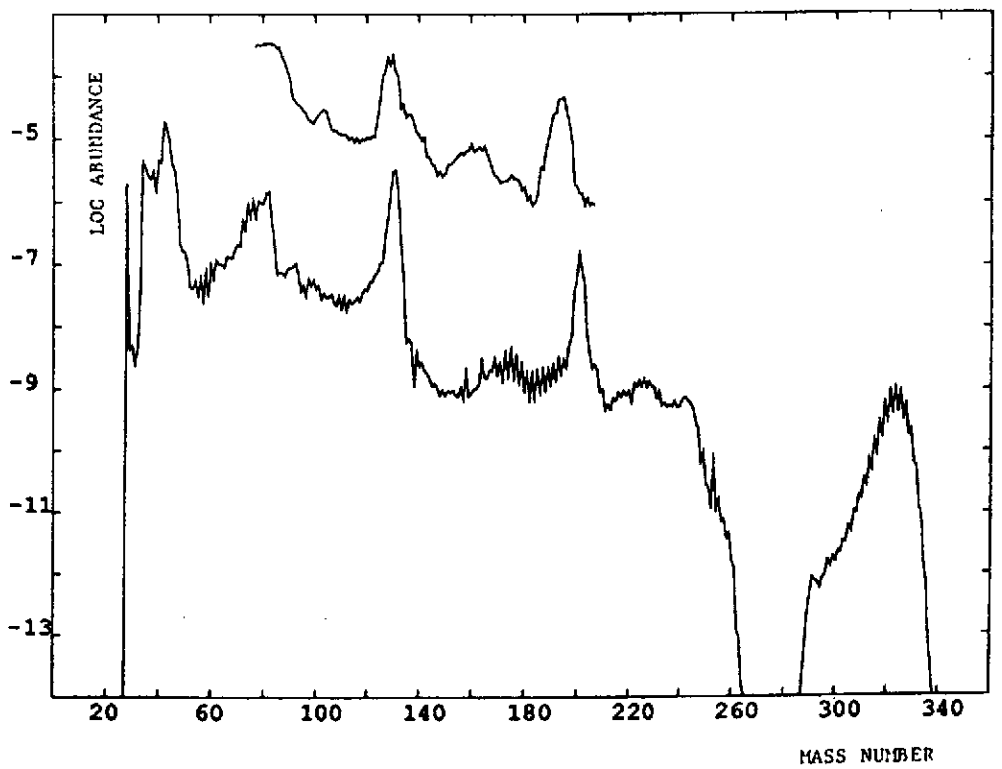

Fig.40. Calculated abundances in a supernova He-driven r-process where the neutrons are provided by $^{13}C(\alpha,n)^{16}O$ (lower curve; the predictions in the $A \gtrsim 260$ range do not have to be considered seriously, namely in view of the neglect of fission processes). The upper curve is the observed solar system r-nuclei abundance curve (arbitrary normalization) (from Cowan et al. 1986).

r-processes in massive star explosions.

Some additional exotic models have also been investigated, like the ejection and decompression of highly neutron-rich material during neutron star collisions or disruptions, or nonuniform Big Bang production (see Sect. 5), which could perhaps account for the observed r-nuclide content of very old stars.

In conclusion, the site(s) of the r-process (in particular the one responsible for the bulk solar system r-nuclei) is(are) still unknown, all the proposed scenarios facing serious problems. On top of those astrophysical difficulties, major nuclear physics problems are also raised by the r-process. It indeed requires a detailed description of the properties of thousands of (mostly unknown) neutron-rich nuclei located very far off the stability line. One is also left with the formidable task of providing reliable evaluations of the rates of transformation of those nuclides under neutron captures or photodisintegrations, β-decays, or fission. The present status of the nuclear physics models adopted in the study of the r-process has been discussed at several occasions (e.g. Takahashi 1988; Thielemann 1989; see also Bender et al. 1988, or Möller and Randrup 1989 for recent theoretical improvements concerning β-decay half-life estimates).

All the astrophysical and nuclear physics difficulties encountered in the modelling of the r-process affect also to a substantial extent the predictions of the age of the solar system r-nuclides based on the study of the ^{232}Th-^{238}U and ^{235}U-^{238}U chronometers. A critical discussion of these

cosmochronological questions can be found in Arnould and Takahashi (1990).

8.3. The p-process

This process is aimed at explaining the synthesis of the p-nuclei observed in the bulk solar system material (Figs. 3,4). It could also provide some explanation for certain isotopic anomalies found in primitive meteorites (Sect. 2.4, and e.g. Anders 1987; Prinzhofer et al. 1989).

As made clear by Figs. 3, 32 and 37, the p-nuclei cannot be produced by the s- and r-processes of neutron captures discussed in Sects. 8.1 and 8.2. In contrast, it seems natural to think of the transformation of pre-existing seed nuclei (especially of the s- or r-type) by the addition of protons (radiative proton captures), or by the removal of neutrons (neutron photodisintegrations).

The rates of (γ, n) photodisintegrations are increasing very rapidly with increasing temperatures and decreasing neutron binding energies. It appears that temperatures $T \gtrsim 10^9$ K are required in order for s- or r-nuclei to have time to be stripped of neutrons in realistic stellar situations. On the other hand, (p, γ) reactions are much less dependent on temperature and binding energy, but their rates are rapidly decreasing with increasing Coulomb barrier heights. More specifically, these rates are reduced by factors $10^6 - 10^9$, at temperatures of a few 10^9 K, when going from Fe to Bi. As a result, proton radiative captures can contribute at best to the production of the lightest p-nuclei (e.g. ^{74}Se to ^{98}Ru) production only, and in highly proton-rich environments. Such considerations have been the main guidelines in the search for stellar environments where the p-nuclei could be synthezised (for a review, see Rayet 1987, Prantzos 1989b).

Following an original suggestion of Burbidge et al. (1957), the explosion of H-rich supernova envelopes has long been held responsible for the synthesis of the p-nuclei. In such a scenario, which has been most thoroughly explored by Audouze and Truran (1975), photodisintegrations of pre-existing seeds appear to dominate the production of the p-nuclei heavier than Sm. In contrast, they bring a relatively minor contribution to the synthesis of lighter p-nuclei, which result predominantly from proton captures. The dominance of these captures is a direct consequence of the high proton concentrations which are available in the invoked stellar envelopes.

In spite of its relative and purely mathematical success in mimicking the solar system p-nuclei abundance distribution, the explosive H-burning model sketched above has to be considered as physically implausible. The required explosion conditions ($\rho_p \approx 10^4 \mathrm{gcm}^{-3}$, $T_p \gtrsim 2 \times 10^9$ K) indeed appear impossible to reach in the considered supernova layers. It has also to be remarked that, from a purely nuclear physics point of view, the rp-process mentioned in Sect. 6.2 could be responsible for the synthesis of some of the lightest p-nuclei. However, the possible net contribution of that mechanism to the bulk solar system composition is entirely unknown.

In view of the difficulties encountered by the explosive H-burning p-process model, various other sites have been proposed, and especially the deep O/Ne-rich zones of massive stars, either in their pre-supernova evolution (Arnould 1976), or during their supernova explosion (Woosley and Howard 1978; Prantzos et al. 1990; Rayet et al. 1990). In such layers, the temperatures are indeed high enough for the seed nuclei, which can be produced more or less abundantly during the previous He- or C-burning phases (Sects. 6.3, 6.4 and 8.1), to be transformed to a significant

extent by (γ,n), (γ,p) or (γ,α) photodisintegrations. In addition, (n,γ) captures can affect the nuclear flow, as well as β-decays, at least in the non-explosive case. In contrast, the paucity of protons in the O/Ne layers largely inhibits the (p,γ) reactions.

The photodisintegration model has originally been developed in the framework of realistic non-explosive O-burning conditions by Arnould (1976), who has shown that several p-nuclides could be produced in significant amounts in such an environment before the eventual explosion of the star.

A simplified photodisintegration model was thereafter applied (Woosley and Howard 1978) to a schematic explosive O-burning model in which the captures of nucleons and α-particles produced during Ne/O burning (Figs. 27,28) are neglected. Recently, this explosion model has been substantially extended (Rayet et al. 1990) by considering an enlarged nuclear reaction network that includes (mainly neutron-deficient) nuclides all the way from C to Bi, takes due account of nucleon and α-particle captures, and makes use of improved nuclear reaction rate predictions (Thielemann et al. 1986a). Figure 41 displays the portion of that reaction network above Germanium, as well as the main nuclear flows for two sets of explosion conditions. The (γ,n) photodisintegrations (not represented for clarity) are the fastest reactions on most stable nuclei, as well as on the unstable neutron-deficient isotopes up to a point where this flow is deflected to lower Z elements by (γ,p) or (γ,α) reactions (vertical arrows). Horizontal arrows also show points where the (n,γ) reactions due to the neutrons produced during the O/Ne burning impede the photodisintegration flows. After freeze-out of all the nuclear reactions, β-decays eventually produce the p-nuclei from more neutron-deficient progenitors. Figure 41 clearly shows the extreme sensitivity of the nuclear flows to the explosion conditions.

Prantzos et al. (1990) have recently performed the first p-process calculation in a realistic supernova model. This particular study deals with SN1987A (Sect. 7), and makes use of the same nuclear physics input and reaction network as Rayet et al. (1990). Figure 42 shows the overproduction (relative to solar) of some selected p-nuclides versus the peak temperatures reached during the explosion. Through the adopted SN1987A model, these temperatures are strictly related to the precise mass location of the burning shells in the exploding star. It is clearly seen that the calculated p-nuclei abundances are extremely sensitive to the explosion conditions, as already concluded from the parametrized p-process calculations. The p-nuclei yields (assuming full homogeneity of the supernova ejecta) derived by Prantzos et al. (1990) are presented in Fig. 43. Although there is no a priori reason why the abundances obtained in this model explosion should exactly follow a solar-like pattern (in this case, all values would be 1 in Fig. 43), it is interesting to remark that a majority of p-nuclei are produced within a factor 3 of the mean value. Qualitatively, this result was also obtained in the parametrized calculations (Rayet et al. 1990). Let us emphasize more particularly the sizeable production of ^{180}Ta in the coolest layers of the considered stellar zone (Fig. 42). The very origin of this nuclide is still very puzzling, despite its very low solar abundance. On the other hand, the calculations predict, as all the previous ones, a severe underproduction of the Mo and Ru p-isotopes, which are by far the most abundant p-nuclei in the solar system. This failure of the models is inescapable with our present knowledge of the astrophysical models and of the nuclear physics in the relevant nuclear mass region.

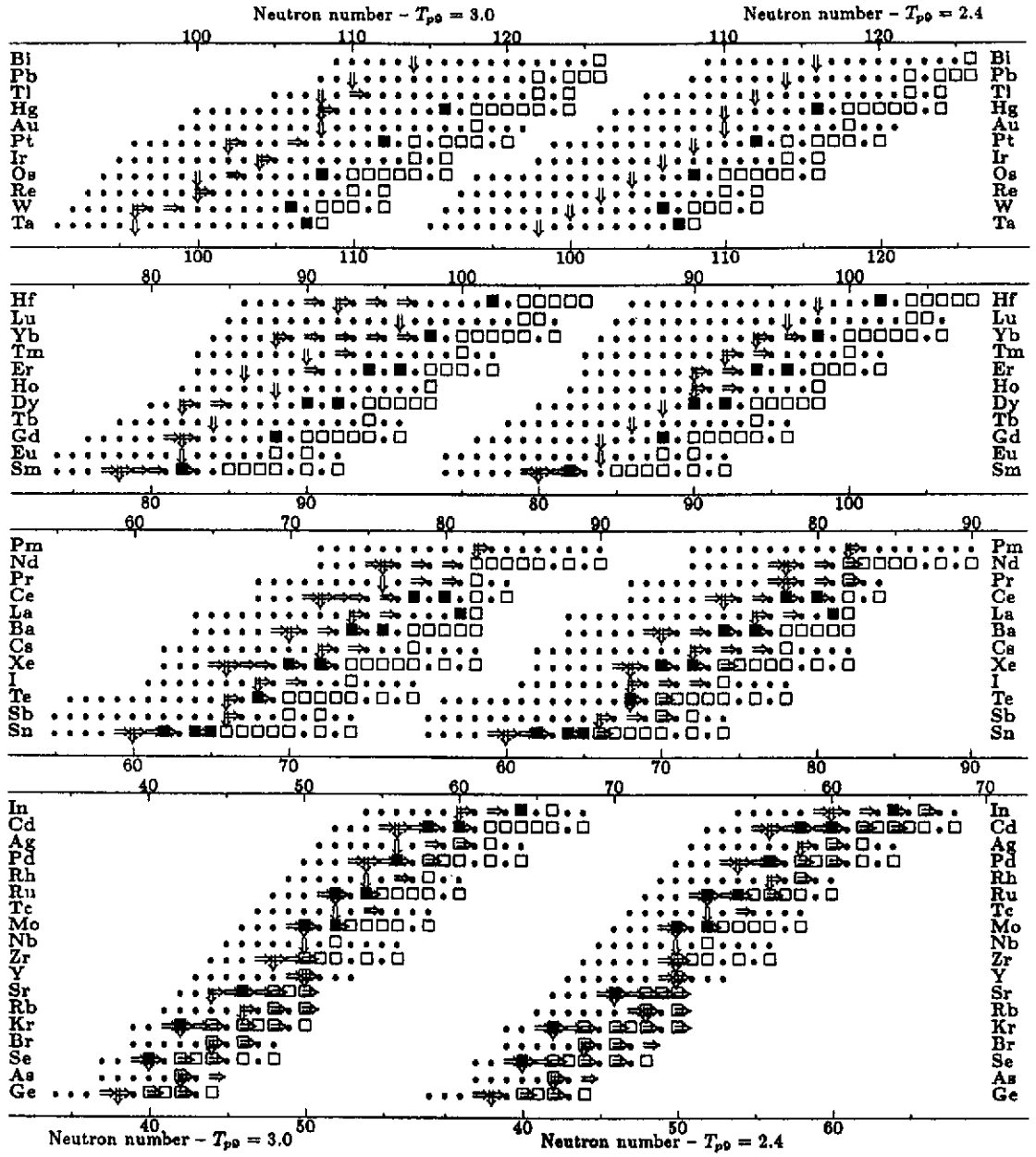

Fig.41. Schematic representation of nuclear flows during the $p-$process in the $Z \geq 32$ range. The neutron number scales are split up in order to show the relevant information on reaction fluxes for two different peak temperatures T_{p9} (where T_9 is the temperature in 10^9 K) reached in the considered layers as a result of the passage of the shock wave associated to the supernova explosion. The left (*resp.* right) part of the diagrams corresponds to $T_{p9} = 3.0$ (*resp.* 2.4), when the maximum neutron concentration $X_n = 6.0 \times 10^{-11}$ (*resp.* 3.7×10^{-14}) has been reached.The symbols have the following meaning: □ : $s-$and $r-$nuclei; ■ : $p-$nuclei; • : other (unstable) isotopes belonging to the network; ⇓ : point where (γ, p) or (γ, α) start to dominate over (γ, n). At the right of such a point, the main nuclear flow is driven to the left by (γ, n) reactions; ⇒ : nuclides for which the (γ, n) isotopic flow is impeded by the (n, γ) reaction (from Rayet et al. 1990).

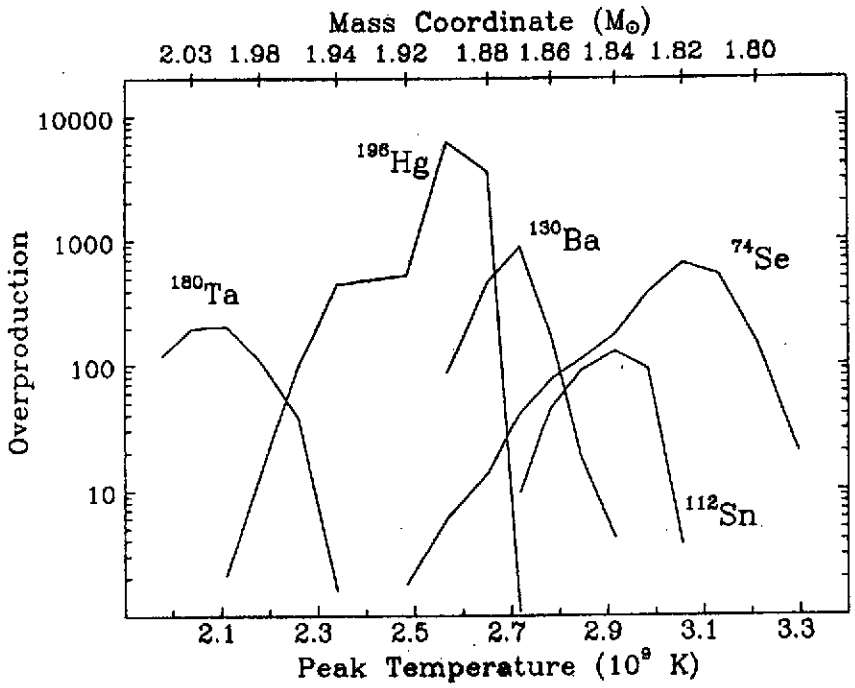

Fig.42. Abundances of the p-nuclei relative to their SC values (overproduction factors) produced in O/Ne-rich layers of a specific model for SN1987A (Sect. 9) that are shock-heated to peak temperatures in the range $(1.9 - 3.3) \times 10^9$ K (from Prantzos et al. 1989a). These peak temperatures correspond to the mass coordinates indicated on the upper scale. No significant p-process develops outside the displayed temperature (mass) range.

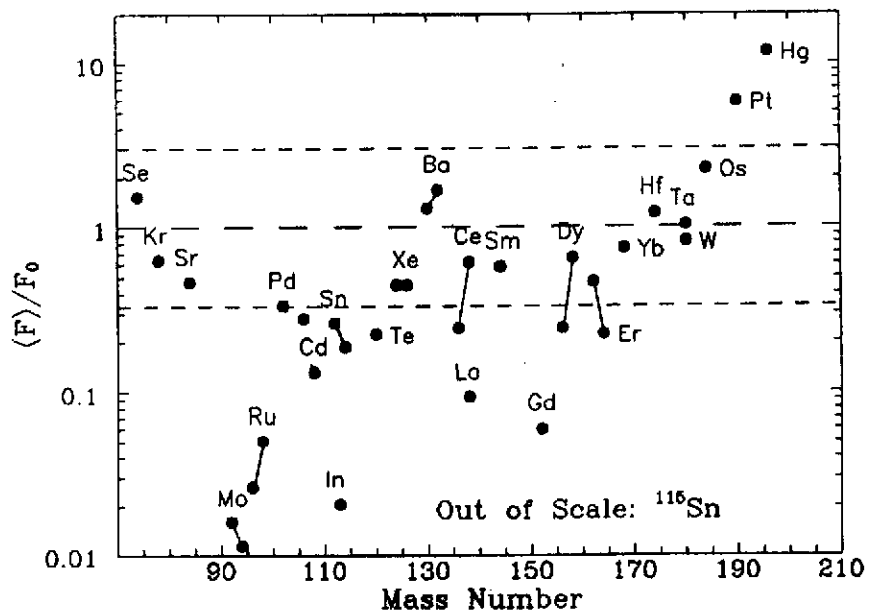

Fig.43. Overproduction of the p-nuclei calculated by Prantzos et al. (1989a) for the model of SN1987A already used in Fig. 42. The overproduction factors are averaged over the whole O/Ne-rich zone defined in Fig. 42, and are normalized to the mean overproduction for all the p-nuclei.

Additional detailed p-process calculations developed self-consistently in the framework of realistic stellar explosion models would be highly desirable. It would also be of great interest to increase the reliability of the predictions of the large body of nuclear physics data requested by such calculations.

Other p-process scenarios than those described here have been proposed (for a review, see e.g. Rayet 1987; Prantzos 1989b). They could be of interest for the synthesis of at least certain p-nuclei.

9. Epilogue

This brief overview of the theories of stellar evolution and of nucleosynthesis makes clear that, within quite a short time span, much progress has been made in our understanding of an impressive body of observations concerning the composition and evolutionary characteristics of many astrophysical sites. In spite of that, we still have to live with a lot of mysteries and puzzles.

Much remains to be done indeed in order to provide a reasonably reliable and detailed explanation for the bulk solar system composition, for the isotopic anomalies in meteorites, as well as for the composition of many chemically peculiar stars, planetary nebulae, novae, or supernovae. All these problems and pending questions certainly make the common adventure of nuclear physics and astrophysics very exciting and challenging.

On the astrophysics side, the mixing processes that can develop at all (non-explosive, as well as explosive) evolutionary stages of a star remain essentially unknown today. Self-consistent models for the evolution of binary stars and for (Type I and II) supernova explosions still have to be constructed. A fortiori, many fundamental aspects and details of the models aimed at describing the chemical evolution of galaxies remain to be worked out, this long-standing problem having been simplified almost beyond recognition in the calculations performed so far.

On the nuclear physics side, and in spite of a considerable experimental and theoretical effort, the rates of many reactions of importance in the energy budget of a star, as well as for stellar and non-stellar (especially inhomogeneous Big Bang; see Sect. 4) nucleosynthesis are still very uncertain at the energies of astrophysical interest. In particular, astrophysics is badly in need of various nuclear properties of radioactive nuclei, and of reliable rates of reactions on such nuclei. This clearly represents a new frontier in science, where the future development of radioactive nuclear beam facilities certainly have to play a pivotal role.

Acknowledgements We thank Marc Rayet and Guy Paulus for their help in the preparation of the manuscript. This work has been performed within the *Programme International de Collaboration Scientifique (PICS)* N° 18, and has also been supported in part by the EEC Science Program SC1-0065. M.A. is Chercheur Qualifié F.N.R.S. (Belgium)

REFERENCES

Aguer, P., Bogaert, G., Kious, M., Landré, V., Lefebvre, A., Thibaud, J.-P., Beck, F., Huck, A. 1989, in *Heavy Ion Physics and Nuclear Astrophysical Problems*, eds. S. Kubono, M. Ishihara, and T. Nomura (World Scientific, Singapore), p. 107

Alpher, R.A., Herman, R.C. 1953, *Ann. Rev. Nucl. Sci.* **2**, 1

Anders, E. 1987, *Phil. Trans. R. Soc. Lond.* **A323**, 287

Anders, E., Grevesse, N. 1989, *Geochim. Cosmochim. Acta* **53**, 197

Arcoragi, J.-P., Langer, N., Arnould, M. 1990, in preparation

Arnett, W.D., Thielemann, F.-K. 1985, *Astrophys. J.* **295**, 589

Arnett, W.D., Bahcall, J.N., Kirshner, R.P., Woosley, S.E. 1989, *Ann. Rev. Astron. Astrophys.* **27**, 629

Arnould, M. 1976, *Astron. Astrophys.* **8**, 436

Arnould, M. 1980, *Explosive Nucleosynthesis,* Cahier n°8, ed. M. Demeur (Physique Nucléaire Théorique, Université Libre de Bruxelles)

Arnould, M. 1985, in *Proc. Accelerated Radioactive Beams Workshop,* eds. L. Buchmann and J. d'Auria (TRIUMF TRI-85-1, Vancouver), p. 29

Arnould, M. 1986a, in *Advances in Nuclear Astrophysics,* eds. E. Vangioni-Flam, J. Audouze, M. Cassé, J.P. Chièze and J. Tran Thanh Van (Editions Frontières, Gif-sur-Yvette), p. 113

Arnould, M. 1986b, in *Progress in Particle and Nuclear Physics,* vol. **17**, ed. A. Faessler (Pergamon Press: Oxford), p. 305

Arnould, M. 1987, *Phil. Trans. R. Soc. Lond.* **A323**, 251

Arnould, M. 1990, in *Proceedings of IAU Symp. 145, Evolution of Stars: The Photospheric Abundance Connection*, Golden Sands, Bulgaria (to appear)

Arnould, M., Beelen, W. 1974, *Astron. Astrophys.* **33**, 215

Arnould, M., Forestini, M. 1989, in *Research Reports in Physics: Nuclear Astrophysics*, eds. M. Lozano, M.I. Gallardo, J.M. Arias (Springer Verlag, Berlin), p.48

Arnould, M., Nørgaard, H. 1975, *Astron. Astrophys.* **42**, 55

Arnould, M., Takahashi, K. 1990, in *Astrophysical Ages and Dating Methods*, eds. E. Vangioni-Flam, M. Cassé, J. Audouze and Tran Than Van (Editions Frontières, Gif-sur-Yvette), to appear

Arnould, M., Nørgaard, H., Thielemann, F.-K., Hillebrandt, W. 1980, *Astrophys. J.* **237**, 931

Audouze, J. 1986, in *Nucleosynthesis and Chemical Evolution*, eds. B. Hauck, A. Maeder and G. Meynet (Observatoire de Genève), p. 186

Audouze, J., Truran, J.W. 1975, *Astrophys. J.* **202**, 204

Audouze, J., Truran, J.W., Zimmerman, B.A. 1973, *Astrophys. J.* **184**, 493

Bahcall, J.N., Ulrich, R.K. 1988, *Rev. Mod. Phys.* **60**, 297

Bao, Z. Y., Käppeler, F. 1987, *At. Data Nucl. Data Tables* **36**, 411

Barnes, C.A. 1986, in *Advances in Nuclear Astrophysics,* eds. E. Vangioni-Flam, J. Audouze, M. Cassé, J.P. Chièze and J. Tran Thanh Van (Editions Frontières, Gif-sur-Yvette), p. 505

Bender, E., Muto, K., and Klapdor, H.V. 1988, *Phys. Lett.* **B208**, 53

Boesgaard A., Steigmann G. 1985, *Ann. Rev. Astron. Astrophys.*, **23**, 319

Bowers, R., Deeming, T. 1984, *Astrophysics I* (Jones and Bartlett Publishers, Boston)

Buchmann, L., D'Auria, J.M., McCorquodale, P. 1988, *Astrophys. J.* **324**, 953

Burbidge, E.M., Burbidge, G.R. Fowler, W.A., Hoyle, F. 1957, *Rev. Mod. Phys.* **29**, 547

Cameron, A.G.W. 1957, *Stellar Evolution, Nuclear Astrophysics, and Nucleogenesis* (Chalk River Rept. CRL-41)

Caughlan, G.R., Fowler, W.A., Harris, M.J., Zimmerman, B.A. 1985, *At. Data Nucl. Data Tables* **32**, 197

Caughlan, G.R., Fowler, W.A. 1988, *At. Data Nucl. Data Tables,* **40**, 283

Chiosi, C. 1986, in *Progress in Particle and Nuclear Physics,* vol. **17**, ed. A. Faessler (Pergamon Press, Oxford), p. 173

Chiosi, C., Maeder, A. 1986, *Ann. Rev. Astron. Astrophys.* **24**, 329

Clayton, D.D. 1983, *Principles of Stellar Evolution and Nucleosynthesis* (The University of Chicago Press, Chicago)

Clayton, D.D., Leising, M.D. 1987, *Phys. Rept.* **144**, 1

Cox, J.P., Giuli, R.T. 1968, *Principles of Stellar Structure* (Gordon and Breach, New York)

Cowan, J.J., Cameron, A.G.W., Truran, J.W., Sneden, C. 1986, in *Advances in Nuclear Astrophysics,* eds. E. Vangioni-Flam, J. Audouze, M. Cassé, J.P. Chièze and J. Tran Thanh Van (Editions Frontières, Gif-sur-Yvette), p. 477

Darquennes, D., Decrock, P., Delbar, T., Huyse, M., Jongen, Y., Lacroix, M., Leleux, P., Licot, I., Lipnik, P., Loiselet, M., Ryckewaert, G., Wa Kitwanga, S., Van Duppen, P., Vanhorenbeeck, J., Vervier, J., Zaremba, S. 1990, in *Proceedings of the First International Conference on Radioactive Nuclear Beams,* eds. W.D. Myers, J.M. Nitschke, and E.B. Norman, (World Scientific, Singapore), p.3

Delbar, T., Huyse, M., Vanhorenbeeck, J. (eds.) 1988, *Belgian Interuniversity Report* RIB-1988-01

Deliyannis C., Demarque P., Kawaler S. 1990, *Astrophys. J. Suppl.*, **73**, 21

de Loore, C. 1980, *Space Sci. Rev.* **26**, 113

Descouvemont, P. 1987, *Phys. Rev.* **C36**, 2206

Descouvemont, P. 1989, *Nucl. Phys.* **A504**, 193

Descouvemont, P. 1989a, private communication

Descouvemont, P., Baye, D. 1987, *Phys. Rev.* **C36**, 1249

Descouvemont, P., Baye, D. 1989, in *Heavy Ion Physics and Nuclear Astrophysical Problems*, eds S. Kubono, M. Ishihara, and T. Nomura (World Scientific, Singapore), p. 97

Dufour, M., Dietrich, K. 1990, preprint (submitted to Astron. Astrophys.)

El Eid, M.F., Prantzos, N. 1988, in *Origin and Distribution of the Elements*, ed. G.J. Mathews (World Scientific, Singapore), p.485

Fernandez, P.B., Adelberger, E.G., Garcia, A. 1989, *Phys. Rev.* **C40**, 1887

Filippone, B.W. 1986, *Ann. Rev. Nucl. Part. Sci.* **36**, 717

Filippone, B.W. Humblet, J., Langanke, K. 1989, *Phys. Rev.* **C40**, 515

Freedman, D.Z., Schramm, D.N., Tubbs, D.L. 1977, *Ann. Rev. Nucl. Sci.* **27**, 167

Fritzsch, H. 1986, in *Progress in Particle and Nuclear Physics*, vol. **17**, ed. A. Faessler (Pergamon Press: Oxford), p. 1

Goriely, S., Jorissen, A., Arnould, M. 1989, in *Proceedings of the 5th Workshop on Nuclear Astrophysics*, Tegernsee, Report MPA/P1, eds. W. Hillebrandt and E. Müller (Max-Planck Institute für Physik und Astrophysik, Garching), p. 60

Harris, M.J., Fowler, W.A., Caughlan, G.R., Zimmerman, B.A. 1983, *Ann. Rev. Astron. Astrophys.* **21**, 165

Hernanz, M., Isern, J., Canal, R., Labay, J., Mochkovitch, R. 1988, *Astrophys. J.* **324**, 331

Hillebrandt, W., Höflich, P. 1989, *Rep. Prog. Phys.* **52**, 1329

Hillebrandt, W., Takahashi, K., Kodama, T. 1976, *Astron. Astrophys.* **52**, 63

Hoff, R. 1986, in *Weak and Electromagnetic Interactions in Nuclei*, ed. H.V. Klapdor (Springer, Heidelberg), p. 207

Hollowell, D.E., Iben, I. Jr. 1989, *Astrophys. J.* **340**, 966

Howard, W.M., Mathews, G.J., Takahashi, K., Ward, R.A. 1986, *Astrophys. J.* **309**, 633

Hoyle, F. 1946, *Monthly Notices Roy. Astron. Soc.* **106**, 343

Iben, I. Jr. 1974, *Ann. Rev. Astron. Astrophys.* **12**, 215

Iben, I. Jr., Renzini, A. 1983, *Ann. Rev. Astron. Astrophys.* **21**, 271

Iliadis, C., Schange, T., Rolfs, C., Schröder, U., Somorjai, E., Trautvetter, H.P., Wolke, K., Endt, P.M., Kikstra, S.W., Champagne, A.E., Arnould, M., Paulus, G. 1989, *Nucl. Phys.* **A512**, 509

Jorissen, A. 1990, Thesis, Université Libre de Bruxelles (unpublished)

Jorissen, A., Arnould, M. 1986, in *Advances in Nuclear Astrophysics*, eds. E. Vangioni-Flam, J. Audouze, M. Cassé, J.P. Chièze and J. Tran Thanh Van (Editions Frontières, Gif-sur-Yvette), p. 419

Jorissen, A., Arnould, M. 1989, *Astron. Astrophys.* **221**, 161

Kajino, T., Boyd, R.N. 1990, preprint

Käppeler, F., Beer, H., Wisshak, K. 1989, *Rep. Prog. Phys.* **52**, 945

Käppeler, F., Gallino, R., Busso, M., Picchio, G., Raiteri, C.M. 1989a, preprint

Kubono, S., Funatsu, Y., Ikeda, N., Yasue, M., Nomura, T., Fuchi, Y., Kawashima, H., Kato, S., Orihara, H., Miyataki, H., Kajino, T. 1989, in *Proceedings of the First International Conference on Radioactive Nuclear Beams*, Berkeley (World Scientific, Singapore), to appear

Kolb E., Turner M. 1990, *The Early Universe*, Addison-Wesley

Krauss L., Romanelli P. 1990, *Astrophys. J.*, **358**, 47

Langer, N., Arcoragi, J.-P., Arnould, M. 1989, *Astron. Astrophys.*, **210**, 187

Leising, M.D., Share, G.H., Chupp, E.L., Kanbach, G. 1988, *Astrophys. J.* **328**, 755

Mahoney, W.A., Ling, J.C., Wheaton, W.A., Jacobson, A.S. 1984, *Astrophys. J.* **286**, 578

Malaney, R.A., Boothroyd, A.I. 1987, *Astrophys. J.* **320**, 866

Malaney, R.A., Fowler, W.A. 1989, *Astrophys. J.*, **345**, L5

Mathews, G.J., Ward, R.A. 1985, *Rep. Prog. Phys.* **48**, 1371

Merrill, P.W. 1952, *Science* **115**, 484

Miller, G.E., Scalo, J.M. 1979, *Astrophys. J. Suppl.* **41**, 513

Möller, P., Randrup, J. 1989, Lawrence Berkeley Laboratory preprint LBL- 27504

Nomoto, K. 1986, in *Progress in Particle and Nuclear Physics*, vol. **17**, ed. A. Faessler (Pergamon Press: Oxford), p.249

Nomoto, K., Hashimoto, M. 1988, *Phys. Rept.*, **163**, 13

Olive K, Schramm D., Steigmann G., Walker T. 1990, *Phys. Let. B*, **236**, 454

Perrin, J. 1920, *Revue du Mois*, **21**, 113

Prantzos, N. 1987, in *Nuclear Astrophysics*, Lecture Notes in Physics **287**, eds. W. Hillebrandt, R. Kuhfuss, E. Müller and J.W. Truran (Springer Verlag, Berlin), p. 250

Prantzos, N. 1989a, in *Research Reports in Physics: Nuclear Astrophysics*, Eds. M. Lozano, M. Gaillardo, J. Arias (Springer-Verlag), p. 1

Prantzos, N. 1989b, in *Research Reports in Physics: Nuclear Astrophysics*, Eds. M. Lozano, M. Gaillardo, J. Arias (Springer-Verlag), p.18

Prantzos, N., Doom, C., Arnould, M., de Loore, C. 1986, *Astrophys. J.* **304**, 695

Prantzos, N., Arcoragi, J.-P., Arnould, M. 1987, *Astrophys. J.* **315**, 209

Prantzos, N., Arnould, M., Cassé, M. 1988, *Astrophys. J.* **331**, L15

Prantzos, N., Hashimoto, M., Nomoto, K. 1990, *Astron. Astrophys.*, **234**, 211

Prantzos, N., Hashimoto, M., Rayet, M., Arnould, M. 1990, in *Supernovae*, ed. S.E. Woosley (Springer Verlag, Berlin), to appear; also *Proceedings of the Elba Workshop on the Chemical and Dynamical Evolution of Galaxies*, to appear; and *Astron. Astrophys.*, in press

Prinzhofer, A., Papanastassiou, D.A., Wasserburg, G.J. 1989, preprint (to appear in *Astrophys. J. Letters*)

Rayet, M. 1987, in *Nuclear Astrophysics, Lecture Notes in Physics* **287**, eds. W. Hillebrandt, R. Kuhfuss, E. Müller, and J.W. Truran (Springer Verlag, Berlin), p. 210

Rayet, M., Prantzos, N., Arnould, M. 1990, *Astron. Astrophys.* **227**, 271

Rebolo R., Molaro P., Beckman J. 1988, *Astron. Astrophys.*, **192**, 192

Rolfs, C., Trautvetter, H.P., Rodney, W.S. 1987, *Rep. Prog. Phys.* **50**, 233

Rolfs, R., Rodney, W.S. 1988, *Cauldrons in the Cosmos* (The University of Chicago Press, Chicago)

Rolfs, C, Jonson, B., Allardyce, B.W., Haas, H., Ravn, H. 1989, *A Concept for a Post-acceleration of Radioactive Ions for Measurements in Astrophysics* (ISOLDE Collaboration, CERN, Geneva)

Russell, H.N. 1919, *Pub. Astron. Soc. Pac.*, **31**, 205

Sackmann, I.-J., Boothroyd, A.I. 1990, in *Procceedings of IAU Symp. 145, Evolution of Stars: The Photospheric Abundance Connection*, Golden Sands, Bulgaria (to appear)

Salpeter, E.E., Van Horn, H.M. 1969, *Astrophys. J.* **155**, 183

Scalo, J.M. 1986, *Fund. Cosmic Phys.* **11**, 1

Schatz, G. 1986, in *Progress in Particle and Nuclear Physics*, vol. **17**, ed. A. Faessler (Pergamon Press, Oxford), p. 393

Schatzmann, E., Praderie, F. 1990, *Les Etoiles* (Interéditions/Editions du CNRS, Paris)

Schramm D., Wagoner R. 1977, *Ann. Rev. Nucl. Sci.*, **27**, 37

Schramm D. 1990, *Fermilab Preprint* 90-120-A

Seuthe, S., Rolfs, C., Schröder, U., Schulte, W.H., Somorjai, E., Spite F., Spite M. 1982, *Astron. Astrophys.*, **115**, 357

Trautvetter, H.P., Waanders, F.B., Kavanagh, R.W., Raven, H., Arnould, M., Paulus, G. 1990, *Nucl. Phys* **A514**, 471

Sugimoto, D., Nomoto, K. 1980, *Space Sci. Rev.* **25**, 155

Takahashi, K. 1988, in *Origin and Distribution of the Elements*, ed. G.J. Mathews (World Scientific, Singapore), p. 542

Takahashi, K., Yokoi, K. 1987, *At. Data Nucl. Data Tables* **36**, 375

Thielemann, F.-K. 1989, in *Research Reports in Physics: Nuclear Astrophysics*, eds. M. Lozano, M.I. Gallardo, J.M. Arias (Springer Verlag, Berlin), p.106

Thielemann, F.-K. 1990, in *Supernovae*, ed. S.E. Woosley (Springer Verlag, Berlin), to appear

Thielemann, F.-K., Arnett, W.D. 1985, *Astrophys. J.* **295**, 604

Thielemann, F.-K., Truran, J.W. 1986, in *Advances in Nuclear Astrophy sics*, eds. E. Vangioni-Flam, J. Audouze, M. Cassé, J.P. Chièze and J. Tran Thanh Van (Editions Frontières, Gif-sur-Yvette), p. 541

Thielemann, F.-K., Wiesher, M. 1990, Harvard Smithsonian Center for Astrophysics preprint No 3001

Thielemann, F.-K., Arnould, M., Truran, J.W. 1986a, in *Advances in Nuclear Astrophysics*, eds. E. Vangioni-Flam, J. Audouze, M. Cassé, J.P. Chièze and J. Tran Thanh Van (Editions Frontières, Gif-sur-Yvette), p. 525

Thielemann, F.-K., Hashimoto, M., Nomoto, K. 1990, *Astrophys. J.*, **349**, 222

Thielemann, F.-K., Metzinger, J., Klapdor, H.V. 1983, *Z. Phys.* **A309**, 301

Thielemann, F.-K., Nomoto, K., Yokoi, K. 1986b, *Astron. Astrophys.* **158**, 17

Thomas, H.-C. 1977, *Ann. Rev. Astron. Astrophys.* **15**, 127

Tinsley, B.M. 1980, *Fund. Cosmic Phys.* **5**, 287

Trimble, V. 1975, *Rev. Mod. Phys.* **47**, 877

Trimble, V. 1982, *Rev. Mod. Phys.* **54**, 118

Trimble, V. 1983, *Rev. Mod. Phys.* **55**, 511

Turck-Chièze, S., Cahen, S., Cassé, M., Doom, C. 1988, *Astrophys. J.* **335**, 415

van Wormer, L., Browne, C.P., Giesen, U., Görres, J., Graff, S., Lamm, L.O., Wiescher, M., Rollefson, A.A. 1989, *Bull. Am. Phys. Soc.* **34**, 1192

von Ballmoos, P., Diehl, R., Schönfelder, V. 1987, *Astrophys. J.* **318**, 654

Wagoner R., Fowler W., Hoyle F. 1967, *Astrophys. J.*, **148**, 3

Wallace, R.K., Woosley, S.E. 1981, *Astrophys. J. Suppl.* **45**, 389

Wallace, R.K., Woosley, S.E. 1984, in *High Energy Transcients in Astrophysics*, ed. S.E. Woosley, AIP Conf. Proc. No. 115 (New York), p. 319

Wang, T.F., Rehm, K.E., Sanders, S.J., Davids, C.N., Glagola, B.G., Holgmann, R., Ma, W.C., Magnus, P.V., Parker, P.D., Smith, M., 1988, *Bull. Am. Phys. Soc. Series II* **33**, 1564

Wasserburg, G.J. 1985, in *Protostars and Planets II*, eds. D.C. Black and M.S. Matthews (University of Arizona Press: Tucson), p. 703

Weinberg S. 1972, *Gravitation and Cosmology*, J. Wiley and Sons

Wiescher, M., Görres, J. 1989, *Astrophys. J.* **346**, 1041

Wiescher, M., Ketner, K.-U. 1982, *Astrophys. J.* **263**, 891

Wiescher, M., Langanke, K. 1986, *Z. Phys.* **A325**, 309

Wiescher, M., Görres, J., Thielemann, F.-K., 1988, *Astrophys. J.* **326**, 384

Wiescher, M., Görres, J., Thielemann, F.-K., Ritter, H. 1986, *Astron. Astrophys.* **160**, 56

Wiescher, M., Görres, J., Graff, S., Buchmann, L., Thielemann, F.-K. 1989, *Astrophys. J.* **343**, 352

Wiescher, M., Harms, V., Görres, J., Thielemann, F.-K., Rybarcyk, L.J., 1987, *Astrophys. J.* **316**, 162

Wiescher, M., Görres, J., Sherril, B., Mohar, M., Winfield, J.S., Brown, B.A. 1988a, *Nucl. Phys.* **A484**, 90

Wolke, K., Harms, V., Becker, H.W., Hammer, J.W., Kratz, K.L., Rolfs, C., Schröder, U., Trautvetter, H.P., Wiescher, M., Wöhr, A. 1989, *Z. Phys.* **A334**, 491

Woosley, S.E. 1986, in *Nucleosynthesis and Chemical Evolution*, eds. B. Hauck, A. Maeder and G. Meynet (Observatoire de Genève), p. 1

Woosley, S.E., Howard, W.M. 1978, *Astrophys. J. Suppl.* **36**, 285

Woosley, S.E., Weaver, T.A. 1986, *Ann. Rev. Astron. Astrophys.* **24**, 205

Woosley, S.E., Arnett, W.D., Clayton, D.D. 1973, *Astrophys. J. Suppl.* **26**, 231

Yang J., Turner M., Steigman G., Schramm D., Olive K. 1984, *Ap.J.*,**281**, 493